Analysis and comparison of the glycoproteomic phenotype of TLR4- and TLR2-induced tolerance in human monocytes

Dissertation zur Erlangung des akademischen Grades

doctor medicinae (Dr. med.)

vorgelegt dem Rat der Medizinischen Fakultät

der Friedrich-Schiller-Universität Jena

von Andrea Behnert

geboren am 15.10.1992 in Hann. Münden

Gutachter

1. Prof. Dr. Hortense Slevogt, Jena
2. Prof. Dr. Bernd Lepenies, Hannover
3. Prof. Dr. Rainer König, Jena

Staatsexamen: 18.05.2018

Table of Contents

List of Abbreviations VIII

1. Summary 1

2. Zusammenfassung 3

3. Introduction 5

3.1 Host immune response in sepsis 5

3.2 Endotoxin Tolerance: A major mechanism of immunosuppression during sepsis 6

3.3 PRRs and their ligands: PAMPS and alarmins 8

3.4 The Toll-like receptor family and its ligands 8

3.4.1 General aspects of LPS-mediated TLR4 activation in naïve and tolerant monocytes 9

3.4.2 Characteristics of LPS as a PAMP and TLR4 ligand 10

3.4.3 S100A12 as alarmin and TLR4 ligand 11

3.4.4 General aspects of TLR2 activation 12

3.5 Characterization of the NOD-like receptor (NLR) family 13

3.5.1 General aspects of the NLR family 13

3.5.2 Signaling of the NOD-like receptors NOD1 and NOD2 13

3.6 Receptor expression profile and glycoproteomics of human monocytes 14

4. Hypothesis and objectives 16

5. Materials and Methods 18

5.1 Laboratory devices and expendable materials 18

5.2 TLR agonists and recombinant proteins 20

5.3 Primers used for semi-quantitative and real-time PCR studies 21

5.4 List of antibodies for flow cytometry and western blot 22

5.5 Cell culture methods 23

5.5.1 Conditions of eukaryotic cell cultivation 23

5.5.2 THP-1 cells (ATCC®-TIB-202™, USA) 23

5.5.3 HEK-Blue™-hTLR4 cells (Invivogen, USA) 23

5.5.4 Cell freezing and thawing 24
5.5.5 Isolation of human peripheral blood monocytes 24
5.5.6 Purity of monocytes for glycoproteomic analysis (MACS and FACS) 25
5.5.7 Cell stimulations 25
5.6 Methods in molecular biology 27
5.6.1 Cell lysis and RNA extraction 27
5.6.2 Determination of RNA concentration and purity 27
5.6.3 Reverse transcription (RT) of RNA into cDNA 27
5.6.4 Primer Design 28
5.6.5 Polymerase chain reaction (PCR) 28
5.6.6 PCR product analysis using agarose gel electrophoresis 29
5.6.7 Gene expression analysis with real-time PCR (qPCR) 29
5.6.8 Cultivation of Escherichia coli 30
5.6.9 Establishing of competent bacteria 30
5.6.10 Plasmid preparation and isolation 31
5.6.11 Ethanol precipitation of DNA 31
5.6.12 Transfection of cells 32
5.6.13 Luminescence measurement 34
5.7 Methods of protein biochemistry 36
5.7.1 Enzym linked immunosorbent assay (ELISA) 36
5.7.2 Cell lysis and isolation of the total cellular protein content 36
5.7.3 SDS-polyacrylamide gel electrophoresis (SDS-page) 37
5.7.4 Staining of protein gels 37
5.7.5 Western blot 38
5.7.6 Immunochemical tests for the detection of proteins on blot membranes 39
5.7.7 Flow cytometry analysis of human monocytes 39
5.7.8 Sample Preparation for Mass Spectrometry 40
5.7.9 Limulus Amebocyte Lysate (LAL) test 42

Table of Contents

5.7.10 Quantitative analysis of NF-κB activation in HEK-Blue-hTLR4 cells....43
5.8 Statistical analysis....44
5.8.1 Analysis of qPCR data and cytokine expression via ELISA....44
5.8.2 Densitometric analysis of Western blot data....44
5.8.3 Analysis of FACS data....44
5.8.4 Analysis of mass spectrometry-based proteomic data....44
5.9 Software....46
6. Results....47
6.1 Characterization of human monocytes....47
6.1.1 Human monocytes express TLR1, TLR2, TLR6, TLR4, CD14, MD-2, RAGE and NLRs....47
6.2 Pro-inflammatory response and tolerance induction in monocytes by TLR- and NLR-agonists....48
6.2.1 TNF-α mRNA expression of LPS-, Pam3CSK4-, MALP2-, iE-DAP or MDP-stimulated monocytes....48
6.2.2 Kinetic analysis of the pro-inflammatory immune response of LPS-treated human monocytes....48
6.2.3 TNF-α mRNA expression is suppressed in LPS-, P3C- or MALP2-prestimulated monocytes but not when pre-stimulated with a NLR-ligand....49
6.3 S100A12: an endogenous ligand and possible inducer of tolerance in monocytes....50
6.3.1 Comparison of the pro-inflammatory effects of commercially obtained S100A12 and LPS in THP-1 cells....50
6.3.2 Confirmation of the purity of S100A12....51
6.3.3 Confirmation of LPS contamination in commercially obtained S100A12 by LAL assay....52
6.3.4 Endotoxin-free S100A12 does not induce TNF-α expression on transcriptional level in THP-1 cells....53
6.4 Adjustment of stimulation concentrations of TLR agonists....55

6.4.1 Standardization by an NF-κB-promoter reporter gene assay is not possible due to malfunctioning transient transfection of THP-1 cells and human monocytes 55
6.4.2 TNF-α- and IL-6-production by naïve and prestimulated monocytes 57
6.4.3 Intercellular adhesion molecule-1 (ICAM-1) expression as a marker of the activation level of stimulated human monocytes 59
6.5 Purity of monocytes for glycoproteomic analysis 61
6.6 Mass spectrometry-based glycoprotein expression in monocytes 61
6.6.1 LPS-, Pam3CSK- and MALP2-stimulated monocytes exhibit changes in their glycoprotein expression 64
6.6.2 Comparison of the glycoprotein expression patterns of all three donors by Principal Component Analysis (PCA) 65
6.6.3 Results of paired analysis 66
6.6.4 Subcellular localization of significantly regulated glycoproteins 73
6.6.5 Comprehensive analysis of CD antigen expression in the tolerant monocyte state 74
6.6.6 Modification of glycosylation enzyme-expression in tolerant monocytes 75
6.6.7 Changes of G protein-coupled receptor expression in tolerant monocytes 77
6.7 Confirmation of glycoproteomic data via qPCR, FACS and immunoblot analysis 78
7. Discussion 81
7.1 Tolerance induction in human monocytes 82
7.2 Glycoproteomic analysis of naïve and tolerant monocytes 86
7.2.1 Donor-dependent purity of isolated cells and impact on glycoproteomic analysis 86
7.2.2 Changes in the glycoproteome of LPS-, Pam3CSK- and MALP2-tolerized monocytes 87
7.2.3 Effects of different TLR ligands 89
7.2.4 Cell surface signature of tolerant monocytes 91
7.2.5 Induction of sialyltransferases and SIGLECs 95
7.3 Perspectives 96
8. Conclusions 97

Table of Contents

9. References 99

10. Appendix 110

10.1 List of figures 110

10.2 List of tables 112

Ehrenwörtliche Erklärung 113

Danksagung 114

List of Abbreviations

ANOVA	Analysis of variance
Asn	Asparagin
BIR	Baculovirus inhibitor of apoptosis protein repeat
BSA	Bovine serum albumin
CARD	Caspase-activation and recruitment domain
CBB	Coomassie Brilliant Blue
CD	Cluster of differentiation
cDNA	Complementary DNA
CEACAM	Carcinoembryonic antigen-related cell adhesion molecule
CLR	C-type lectin receptor
CSE	Control Standard Endotoxin
Ct	Threshold cycle
CIITA	Class II transactivator
DAMPs	Danger-associated molecular pattern
DAVID	Database for Annotation, Visualization and Integrated Discovery
DF	Dirk Foell
DMEM	Dulbecco's Modified Eagle Medium
DMSO	Dimethylsulfoxid
DNA	Deoxyribonucleic acid
dNTP	Deoxyribonucleoside triphosphate
DPBS	Dulbecco's phosphate-buffered saline
DTT	Dithiothreitol
EDTA	Ethylenediaminetetraacetic acid
ELISA	Enzyme-linked immunosorbent assay
ER	Endoplasmic reticulum
ET	Endotoxin tolerance
FACS	Fluorescence-activated cell sorting
FC	Fold change
FCS	Fetal calf serum

FDR	False discovery rate
Fig.	Figure
FSC	Forward scatter
GO	Gene Ontology
GPCR	G protein-coupled receptor
GPI	Glycosylphosphatidylinositol
HEK293	Human embryonic kidney 293
HLA	Human leukocyte antigen complex
HMGB1	High mobility group box-1
HPRT1	Hypoxanthine phosphoribosyltransferase 1
hPSC	Human pluripotent stem cell
HRP	Horseradish peroxidase
IAP	Inhibitor of apoptosis
ICAM-1	Intercellular-adhesion molecule 1
iE-DAP	D-γ-glutamyl-meso- Diaminopimelic acid
IFN	Interferon
IKK	IkappaB (IκB) kinase
IL	Interleukin
IRAK	Interleukin-1 receptor-associated kinase
IRF	Interferon regulatory transcription factor
ITGB8	Integrin subunit beta 8
KEGG	Kyoto Encyclopedia of Genes and Genomes
LAL	Limulus amebocyte lysate
LB medium	Lysogeny broth medium
LBP	LPS-binding protein
LC-MS/MS	Liquid chromatography–tandem mass spectrometry
LP	Lipopeptide
LPAR6	Lysophosphatidic acid receptor 6
LPS	Lipopolysaccharide
LRR	Leucin rich repeat domain
Ly96	Lymphocyte antigen 96 (= MD-2)

MACS	Magnetic-activated cell sorting
MALP2	Macrophage-activating lipopeptide-2
MAPK	Mitogen-activated protein kinase
MD-2	Myeloid differentiation factor 2
MDP	Muramyl dipeptide
MHC	Major histocompatibility complex
MW	Molecular weight
MyD88	Myeloid differentiation primary response protein 88
NF-κB	Nuclear factor kappa-B
NGF	N-glycosylated peptide fraction
NLR	Nucleotide-binding oligomerization domain (NOD)-like receptor
NOD	Nucleotide-binding oligomerization domain
OD	Optical density
Pam3CSK, P3C	Pam3CysSerLys4
PAMP	Pathogen-associated molecular pattern
PBMC	Peripheral blood mononuclear cell
PC	Primary component
PCA	Principal component analysis
PCR	Polymerase chain reaction
PD-L1	Programmed cell death-ligand 1
PGN	Peptidoglycan
PMA	Phorbol-12-myristate-13-acetate
PMB	Polymyxin B
pNA	P-nitroaniline
PNGase F	Peptide-N-Glycosidase F
PPIB	Peptidylpropyl isomerase B
PRR	Pattern-recognition receptor
PVDF	Polyvinylidene fluoride
PYD	Pyrin domain
qPCR	quantitative PCR
RAGE	Receptor for advanced glycation endproducts

RLR	Retinoic acid inducible gene (RIG)-I-like receptors
RNA	Ribonucleic acid
RPMI	Roswell Park Memorial Institute
RT	Reverse transcription
TBS	Tris-buffered saline
TGF-β	Transforming growth factor-beta
TIR	Toll/interleukin-1 receptor domain
TLR	Toll-like receptor
TMB	3,3',5,5'-Tetramethylbenzidine
TMD	Transmembrane domain
TMHMM	Transmembrane hidden Markov model
TNF-α	Tumor necrosis factor-alpha
TPF	Tryptic peptide fraction
TRAF	Tumor necrosis factor receptor-associated factor
TRAM	TRIF-related adaptor protein
TRIF	TIR-domain-containing adaptor-inducing interferon-β
TRIS	Tris(hydroxymethyl)aminomethane
SD	Standard deviation
SDS	Sodium dodecyl sulfate
SEAP	Secreted embryonic alkaline phosphatase
SEC	Size Exclusion Chromatography
SEM	Standard error of the mean
SIGLEC	Sialic acid (Sia)-binding Ig-like lectin
SIRS	Systemic inflammatory response syndrome
SLAMF	Signaling lymphocytic activation molecule family member
SSC	Side scatter

1. Summary

Endotoxin tolerance of human monocytes contributes to sepsis-induced immunosuppression, a leading cause of sepsis-related deaths worldwide. Although several studies already demonstrated distinct alterations of cytokine expression, phagocytotic capability and expression changes of particular receptor- and glycoproteins to be linked with the tolerant state in human monocytes, no study investigated changes of the whole glycoproteome on a global level. Due to the fact that most membrane-bound receptors are glycosylated, the characterization of the tolerant monocyte cell state by glycoproteomics using tandem mass spectrometry (LC-MS/MS) might reveal new and useful markers to distinguish tolerant from naïve cells and can provide possible new targets for improving immune-modulatory therapies.

In this doctoral thesis, (a) PAMPs binding to cell surface-expressed pattern recognition receptors (PRRs) (TLR4 agonist LPS, TLR2/1 agonist Pam3CSK and TLR2/6 agonist MALP2), (b) PAMPs binding to intracellular PRR (NOD-like receptor (NLR) ligands 1 and 2; iE-DAP and MDP) and (c) the alarmin S100A12, signaling via the receptor for advanced glycation endproducts (RAGE) and TLR4, were examined for their capability to induce the monocyte tolerant state. Qualitative and quantitative analysis of glycoprotein expression changes in purified monocytes of three different peripheral blood donors were assessed with and without LPS-, Pam3CSK- and MALP2-stimulation and analyzed in the naïve and tolerant state.

Tolerance was measured by restimulation with LPS of monocytes that were prestimulated with adjusted concentrations of either LPS, Pam3CSK or MALP2. Prestimulation with all three PRR agonists led to highly decreased expression of the pro-inflammatory cytokines TNF-α and IL-6, which is consistent with the cells entering a tolerant state. NLR ligands iE-DAP and MDP induced only weak pro-inflammatory responses in human monocytes and none of the NLR ligands demonstrated a reduction of TNF-α expression in subsequent LPS challenges. Commercially available S100A12, that was efficient in inducing pro-inflammatory activation of monocytic THP-1 cells, was found to be significantly contaminated with LPS, as revealed by Limulus Amebocyte Lysate (LAL) test. Further experiments with endotoxin-free, granulocyte-derived, purified S100A12 induced neither a pro-inflammatory activation of human monocytes nor tolerance. Thus, only the glycoproteomes of LPS-, Pam3CSK- and MALP2-stimulated monocytes, that induced the tolerant state, were analyzed in a mass spectrometry approach.

Comparable numbers of glycoproteins (1003, 966 and 1033) were identified in purified human monocytes from each of the three donors, respectively. Altogether, 1176 annotated proteins were

identified, originating from various cellular organells. 898 of the 1176 identified glycoproteins were predicted to contain at least one transmembrane domain, demonstrating that a high number of membrane spanning glycoproteins has been found. The majority of the identified glycoproteins were annotated in Gene Ontology (GO) as “plasma membrane” associated including 202 CD antigens and 54 GPCRs. Stimulation of the purified human monocytes with LPS, Pam3CSK or MALP2 induced significantly differential expression levels of 135 glycoproteins. From 75 glycoproteins annotated to be involved in glycan processing and maturation, only 4 demonstrated significantly expression changes, indicating no major changes in the glycosylation of the proteins which might have affected enrichment and quantification during LC-MS/MS analysis. The largest subset of differentially expressed glycoproteins was again annotated as plasma membrane-resident glycoproteins comprising 35 significantly regulated CD antigens. KEGG pathway analysis revealed an enrichment of CD antigens involved in cell adhesion processes (e.g. ITGAV (CD51) and ICAM-1(CD54)). Interestingly, all three TLR agonists led to highly similar changes in the glycoproteomes of the stimulated cells. Resemblance of the glycoproteomic signature was higher among the different stimuli than between the three donors due to interindividual differences in glycoprotein expression (e.g. HLA molecules) and donor-dependent sample purity. 75 glycoproteins demonstrated significantly increased expression levels, with PD-L1 (CD274), ITGB8 and IL7R (CD127) among the most highly upregulated glycoproteins. Collectin 12 (COLEC12) and lysophosphatidic acid receptor 6 (LPAR6) displayed the strongest decrease in their expression out of 60 significantly down-regulated glycoproteins. Whereas upregulation of PD-L1 and IL7R expression in monocytes of septic patients is a well-described phenomenon in the literature, this study identifies, for the first time, strongly upregulated expression of ITGB8 in tolerant human monocytes. ITGB8 is involved in the activation of latent TGF-β, a cytokine which was shown to contribute to and to be expressed increased during sepsis-induced immunosuppression.

Taken together, the tolerant monocyte cell state is accompanied by differential expression of a series of glycoproteins. Changes in the monocytes glycoproteome were highly similar in cases of TLR2- and TLR4-mediated tolerance and revealed possible new biomarkers of the tolerant monocyte state like ITGB8, which should be validated in future *in vivio* studies.

2. Zusammenfassung

Eine hohe Zahl septischer Patienten entwickelt eine Immunsuppression, die zu den wichtigsten Gründen Sepsis bedingter Todesursachen zählt. Endotoxin Toleranz menschlicher Monozyten trägt entscheidend zur Sepsis induzierten Immunsuppression bei und eine Reihe von Studien konnte zeigen, dass dieses tolerante Zellstadium in Monozyten mit spezifischen Veränderungen der pro- und anti-inflammatorischen Zytokinexpression, der phagozytotischen Aktivität und der Expression bestimmter Rezeptor- und Glykoproteine assoziiert ist. Bisher erfolgte jedoch noch keine Untersuchung des Glykoproteoms toleranter Monozyten auf globaler Ebene: Dies wäre ein vielversprechender Ansatz neue Biomarker des toleranten Zellstadiums zu entdecken, da der größte Teil der auf der Zelloberfläche-exprimierten Rezeptoren glykosyliert ist. Diese Biomarker könnten einerseits der Unterscheidung toleranter von naiven Zellen dienen und andererseits mögliche neue pharmakologische Angriffspunkte darstellen.

Die vorliegende Studie untersuchte die pro-inflammatorische Aktivierung und Toleranz-Induktion in aufgereinigten CD14+ Monozyten durch verschiedene bakterielle Zellwandbestandteile (PAMPs). Verwendet wurden (a) PAMPs, die an PRRs der Zelloberfläche binden (TLR4-Ligand LPS, TLR2/1-Ligand Pam3CSK, TLR2/6-Ligand MALP2), (b) PAMPs, die an intrazellulär lokalisierte PRRs binden (NOD-like receptor (NLR)-Liganden 1 und 2; iE-DAP und MDP) und (c) das von Granulozyten synthetisierte Alarmin S100A12, ein Agonist des Receptor for Advanced Glycation Endproducts (RAGE) und von TLR4. Veränderungen des Glykoprotein-Expressionsmusters naiver und LPS-, Pam3CSK- und MALP2-stimulierter Monozyten wurden von drei unterschiedlichen Blutspendern mittels Tandem-Massenspektroskopie (LC-MS/MS) qualitative und quantitative erfasst und verglichen.

LPS-Restimulation LPS-, Pam3CSK- und MALP2-(vor)stimulierter Monozyten führte zu einer signifikant verminderten Expression pro-inflammatorischer Zytokine (TNF-α, IL-6), ein Merkmal, dass sich die entsprechend stimulierten Monozyten im toleranten Zustand befinden. Beide NLR-Agonisten, iE-DAP und MDP, induzierten eine messbare pro-inflammatorische Aktivierung, resultierten jedoch im Gegensatz zu den oben genannten TLR-Agonisten nicht in der Abnahme der TNF-α Expression bei anschließender LPS-Restimulation. Kommerziell erhältliches S100A12, zeigte eine pro-inflammatorische Aktivierung monozytärer THP-1 Zellen. Allerdings bestätigte der Limulus-Amöbozyten-Lysat (LAL)-Test eine messbare Kontamination mit LPS. LPS-freies, von Granulozyten-gewonnen und aufgereinigtes S100A12 zeigte weder ein pro-inflammatorische Aktivierung noch eine Toleranzinduktion in Monozyten.

Daher wurden in der nachfolgenden massenspektroskopischen Analyse nur die Glykoproteome naiver und LPS-, Pam3CSK- und MALP2-stimulierter Monozyten untersucht.

Insgesamt wurden 1176 Glykoproteine der aufgereinigten Monozyten von annähernd allen vorhanden Zellkompartimenten identifiziert und eine vergleichbare Anzahl an Glykoproteinen (1003, 966 und 1033) von allen 3 Spendern detektiert. 898 der 1176 identifizierten Glykoproteine enthielten mindestens eine Transmembran Domäne, entsprechend gelang es eine hohe Zahl an Membran-überspannenden Glykoproteinen zu isolieren. Der größte Anteil identifizierter Glykoproteinen wurde mittels Gene Ontology (GO) als „plasma membrane"-assoziiert annotiert und enthielt 202 CD Antigene und 54 G-Protein gekoppelte Rezeptoren. Stimulation der Monozyten mit LPS, Pam3CSK und MALP2 führte zur signifikant veränderten Expression von 135 Glykoproteinen. Nur 4 von insgesamt 75 Glykoproteinen, annotiert als involviert in unterschiedlichen Schritten der Protein-Glykosylierung, zeigten eine signifikant veränderte Expression, weshalb von keiner Beeinflussung der Glykoprotein Anreicherung oder massenspektroskopischen Quantifizierung auszugehen ist. Glykoproteine der Plasmamembran bildeten auch die größte Gruppe signifikant regulierter Glykoproteine, darunter 35 CD Antigene. KEGG Analyse ergab eine Anreicherung von CD Proteinen involviert in Zelladhäsions Prozessen (z.B. ITGAV (CD51) und ICAM-1 (CD54)). Interessanterweise resultierte die Stimulation der Monozyten mit allen 3 TLR Liganden in sehr ähnlichen Veränderungen des Glykoproteoms. Die Ähnlichkeit der Glykoprotein-Expressionsmuster war sogar größer zwischen den einzelnen Stimuli als zwischen den verschiedenen Blutspendern, wozu einerseits interindividuelle Unterschiede der Glykoproteinexpression (z. B. der HLA Antigene) und andererseits die Spender-abhängige Reinheit der verwendeten Proben beitrugen. 75 Glykoproteine demonstrierten signifikant erhöhte Expressionsraten, wobei sich PD-L1 (CD274), ITGB8 und IL7R (CD127) unter den am stärksten herauf regulierten Glykoproteinen befanden. Collectin 12 (COLEC12) und Lysophosphatic acid receptor 6 (LPAR6) zeigten unter den insgesamt 60 herunter regulierten Glykoproteinen die stärkste Abnahme ihrer Expression. Während die erhöhte Expression von PD-L1 und IL7R auf Monozyten septischer Patienten, und ihr Beitrag zur Sepsis induzierten Immunsuppression, ein in der wissenschaftlichen Literatur bekanntes Phänomen ist, konnte die vorliegende Studie zum ersten Mal deutlich erhöhte Expressionsraten von ITGB8 zeigen. ITGB8 ist in der Aktivierung des latenten, immunsuppressiven TGF-β involviert und stellt somit ein möglichen neuen Glykoprotein-Biomarker des toleranten Status von Monozyten dar, der unter Umständen sogar von pharmakologischen Interesse sein könnte. Die Validität dieses möglichen neuen Biomarkers bleibt jedoch in weiteren *in vivo* Studien zu überprüfen.

3. Introduction

3.1 Host immune response in sepsis

The inflammatory host response to severe infections, caused by invading pathogens, is defined as sepsis (Hotchkiss et al. 2013). Sepsis is one of the most frequent causes of mortality among hospitalized patients and responsible for more than 120.000 deaths each year, solely in the USA (Reinhart et al. 2012, Martin et al. 2003). In clinical observations, it was recognized that patients, who survive the initial hyperinflammatory phase, often enter a prolonged immunosuppressive phase. While improved diagnostics and treatments result in increasing survival rates of the first hyperinflammatory phase of sepsis, the mortality rate of the subsequent immunosuppressive state remains unaffectedly high at about 30% (Jawad et al. 2012). The disability to efficiently control the initial infection and the acquisition of secondary hospital-acquired infections are the primary causes of death in these patients (Hotchkiss et al. 2013). Generally, a complex interaction of the innate and the acquired immune system ensure an efficient and fast elimination of invading pathogens. Focusing on the cellular level, especially monocytes, macrophages and granulocytes, as important members of the innate immunsystem, play a central role in the early detection of microbial infections. Due to the vast variety of highly conserved pathogen-recognition receptors (PRRs) expressed on their cell surface, monocytes and macrophages are able to recognize different microbes and to initiate an inflammatory response. They can phagocytose pathogens or initiate the host response by releasing antimicrobial compounds and pro-inflammatory cytokines. Moreover, monocytes and macrophages induce and regulate the activation of an appropriate adaptive immune response by presenting antigens to naïve T cells (reviewed in Aziz et al. 2013, Gordon 2007). Additionally to the recognition of broadly shared and conserved structures among bacterial species, so called “pathogen-associated molecular patterns” (PAMPs), PRRs have been shown to bind endogenous host-derived molecules, the so called “alarmins” that can be either released by dying cells or actively secreted by activated immune cells (reviewed in Kumar et al. 2013). Once activated by specific ligands, PRRs induce signaling cascades which result in an upregulated transcription of various genes encoding molecules that are involved in the pro-inflammatory response (e.g. pro-inflammatory cytokines, type I interferons (IFNs), chemokines, antimicrobial proteins, proteins involved in the regulation of PRR signaling). All these molecules have pleiotropic effects on major cellular functions, e.g. by modifying growth, metabolism, replication processes, cell adhesion and migration, and are also directly involved in the regulation of vascular endothelial permeability, the production of acute phase proteins, recruitment of blood cells to inflamed tissues and cell death occurring in inflamed tissues (Takeuchi und Akira 2010). Due to

this, a tight regulation of the expression of PRRs and of receptor-downstream signaling cascades is necessary in order to achieve an appropriate and efficient elimination of the invading pathogens on the one hand, while restoring the immune balance and preventing massive host tissue damage on the other hand.

As mentioned above, sepsis is characterized by an initial dominant and overwhelming hyper-inflammatory immune response followed by an immunosuppressive state. For years, it was a paradigm that hyperinflammation with subsequent immunosuppression was an orderly process, while recent studies support the current opinion that both, the pro- and anti-inflammatory host response, occur early and simultaneously (Pena et al. 2014, Hotchkiss et al. 2013). The net effects of these opposing processes result in an early pro-inflammatory state and a prolonged immunosuppressive phase with various mechanisms leading to immune dysfunction and disease severity (Fig. 1). Especially, dysfunctional monocytes and macrophages, that become refractory to subsequent PAMP activation and enter a state of hyporesponsiveness, seem to play a key role in the development of sepsis-associated immunosuppression (Monneret et al. 2004, Biswas and Lopez-Collazo 2009). The phenomenon described above is called “endotoxin tolerance” and will be described more detailed in the following chapter.

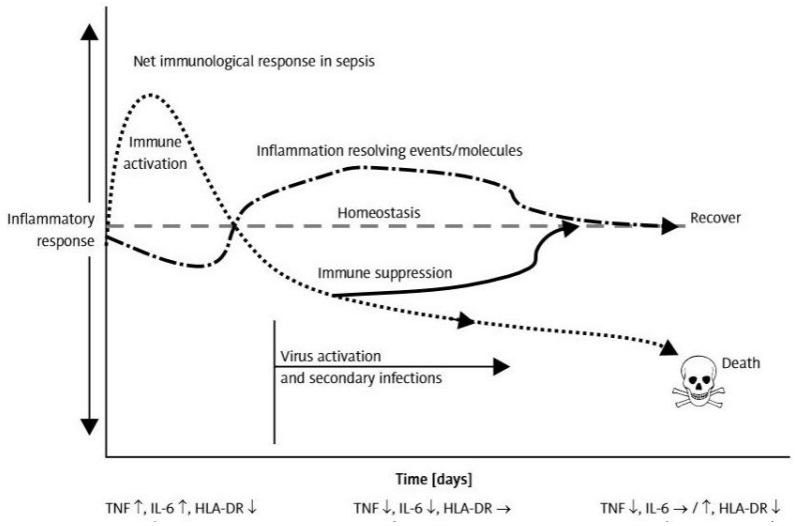

Fig. 1: Theory of host immune response in sepsis. Both, pro- and anti-inflammatory immune response occur early in course of sepsis. Initially, the pro-inflammatory activation of the cells dominates with upregulated expression levels of pro-inflammatory cytokines e.g. TNF-α and IL-6. But if sepsis persists, the anti-inflammatory response prevails, leading to immune suppression in septic patients, which is linked with an increased risk for secondary infections and mortality. Fig. 1 represents a modified version of the scheme by Das et al. (2014).

3.2 Endotoxin Tolerance:
A major mechanism of immunosuppression during sepsis

The anti-inflammatory response of monocytes dominates rapidly after the initial release of pro-inflammatory cytokines, inducing a state of immunosuppression. One important aspect among many other severe alterations in the innate and adaptive immune system, contributing to this immunosuppressive state, is a phenomenon called “endotoxin tolerance” (ET). For example,

monocytes/macrophages that are exposed to low concentrations of the TLR4 agonist lipopolysaccharide (LPS, endotoxin) enter into a transient state of hyporesponsiveness and are less sensitive to respond to further challenges with LPS and other PAMPs. Several studies showed that the tolerant phenotype of monocytes is associated with down regulated transcription of genes encoding pro-inflammatory cytokines (e.g. tumor necrosis factor (TNF)-α, IL-1β, IL-6), while the expression of anti-inflammatory cytokines (like IL-10, IL-1RA, TGF-β) and inhibitory receptors (e.g. programmed cell death ligand receptor 1 (PD-L1)) is upregulated (reviewed in Hotchkiss et al. 2013). Moreover, tolerant cells display increased phagocytic capability but impaired antigen presenting capacity due to the reduced expression of several MHC class II molecules (e.g. HLA-DR) (del Fresno et al. 2009). Both, decreased HLA-DR expression and enhanced expression of anti-inflammatory cytokines have been shown to be associated with a worse outcome in sepsis (van Dissel et al. 1998, Hynninen et al. 2003, Gogos et al. 2000). Although LPS tolerance has been studied extensively, underlying mechanisms responsible for endotoxin tolerance remain poorly understood, but a number of studies suggest first explanations. Previous reports found that the activation of several central regulators of gene expression, including nuclear factor kappa B (NF-κB) and mitogen-activated protein kinases (MAPKs), was reduced in tolerant macrophages (Foster et al. 2007). The transcription factor NF-κB and the phosphorylating MAPKs, which regulate a variety of immune-relevant transcript factors, are central elements of the PRR/TLR-induced down-streaming signaling cascades. In addition, epigenetic modifications such as histone modification and gene-specific chromatin remodeling seem to play a major role in the impaired immune response of tolerant monocytes to secondary stimuli by selectively silencing genes that encode pro-inflammatory cytokines.

Recently published data of Pena et al. (2014) provided a description of a unique endotoxin tolerance gene expression profile, already present in the early clinical course of sepsis. Due to its specific linkage to sepsis pathogenesis and organ dysfunction, testing for this endotoxin signature is a promising approach to identify septic patients with impaired immune functions and, therefore, of high diagnostic and therapeutic potential. As mentioned above, several studies already demonstrated distinct alterations of cytokine release and phygocytotic capabilities in tolerant monocytes, but so far, only few investigations studied monocytes protein expression changes on a global protein level. Nevertheless, various studies examined changes of e.g. cell adhesion surface receptors and also of HLA molecules, like upregulated expression levels of ICAM-1 and decreased abundance of HLA-DR (Sosa-Bustamante et al. 2011, Zhao et al. 2014, Hynninen et al. 2003). These changes in protein expression were shown to be of clinical importance as they can be used as markers for tolerance or as drug targets interfering with sepsis pathology. Assessing the global

glycoproteome of tolerant human monocytes may contribute to a better understanding of the phenomenon “endotoxin tolerance” and, thus, could provide helpful information to develop new diagnostic strategies and immunmodulatory therapies.

3.3 PRRs and their ligands: PAMPS and alarmins

The initial sensing of infection and, thus, the induction of tolerance and cellular reprogramming is mediated by innate PRRs, which are highly conserved receptors including transmembrane proteins such as Toll-like receptors (TLRs) and C-type lectin receptors (CLRs) as well as cyotplasmic receptors such as Retinoic acid inducible gene (RIG)-I-like receptors (RLRs) and Nucleotide-oligomerizatian domain (NOD)-like receptors (NLRs) (reviewed in Takeuchi and Akira 2010). Besides the well studied tolerance induction mediated by the LPS-sensing TLR4, several other members of the PRR-family (e.g. TLR2) have been shown to be able to induce cellular reprogramming as reviewed by Buckley et al. (2006). The following chapter, therefore, summarizes key players of tolerance induction within the PRR-family.

3.4 The Toll-like receptor family and its ligands

Toll-like receptors (TLRs) were the first PRRs to be identified and are now among the most extensively studied germline encoded PRRs (Kawai and Akira 2011). So far, eleven members (TLR1-11) were described in the human system, each receptor displaying a distinct organ- and tissue-specific expression, cellular localization and ligand specifity. These type-1 transmembrane proteins play a key role in PAMP recognition and responses to invading pathogens initiating and coordinating the innate and adaptive immunity. TLRs are widely expressed in both, immune and non-immune cells. They are evolutionary highly conserved membrane-anchored proteins consisting of an ecto-, a transmembrane and a cytoplasmic domain. The leucin-rich extracellular domain of each TLR mediates the recognition of distinct PAMPs, which are broadly shared and conserved components derived from viruses, bacteria, mycobacteria, fungi and parasites including: lipoproteins (recognized by TLR1, TLR2, and TLR6) and lipopolysaccharide (LPS, recognized by TLR4) as well as components of the microbial cell wall, viral double-stranded (ds)/ single-stranded (ss) RNA (TLR3, TLR7 and TLR8),), flagellin (TLR5) and unmethylated CpG motifs (TLR9) (Akira et al. 2006). Whereas TLR1, TLR2, TLR4, TLR5 and TLR6 are localized on the cell surface for optimal detection of microbial membrane components, all nucleid acid sensing members of the TLR family (TLR3, TLR7, TLR8 and TLR9) are expressed within intracellular vesicles. Upon activation, the TLR proteins undergo homo- or heterodimeric oligomerization due to conformational changes induced by ligand binding. This allows the recruitment of a specific subset

of adaptor molecules (e.g. Myd88 and TRIF) to the cytoplasmic Toll-IL-1 receptor (TIR) domain with subsequent initiation of downstream signaling events resulting in the regulation of transcriptional activity and production of cytokines (e.g. TNF-α, IL-6), chemokines (e.g. IL-8), antimicrobial peptides. These mechanisms aim at the fast and efficient elimination of the infection-causing pathogens. As mentioned above, TLRs are not limited to the detection of PAMPs, but seem also capable to sense endogenous ligands of the host, so called alarmins, e.g. high mobility group box-1 (HMGB1, recognized by TLR2, TLR4 and RAGE) and S100A12 (recognized by TLR4 and RAGE). Thus, and in accordance to the already in 1994 postulated "danger model" from Polly Matzinger, PRRs, and TLRs in particular, seem to differentiate between "dangerous" (PAMPs and alarmins) and "non-dangerous" rather than between "self" and "non-self/foreign" (Matzinger 1994 and 2002, Kono and Rock 2008).

3.4.1 General aspects of LPS-mediated TLR4 activation in naïve and tolerant monocytes

TLR4 is able to sense LPS, a component of Gram-negative bacterial cell walls, although LPS alone cannot bind directly to TLR4 efficiently (Park et al. 2009). Thus, the co-receptor MD-2, a secretory, lipid binding glycoprotein is necessary in order to enhance the intrinsic affinity of TLR4 towards LPS. MD-2 contains a large hydrophobic pocket allowing the binding of the lipid A domain of LPS (Park et al. 2009). Nevertheless, LPS-binding protein (LBP) and the CD14 are additionally required for efficient transfer of LPS monomers to the TLR4:MD-2 dimeric complex (1:1 complex). Upon ligand recognition, the LPS:TLR4:MD-2 complex undergoes subsequent dimerization with a second TLR4:MD-2 heterodimer. Once activated, four adaptor proteins are recruited to the cytoplasmic domain of the TLR4-receptor complex resulting in the activation of two distinct pathways: the "MyD88-dependent" pathway, which is shared by all TLRs (except of TLR3), and the "TRIF-dependent" pathway (Fig. 2) (Kawai and Akira 2011). Both pathways are resulting in the activation of NF-κB and MAP kinases, but differ in their kinetics. Initially, MyD88 is recruited to the plasma membrane-bound TLR4 with the help of the adaptor protein TIRAP. Subsequent activation of IRAKs, TRAF6 and the TAK1 complex by MyD88 lead to an early phase activation of NF-κB and MAP kinases (reviewed in Kawai and Akira 2011). After endocytosis of TLR4 in bacteria containing phagosomes, internalized TLR4 forms complexes with TRAM and TRIF inducing signaling cascades that, on the one hand, lead to IRF3-dependent expression of type I IFN and, on the other hand, mediate late phase activation of NF-κB and MAP kinases (Kawai and Akira 2011). In tolerant cells, a variety of alterations in the TLR4-mediated intracellular signaling were observed affecting the expression of receptor-, adaptor-, signaling-molecules and transcription factors, representing a negative feedback loop at multiple levels (Fig. 2) (Bohannon

et al. 2013). So far, most of these alterations are mapped to the MyD88-dependent pathway, although this might be possibly due to lacking investigations of changes in the TRIF-dependent pathway (Biswas and Lopez-Collazo 2009). Changes in TLR4 signaling were associated with decreased TLR4-MyD88 complex formation and upregulated expression of several TLR4- and NF-κB-inhibitors such as IRAK-M, suppressor of cytokine signaling-1 (SOCS-1) and inhibitor of κB (IκB), thereby attenuating translocation and activation of NF-κB (reviewed by Bohannon et al. 2013, Biswas and Lopez-Collazo 2009). Together with the above mentioned epigenetic changes, this phenomenon is referred to as "cellular reprogramming" in the tolerant cell state.

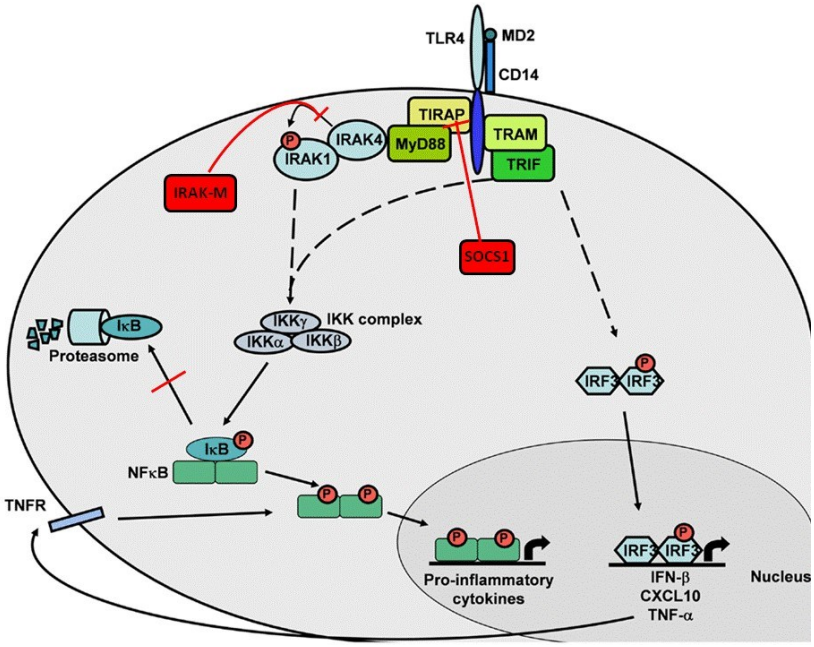

Fig. 2: Simplified model of the TLR4 intracellular signaling cas-cade and its negative regulation in endotoxin tolerance. Upon binding of LPS, the TLR4-receptor complex signals via two different pathways using either the adaptor protein MyD88 or TRIF. MYD88-dependent activation of IRAK4, IRAK1 and the IKK complex results in the activation and nuclear translocation of NFκB, which induces the transcription of a series of pro-inflammatory cytokines. TRIF-mediated activation of IRF3 induces IFN-inducible genes e.g. IFN-β and CXCL10. In tolerant monocytes, alterations in the downstream signaling cascades were especially found in the MyD88-dependent pathway, involving upregulated expression levels of inhibitors such as SOCS-1, IRAK-M and IκB. The figure represents a modified version of the scheme by Vaure et al. (2014).

3.4.2 Characteristics of LPS as a PAMP and TLR4 ligand

Lipopolysaccharides are major components of the outer membrane of Gram-negative bacteria, operating as membrane stabilizers and increasing the negative charge of the cell surface (Rietschel et al. 1996). Bacterial lipopolysaccharides share a common architecture, although biological activity is strongly influenced by structural details, which varies from one bacterium to another. LPS comprises three main parts: an inner lipid moiety, called lipid A, which is considered to be the endotoxic component, a glycosidic unit consisting of a core of approximately 10 monosaccharides and, in "smooth-type" lipopolysaccharides, a third region, named O-chain,

containing repetitive subunits of one to eight monosaccharides responsible for the immunospecificity of the bacterial cell (Caroff and Karibian 2003). Therefore, it can be distinguished between the predominantly expressed smooth (*S*-) LPS-chemotype and a rough (*R*-) LPS-chemotype. LPS can be released into the environment during each cell division and also by bacteria killed during phagocytosis, the complement system or antibiotic treatment. Once released, LPS molecules form micellar aggregates due to their amphiphilic character when critical micellar concentration is exceeded. The type of supramolecular aggregate plays also a crucial role of their potential to be recognized by TLR4 (reviewed Brandenburg et al. 2003). Moreover, *R*-LPS gains a considerably higher potential to activate the TLR4:MD-2 receptor complex than the smooth chemotype, hence, *S*-LPS requires CD-14 as a third co-receptor for efficient binding (Jiang et al. 2005). In addition, LPS-binding protein (LBP) can accelerate the transfer of LPS monomers to CD14 molecules, thereby enhancing, LPS mediated TLR4 activation (Yu and Wright 1996, Hailman et al. 1994).

3.4.3 S100A12 as alarmin and TLR4 ligand

Phagocyte-specific S100A12 (Calgranulin C) is a member of the calcium-binding, EF-handed S100-family, expressed by phagocytic myeloid cells, in particular by granulocytes and, to smaller amounts, by monocytes (Kessel et al. 2013). Clinical observations demonstrated highly increased serum levels of S100A12 correlating to disease activity in patients with sepsis and chronic inflammation, which emphasizes a putative role of extracellular S100A12 in the pro-inflammatory and chemotactic responses (Achouiti et al. 2013). Until recently, it was widely believed that these pro-inflammatory effects of S100A12 were mediated by the receptor for advanced glycation endproducts (RAGE). Now, data of the Foell group suggest a monocyte activation by S100A12 that is mediated via the TLR4 receptor complex rather than RAGE (Foell et al. 2013). Through binding to PRRs like TLR4 and RAGE, extracellular S100A12 can act as a prototypic alarmin, triggering the transcription of several pro-inflammatory cytokines and chemokines. Tolerance induction in monocytes by host-derived alarmins was already shown for HMGB1 that binds to TLR4, TLR2 and RAGE. Published data reveal that HMGB1-pretreated THP-1 cells become refractory to subsequent LPS- and LTA-challenges (Aneja et al. 2008, Robert et al. 2010). Therefore, similar to other TLR4 agonists, S100A12 might have the potential to induce tolerance and may contribute to the development of functionally immunosuppressed monocytes during the course of sepsis.

3.4.4 General aspects of TLR2 activation

TLR2 plays a central role in the recognition of a wide variety of lipoproteins and peptidoglycans (PGNs), found as bacterial cell wall components in both Gram-negative and Gram-positive bacteria, in viruses, fungi and parasites. TLR2 forms heterodimeric complexes with TLR1, TLR6 and several other cell surface molecules (such as Dectin and CD36) in order to discriminate between PAMP structures of Gram-positive bacteria (Akira et al. 2006). Both, stimulation of the TLR2/TLR1 receptor complex with Pam3CSK, a synthetic triacylated lipopeptide (LP) mimicing the acylated amino terminus of bacterial LP, as well as the exposure of TLR2/TLR6 heterodimers to mycoplasma-derived MALP2, a 2 kDa synthetic derivate of the macrophage-activating lipopeptide, induce the MyD88-mediated activation of NF-κB and the production of various pro-inflammatory cytokines (reviewed in Takeuchi and Akira 2010). Published data showed that TLR2-mediated inflammatory responses differ depending on the pathogen involved: TLR2-induced type I IFN-production in monocytes was observed when cells were stimulated with viruses, but not in the presence of bacteria (Barbalat et al. 2009).

There are conflicting data about TLR2 agonists inducing tolerance in macrophages and monocytic cell lines. Several studies demonstrated that TLR2 agonists can induce self- and cross-tolerance in monocytic cell lines and macrophages: Whereas Kreutz et al. (1997) demonstrated Pam3CSK to induce tolerance in human monocytes, the group of Dobrovolskaia (2003) observed pretreatment of murine macrophages with Pam3CSK not to be efficient in inducing tolerance to a subsequent LPS-challenge. Moreover, murine macrophages pretreated with MALP2 showed a subsequent hyporesponsiveness towards further MALP2- or LPS-stimulations, which is consistent with the cells entering a tolerant state after a first exposure to PAMPs (Sato et al. 2000).

3.5 Characterization of the NOD-like receptor (NLR) family

Among the wide repertoire of conserved PRRs, NLRs are a growing family of intracellular sentinels triggering pro-inflammatory and antimicrobial responses in the presence of e.g. bacterial peptidoglycan. The presence of NLRs across different species and the linkage of NLR mutations to a higher susceptibility of chronic inflammatory disorders (e.g. Cohn's disease), bacteremia and a worse outcome in sepsis patients highlights the essential role of NLRs in inflammatory processes (Caruso et al. 2014, Tekin et al. 2012).

3.5.1 General aspects of the NLR family

All members of the NLR family share a conserved, tripartite domain structure consisting of: an N-terminal protein–protein interaction domain required for signal transduction, a central NACHT (or NBD) domain facilitating self-oligomerization, and a C-terminal leucine-rich repeat (LRR) that is involved in ligand recognition but also acts as a repressor of NLR signaling in the absence of ligand stimulation by masking the N-terminal domain (reviewed in Barbe et al. 2014). Most of the diversity in this family is found in the variable N-terminal domain and, so far, five classes of mammalian NLRs are defined according to the type of oligomerization-inducing N-terminal domain: NLRA or Class II transactivator (CIITA) contains an acidic transactivation domain, NLRBs or neuronal apoptosis inhibitor proteins (NAIPs) have a baculovirus inhibitor of apoptosis protein (IAP) repeat (BIR), NLRCs possess a caspase-activation and recruitment domain (CARD), NLRPs a pyrin domain (PYD) and NLRX1 contains a CARD-related X effector domain of unknown function (Barbe et al. 2014). Additionally, NLRs can be classified according to their ability of inducing inflammasome activation, leading to recruitment and activation of caspase enzymes that initiate the activation of IL-1β and IL-18 (Li et al. 2014). As mentioned above, unlike TLRs, that sense their ligands at the cell surface or within endosomes, NLRs are cytoplasmic receptors forming another level of antimicrobial defense by surveying the intracellular environment.

3.5.2 Signaling of the NOD-like receptors NOD1 and NOD2

NOD1 (NLRC1, CARD4) and NOD2 (NLRC2, CARD15) are examples for CARD-domain containing and non-inflammasome forming NLRs and were first discovered in 1999 and 2001 (Bertin et al. 1999, Inohara et al. 1999, Ogura et al. 2001). Both receptors detect distinct sub-structures of internalized bacterial peptidoglycan (PGN): NOD2 that contains one additional CARD motif compared to NOD1 and that is almost exclusively expressed in antigen presenting cells, senses muramyl dipeptide (MDP, MurNAc-L-Ala-D-isoGln), the largest peptidoglycan

motif common in both Gram-negative and Gram-positive bacteria. Whereas NOD1 is predominantly expressed in epithelial cells and binds specifically to TriDAP (L-Ala-D-Glu-meso-DAP)-, TetraDAP (L-Ala-D-Glu-meso-DAP-D-Ala) and iE-DAP (γ -D-Glu-meso-DAP)-containing structures from Gram-negative bacteria, respectively.

Upon activation, NOD1 and NOD2 induce NF-κB- and MAP kinases-dependent inflammatory responses (Le Bourhis et al. 2007). An involvement of NOD2 in tolerance induction was shown in the intestinal mucosa by Hedl et al. (2007). In their study, pretreatment of primary human monocytes-derived macrophages with MDP led to a significant decrease in the production of pro-inflammatory cytokines like TNF-α, IL-1β and IL-8 upon restimulation with NOD2-, TLR4- and TLR2-agonists. Therefore, it would be interesting to analyze and compare if NLR ligands are able to induce tolerance in primary human monocytes and if the cellular reprogramming by cytoplasmic NLRs shows distinct alterations compared to tolerance induced by membrane-bound PRRs.

3.6 Receptor expression profile and glycoproteomics of human monocytes

So far, most studies that aim at the description of the tolerant phenotype of monocytes have been focusing on transcriptome analysis and cytokine expression analysis by performing whole transcriptome sequencing, qPCR and ELISAs, respectively. It was shown that monocytes purified from the peripheral blood of septic patients display similar alterations in the transcriptional regulation of pro- and anti-inflammatory cytokines and receptor proteins as endotoxin tolerant monocytes stimulated *in vitro*, thus, mimicking the effects of two consecutive bacterial infections (reviewed in Biswas and Lopez-Collazo 2009). This immune-compromised state is also accompanied by expression changes of several cell surface proteins (e.g. down-regulation of HLA-DR, CD86 and CIITA), but to date, no comprehensive characterization of the global monocyte cell surface protein repertoire (the surfaceome) in the tolerant state was performed. Moreover, the correlation between mRNA levels and protein abundance has been proven to be specifically low in relation to cell surface proteins due to the intrinsic half-live of membrane proteins (Bausch-Fluck et al. 2015). All classical approaches to investigate the abundance of cell surface receptors, like flow-cytometry, employ antibodies directed against known proteins and, therefore, are limited to a small subset of proteins. Due to the key role of cell surface proteins in mediating the cell's interaction with the surrounding environment (cell-cell/cell-matrix interactions, recognition of soluble factors) and transducing the manifoldness of signals into the cell, it is of particular interest to characterize the cell surface proteome as a whole. Current development of proteomic and glycoproteomic technologies allow to perform a global protein expression analysis and to detect quantitative changes. Thus, the value of this resource is exemplified by the identification of (1)

bio markers determining the fate or functional capability of monocytes/cells, (2) proteins and epitopes useful for immunophenotyping and (3) possible drug targets as recently shown for human pluripotent stem cells (hPSC) in a study by Boheler et al. (2014).

Approximately 97% of all membrane proteins, including most relevant receptors of the innate immunity (e.g. HLA-DR, TLRs, CLRs), are glycosylated and, therefore, accessible by using a method described by Zhang et al. (2003), which targets these glycostructures based on oxidation of carbohydrates and hydrazide chemistry for glycoprotein enrichment. Dr. M. Müller in the group of Prof. H. Slevogt established an enrichment protocol for the purification of membrane glycoproteins from whole cell lysates enabling us to identify and quantify these proteins in a global liquid chromatography–tandem mass spectrometry (LC-MS/MS) shot gun proteomic approach. Thus, it allows a unique description of the global cellular glycoproteome including cell surface plasma membrane associated receptors or intracellular component-derived glycoproteins. Glycoproteomic analysis of naïve and tolerant monocytes might reveal biomarkers for staging the patient's immunsystem and for deciding whether to initiate rather a pro- or anti-inflammatory therapy. Moreover, this study might provide possible targets for reversing sepsis-induced immunosuppression and, thereby, allowing important advances towards personalized medicine.

4. Hypothesis and objectives

Systemic infections like severe sepsis or septic shock are associated with a pronounced pro-inflammatory response contributing to organ failure. Subsequently, the immune response becomes deregulated and evolves into a state of immunoparalysis when immunosuppressive mediators dominate pro-inflammatory factors. This state of immunosuppression is associated with a high risk for secondary infections and high mortality of septic patients. Most of the current therapies aim at the blockage of pro-inflammatory signaling mediators to control the host response in sepsis, but show only little success to reduce the 28-day mortality of septic patients. Therefore, targeting the immunosuppressive cell state of immune cells might be an option to prevent the occurrence of secondary infections and to reduce mortality. Monocytes and macrophages are one of the first defense mechanisms against invading pathogens and functionally altered in immunoparalysis. Cellular reprogramming of monocytes is a major contributor to immunosuppression in the course of sepsis and has been shown to be evoked by bacterial cell wall components (PAMPs) like LPS but also by endogenous factors of the host (alarmins) like HMGB1. Thus, characterization of naïve and tolerant monocytes at the global glycoprotein level may help in the identification of new and better suited biomarkers, serving for a better understanding of monocytes functional behavior in septic conditions.

We propose the hypothesis that activation of monocytes with cell surface-associated TLR-ligands and intracellular located NLR-ligands causes pro-inflammatory responses, that, consecutively, result in the development of an immunosuppressed cell state. This immunosuppressed, tolerant cell state is accompanied by transcriptional changes, which also affects the expression of glycoprotein cell surface markers. These differential expressions can be identified and analyzed by glycoproteomics. Activation by different PAMPs, and in case of the TLR4 also by alarmins, may differ in their potency to induce a tolerant phenotype. Although, all stimuli used in the present study are known to be pro-inflammatory triggers inducing NF-κB activation and pro-inflammatory cytokine release in human monocytes, the usage of diverging secondary and tertiary signal transduction pathways may differentially affect the global glycoprotein expression. Therefore, receptor signatures might vary between PAMP- and alarmin-stimulated monocytes, but also between the different TLR agonists.

The primary aim of this study is to analyze and compare global alterations in the glycoproteome and inflammatory response of naïve and TLR4-ligand (LPS and S100A12), TLR2-ligand (Pam3CSK and MALP2) and NLR-ligand (iE-DAP and MDP)-stimulated human monocytes in the tolerant state. Pro-inflammatory responses of naïve and tolerized cells will be characterized

by cytokine expression analysis on transcriptional and protein level for each stimulus to adjust the initial activation levels. Glycoproteomics will be performed with highly purified monocyte preparations, enriched by sorting magnetically and fluorescently labelled cells (MACS and FACS), to discover monocyte activation markers associated with the tolerant state.

5. Materials and Methods

Unless indicated elsewhere, all chemicals were obtained from the following companies: Gibco (USA), Invitrogen (Germany), Pierce (USA), ROTH (Germany), Serva (Germany), Sigma-Aldrich (Germany).

5.1 Laboratory devices and expendable materials

Table 1: List of laboratory devices

Laboratory devices	**Company**
Automated cell counter Countess™	Invitrogen™, Darmstadt
Axio Vert.A1 Microscope	Carl Zeiss, Jena
Bio-Plex® 200 Systems Bio-Plex Manager™ software Bio-Plex Pro™ Wash Stations	Bio-Rad, Munich
CAS-1200 pipetting robot	Qiagen, Germany
Centrifuges: Type 5810 R (cooling function) Type 5804 R Type 5415 Type 5418 R (cooling function) Mini centrifuge D-6015 MiniSpin	Eppendorf, Hamburg neoLab, Heidelberg
Cell culture microscope Primo Vert	Carl Zeiss Microimaging GmbH, Jena
Corbett-Rotor Gene 6000	Qiagen, Germany
Flow cytometer Attune™ auto sampler	Applied Biosystems®, USA
Flow cytometer Aria II™	BD Biosciences, Heidelberg
Incubator Galaxy 170S	New Brunswick, Wesseling-Berzdorf
Incubator HERA Cell 150	Thermo Scientific, USA
Incubator Shaker Series I26	New Brunswick, Wesseling-Berzdorf
Laminar flow Maxisafe™ 2020	Thermo Scientific, USA
NanoDrop 1000 Spectrophotometer	Thermo Scientific, USA
Neubauer-improved counting chamber	Roth, Germany
4D-Nucleofector X-Unit 4D-Nucleofector Core Unit	Lonza Group , Switzerland
Magnetic heat stirrer VMS-C7 advanced®	VWR, Darmstadt
Multi-imaging system Fusion FX7™	PEQlab, Erlangen
PCR Thermal cyclers: MJ Mini Thermal Cycler S1000™ Thermal Cycler	Bio-Rad, Munich
pH meter S20-Seven Easy™	Mettler-Toledo AG, Gießen

Pipetboy	INTEGRA Biosciences, Fernwald
Pipettes, Research plus	Eppendorf, Hamburg
Plate reader Tecan infinite® M200	TECAN, Switzerland
Precision scale M-power	Satorius, Göttingen
Precision scale EWB 620-2M	KERN, Balingen
Shaker	VWR, USA
SpeedVac®SPD1010	Thermo Scientific, USA
Tank blot system Mini PROTEAN® II	Bio-Rad, Munich
Thermomixer compact	Eppendorf, Hamburg
Vortexer Vortex 1	IKA®, Staufen
Water bath TW20	Julabo, Seelbach

Table 2: List of expendable materials

Expendable materials	**Company**
Cover glasses	Thermo Fisher GmbH
ELISA: Human IL-6 ELISA Kit Human TNF alpha ELISA Kit	 BD Bioscience, Heidelberg Thermo Scientific, USA
High Capacity cDNA Reverse Transcription Kit	Thermo Scientific, USA
Kinetic Turbidimetric LAL Assay PYROGENT™–5000	Lonza Group AG, Switzerland
Microtiter plates, flat bottom : 6-, 12-, 48-, 96-well microtiter plates	Corning/Life Science, USA
Mini-Protean TGX Gels 4-15% 15well	Bio-Rad, Munich
Monocyte isolation kit II, human	Miltenyi Biotec, Germany
Plasmid preparation/Isolation kits: PureYield™ Plasmid Midiprep System QIAGEN Plasmid Maxi Kit	 Promega, USA Qiagen, Germany
Renilla Luciferase Assay System	Promega, USA
Luciferase Reporter Gene Assay, high sensitiyity	Roche Diagnostics GmbH, Switzerland
Transfection kits: GeneCellin™ Transfection Reagent Lipofectamine® 2000 Transfection Reagent P3 primary cell 4d-nucleofector X kit SG Cell Line 4D-Nucleofector® X Kit L	 BioCell Challenge, France Invitrogen/ Life Technologies, USA Lonza Group AG, Switzerland

5.2 TLR agonists and recombinant proteins

Table 3: List of used PRR agonists

Agonist	Species	Receptor	Company
LPS (Lipopolysaccharide)	*Salmonella enterica minnesota R595*	TLR4	Invivogen, USA
	Escherichia coli O111:B4		Sigma-Aldrich, USA
MALP2 (macrophage-activating lipopeptide-2)	*Mycoplasma fermentas*	TLR2/6	Enzo Life Sciences, USA
Pam3CSK (Pam3CysSerLys4)	Synthetic compound	TLR2/1	Invivogen, USA
S100A12: Recombinant Human EN-RAGE/S100A12	*Escherichia coli*	TLR4 (RAGE)	R&D Systems, UK
Human S100A12 / CAGC / Calgranulin-C Protein	*Escherichia coli*		Sino Biological, China
Human EN-RAGE/S100A12	*Human Granulocytes*		Research group of Prof. Dr. med. Dirk Foell
Human recombinant TNF-α			R&D Systems, UK
Human recombinant LPS-binding protein (LBP)			R&D Systems, UK
Peptide-N-glycosidase F (PNGaseF)			Sigma-Aldrich, USA
Trypsin			Thermo Scientific, USA

5.3 Primers used for semi-quantitative and real-time PCR studies

Table 4: Primer list

Gene	Primer pairs	Product length (bp)
CD14	forw. 5`-GCAGCCGAAGAGTTCACAAG-3` rev. 5`-ATCGTCCAGCTCACAAGGTT-3`	206
DPEP2	forw. 5`-AAGGGCGTCCACTCCTTCTA -3` rev. 5`-ACAGCATCTGAGACATGGGA -3`	119
GPR84	forw. 5`-TGATCTCCTCTACTGCACGC -3` rev. 5`-AAGGAGGAGCCCAAATACCC-3`	106
HPRT1	forw.5`-GACCAGTCAACAGGGGACAT-3` rev. 5`-AACACTTCGTGGGGTCCTTTTC-3`	195
IL-1β	forw.5`-AGGAAGATGCTGGTTCCCTG-3` rev. 5`-GCATCGACATAAGCCTC-3`	128
IL-6	forw. 5`-GAGGAGACTTGCCTGGTGAA-3` rev. 5`-TGGGTCAGGGGTGGTTATTG-3`	186
IL-10	forw. 5`-GCTGAGAACCAAGACCCAGA-3` rev. 5`-GCATTCTTCACCTGCTCCAC-3`	143
ITGB8	forw. 5`-GTCCAGAATGTGGATGGTGTG -3` rev. 5`-ACTGAGCAGCCTTTGCTTATTAAA -3`	103
LAMP3	forw. 5`-AGTGGGAGCCTATTTGACCG -3` rev. 5`-TGGAGGCTCTGTTCACTCAC -3`	123
LY96	forw. 5`-GCTCTGAAGGGAGAGACTGT-3` rev. 5`-GAGCATTTCTTCTGGGCTCC-3`	120
MMP9	forw. 5`-CAACTACGACACCGACGACC-3` rev. 5`-TGGCCTTGGAAGATGAATGGA-3`	111
NOD1	forw. 5`-GCCTTTGATGGCAAGAGGTG-3` rev. 5`-GCGCAGCCCCTTTTTAAGTTT-3`	204
NOD2	forw. 5`-AGGCAACACCTCCTTGCAGT-3` rev. 5`-CATGACGTTCTTTGCCAGCATC-3`	181
PPIB	forw. 5`-ATGTAGGCCGGGTGATCTTT-3` rev. 5`-TGAAGTTCTCATCGGGGAAG-3`	219
RAGE	forw. 5`-GACCAGGAGACACCCTGAGA-3` rev. 5`- CTGGGCTGAAGCTACAGGAG-3`	110
TLR1	forw. 5`-CAGGCCCTCTTCCTCGTTAG-3` rev. 5`-TGGCAAAATGGAAGATGCTAGT-3`	157
TLR2	forw. 5`-TGCATTCCCAAGACACTGGA-3` rev. 5`-AGGGAGGCATCTGGTAGAGT-3`	131
TLR4	forw. 5`-CAACCTCCCCTTCTCAACCA-3` rev. 5`-CTGGATGGGGTTTCCTGTCA-3`	196
TLR6	forw. 5`-GCCCTGGTATCTCAGGATGG-3` rev. 5`-TCACTTTTCACCCAGGCAGA-3`	144
TNF-α	forw.5`-TTCTCCTTCCTGATCGTGGC-3` rev. 5`-ACTCGGGGTTCGAGAAGATG-3`	150

5.4 List of antibodies for flow cytometry and western blot

Table 5: Primary antibodies

Antigen (all human)	Epitope specifity	Host/isotype/ clone	Format/ Conjugate	Applied concentration		Company
				FACS	WB	
anti-CD14	mono-clonal	Mouse/ IgG1,κ / 61D3	FITC	0.5 µg/50 µl		eBioscience, USA
anti-CD3	mono-clonal	Mouse/ IgG1,κ / MOPC-21	PE	1:50 all		BD Bioscience, Germany
anti-CD19	mono-clonal	Mouse/ IgG1,κ / HIB19	PE			BD Bioscience, Germany
anti-CD42b (GPIbα)	mono-clonal	Mouse/ IgG1 / HIP1	PE			Immuno Tools, Germany
anti-CD54 (ICAM-1)	mono-clonal	Mouse/ IgG2b / 1H4	APC			Immuno Tools, Germany
anti-CD80	mono-clonal	Mouse/ IgG_1,κ / 2D10	PE			Miltenyi Biotec, Germany
anti-CD86	mono-clonal	Mouse/ IgG1,κ / FUN-1	PerCP-Cy™5.5			eBioscience, USA
anti-CD127 (IL7R)	mono-clonal	Mouse/ IgG_1,κ / eBioRDR5	APC			eBioscience, USA
anti-CD274 (PD-L1)	mono-clonal	Mouse/ IgG_1,κ / MIH1	APC			eBioscience, USA
anti-CD319 (SLAMF7)	mono-clonal	Mouse/ IgG2a,κ / RUO	Alexa Fluor® 647			BD Bioscience, Germany
anti-CD371 (CLEC12A)	mono-clonal	Mouse/ IgG_1,κ / HB3	PE			eBioscience, USA
anti-CEACAM6 (1H4-4B)	mono-clonal	Mouse			1:2000	Merck Millipore, Germany
anti-PECAM-1 (M-200)	polyclonal	Rabbit			1:2.500	Santa Cruz, USA
anti-TLR4 (H80)	polyclonal	Rabbit			1:1000	Santa Cruz, USA

Table 6: Secondary antibodies used in Western Blot (WB) analysis

Antigen	Epitope specifity	Host	Applied concentration	Company
anti-mouse IgG	polyclonal	goat, peroxidase	40 ng/ml	Jackson ImmunoResearch, USA
anti-rabbit IgG	polyclonal	goat, peroxidase	1:5000	Jackson ImmunoResearch, USA

5.5 Cell culture methods

5.5.1 Conditions of eukaryotic cell cultivation

All human cell lines were cultured at 37°C in a humidified atmosphere containing 5% CO_2, ensuring sterile conditions by using sterile materials and by working under a laminar flow hood.

Cells were counted either using a Neubauer-improved counting chamber or with assistance of the automated cell counter Countess™ from Invitrogen™ (Germany). In this context cell viability was determined via the trypan blue exclusion assay.

5.5.2 THP-1 cells (ATCC®-TIB-202™, USA)

THP-1 is a human monocytic leukemic cell line and was first described by Tsuchiya et al. in 1980 and was derived from the peripheral blood of a 1-year old male patient suffering from acute monocytic leukemia.

THP-1 cells were maintained in RPMI 1640 supplemented with 10% heat inactivated fetal bovine serum (FBS), 50 U/ml penicillin and 50 µg/ml streptomycin. They were passaged every 2-3 days. After 3-5 min centrifugation at 150x g, the cell pellet was resuspended in fresh RPMI medium and afterwards diluted in order to adjust a cell density of $2\text{-}3*10^5$ cells/ml.

5.5.3 HEK-Blue™-hTLR4 cells (Invivogen, USA)

The HEK-Blue™-hTLR4 cell line is a genetically modified human embryonic kidney 293 (HEK293) cell line, stably co-expressing all components of the TLR4 receptor complex (TLR4, MD2 and CD14) and an NF-κB-inducible SEAP (secreted embryonic alkaline phosphatase) reporter gene. With this cell line it is possible to detect TLR4 agonists that are activating the NF-κB downstream signaling pathway by measuring the amount of SEAP. In the presence of a TLR4 agonist, NF-κB will translocate into the nucleus, where it then specifically binds to the promoter region of the SEAP reporter gene. The expression of SEAP directly correlates with the activation and nuclear translocation of NF-κB.

HEK-Blue™-hTLR4 cells were grown in 75 cm^2 cell culture flask in DMEM-medium containing 10% heat-inactivated fetal calf serum and 1% Penicillin/Streptomycin (P/S) and, thereafter, incubated in 5% CO_2 at 37°C. When reaching confluency at about 80-90%, cells were passaged (all 3-4 days), using Trypsin/EDTA solution (0.025% and 0.01% in DPBS, respectively) for detachment.

5.5.4 Cell freezing and thawing

Cell pellets (3-5*10^6 cells) were resuspended in 1 ml medium containing 10% DMSO and 20% FCS, and added into a cryotube. Cells were first frozen overnight in an iso-propanol freezing box at -80°C, following long-term storage in liquid nitrogen. Thawed cells were immediately transferred in 5 ml pre-warmed medium, centrifuged and resuspended in fresh medium supplemented with 20% FCS. Cells were further cultivated in medium containing 10% FCS in cell culture flasks.

5.5.5 Isolation of human peripheral blood monocytes

Human monocytes were isolated from buffy coats, obtained from healthy male donors of the Institute for Transfusion Medicine in Jena (Jena University Hospital, Germany).

50 ml Leucosep™ falcon tubes (Greiner Bio-One, Germany) were prefilled with 15 ml Ficoll solution (Ficoll-Paque™ Premium, GE Healthcare, UK) and shortly centrifuged at 1000x g to place Ficoll medium below the separation membrane. After mixing the buffy coat with DPBS (1:1), 20 ml of the diluted cell suspension was transferred into each Leucosep™ falcon tube. The following gradient density centrifugation (800x g, 15 min., without brake) led to the separation of the cell suspension into several distinguishable fractions. Beginning with lowest fraction, these were: a) cell fraction 1 (erythrocytes, granulocytes), b) ficoll reagent, c) cell fraction 2 (PBMCs), d) plasma.

PBMCs were carefully removed using a Pasteur pipette and collected into a new 50 ml falcon tube, placed on ice. Repeated washing steps aimed at the removal of contaminants (erythrocytes, thrombocytes, granulocytes) from the PBMC isolate. After diluting PBMCs in ice-cold 0.45% sodium chloride (w/v)) solution and centrifugation (300x g, 4°C, 10 min), cells were resuspended in 5 ml ammonium-chloride-potassium (ACK) lysing buffer (Gibco®, USA). The co-incubation of hypotonic ACK lysing buffer for 5 min at 4°C resulted in the bursting of remaining erythrocytes. Depending on the amount of remaining erythrocytes, this step was repeated. PBMCs were washed three times with cooled DPBS, intermitted by centrifugation (250x g, 4°C, 10 min). Cell number and purity was assessed using the Neubauer improved chamber for microscopy.

Monocytes, which represent 5-10% of the whole peripheral blood leucocytes, were isolated from the collected PBMCs via MACS® monocytes isolation kit II (Miltenyi Biotec, USA). Fc receptors (FcRs) were blocked with FcR blocking reagent and, to separate them from other mononuclear cells (T and B lymphocytes, dendritic cells, NK cells), PBMCs were incubated (15 min., 4°C) with a biotinylated antibody cocktail, specific for surface markers (CD3, CD7, CD16, CD19, CD56,

CD123 and Glycophorin A) of non-monocytes. Anti-biotin MicroBeads, as secondary labeling reagent, were added. The cell suspension was poured onto the columns of the MACS separator after another incubation period of 20 min at 4°C. Magnetically labeled non-monocytic cells were bound in the magnetic field of the MACS separator, while the flowthrough was collected containing the purified monocyte fraction (negative selection). During the labeling procedure a buffer consisting of cooled DPBS supplemented with 2 mM EDTA and 2% FCS was used to prevent cell agglutination. Purified monocytes were counted with the Neubauer-improved chamber, centrifuged (300x g, 10 min) and resuspended in RPMI 1640 with 20% heat-inactivated human serum.

5.5.6 Purity of monocytes for glycoproteomic analysis (MACS and FACS)

MACS-sorted monocytes that were left untreated or stimulated with either LPS (50 ng/ml), Pam3CSK4 (200 ng/ml) or MALP2 (10 ng/ml) for 24 h or 48 h, were labeled with an anti-CD14 antibody and sorted again using fluorescence activated cell sorting (FACS analysis). To deplete platelets (anti-CD42b) and lymphocytes (anti-CD3 against T-lymphocytes and anti-CD19 against B-lymphocytes), they were stained and separated from CD14 positive cells in order to enrich the monocytic population.

5.5.7 Cell stimulations

5.5.7.1 Kinetic studies of TNF alpha gene expression

THP-1 cells ($2*10^6$/ml cells in 1.5 ml RPMI + 10% FCS) and human monocytes ($8*10^6$ cells in 2 ml RPMI + 10%FCS) were cultivated in 12- and 6-well plates and stimulated for 1, 2, 3 and 4 h at 37°C with or without LPS *E. coli* O111:B4 (20 ng/ml). Cell lysates were prepared for RNA isolation. Transcriptional regulation of TNF-α expression was examined in qPCR analysis using gene-specific primers.

5.5.7.2 Adjusting the concentrations of the stimuli used

Human monocytes ($2*10^6$ cells in 0.5 ml RPMI supplemented with 20% human serum) were seeded in 24-well-plate and treated with one of the following stimuli: LPS *E. coli* O111:B4, Pam3CSK, MALP2 for 24 hours at 37°C. Supernatants were transferred into new tubes and detrital material removed by several steps of centrifugation. All samples were performed as triplicates. Untreated monocytes, as negative control, were always included.

5.5.7.2 Induction of endotoxin tolerance in human monocytes

Human monocytes (2 ml of $4*10^6$cells/ml for qPCR-analysis and $2*10^6$ cells in 500 µl for ELISA) were cultured in 6- or 24-well-plates at 37°C. Cells were prestimulated with one of the following stimuli: LPS *E. coli* O111:B4 (50 ng/ml), S100A12 (10 µg/ml), Pam3CSK4 (100 ng/ml or 200 ng/ml), MALP2 (10 ng/ml), iE-DAP (1 µg/ml) or MDP (10 µg/ml) for 20 h and 24 h, always including untreated cells as negative control. Pretreated monocytes were either re-stimulated or left untreated. Further, adherent cells were washed in the wells, while non-adherent cells were transferred into new tubes and washed three times with fresh RPMI (+ 20% heat-inactivated human serum) before restimulation (LPS *E. coli* O111:B4 (50 ng/ml), S100A12 (10 µg/ml)) for 1 h in case of further qPCR-analysis and for 16 h when supernatants were analyzed by ELISA.

For qPCR analysis cell lysates were prepared to isolate RNA and to examine the cytokine mRNA expression. Supernatants of the 24 h prestimulated and of the additionally 16 h restimu-lated monocytes were collected and frozen at -20°C.

5.5.7.3 Stimulation of human monocytes for mass spectrometry analysis

Human monocytes ($1*10^7$ cells in 2 ml RPMI + 20% heat inactivated human serum) were stimulated with either LPS *E. coli* O111:B4 (50 ng/ml), Pam3CSK4 (200 ng/ml) or MALP2 (10 ng/ml) for 24 h and 48 h. Un-stimulated cells as negative control were included for each time point. Before performing further sample preparation for mass spectrometry analysis, the already MACS-sorted and stimulated monocytes were purified again via fluorescence-activated cell sorting (Chapter 6.5).

5.6 Methods in molecular biology

5.6.1 Cell lysis and RNA extraction

Depending on cell type and experimental setting, different cell concentrations ($1*10^6$ – $1*10^7$) were washed once with DBPS before the corresponding amount of lysis buffer (about $1*10^6$ cells/ 200 µl lysis buffer) was added.

RNA isolation from eukaryotic cells was performed according to the manufacturer's protocol (RNeasy® Mini Kit, Qiagen). Briefly, RNA was precipitated and bound to a silica membrane providing high salt conditions. DNA, proteins, guanidinium thiocyanate and other contaminants were removed by several washing steps, including a DNase digestion step. Samples were eluted by centrifugation and solved in 40 µl RNase-free H2O. RNA was stored at -20°C or -80°C.

5.6.2 Determination of RNA concentration and purity

Concentration (in ng/µl) and purity of the obtained RNA were examined using the spectrophotometer NanoDrop 1000. Since nucleic acids absorb at 260 nm, their concentration can be calculated by making use of the Lambert-Beer law. Contaminations may limit down-stream application and thus, information about the RNA purity is required. Detrimental contaminants, like proteins and guanidinium thiocyanate have their maximum absorbance at 280 and 230 nm, respectively purity is assessed by estimating the 260/280 and 260/230 ratios.

Pure RNA: 260/280 OD ratio: 1.8 – 2.2
260/230 OD ratio: 2.0

5.6.3 Reverse transcription (RT) of RNA into cDNA

Retroviral RNA-dependent DNA polymerases, so-called reverse transcriptases, generate complementary DNA templates from RNA. Two micrograms of THP1-RNA and one-point-five micrograms of monocytic RNA were reverse transcribed to cDNA for each sample and experiment. The synthesized cDNA was resuspended in 0.5 M Tris/EDTA buffer in a ratio of 1:10 for a final volume of 200 µl. Mix composition and program of the thermocycler used for cDNA synthesis are listed in more detail table 7 and table 8.

Table 7: Mix composition using the *High Capacity cDNA Reverse Transcription Kit (Thermo Scien., USA)*

Reagents	Volume (µl)
Buffer (10x)	2
dNTPs (25x, 100 mM)	0,8
Random primers (10x)	2
RNase Inhibitor	1
Reverse Transcriptase (50 U/µl)	1
RNA (sample)	Corresponding to 2 µg (THP-1), 1.5 µg (monocytes)
Nuclease-free H_2O	Up to total vol. 20 µl

Table 8: Program of the thermo cycler used for cDNA synthesis

Step in synthesis	Thermal cycler condition	
	[°C]	[min]
Primer annealing	25	10
Reverse transcription	37	120
Enzyme inactivation	85	5
Storage	4	∞

5.6.4 Primer Design

The synthesis of the complementary strand through the DNA polymerase requires the binding of a short oligonucleotide sequence (primer) to the template DNA. Thus, primers have to be orientated in sense and antisense direction, corresponding to their binding at 3` and 5` end on the DNA strand, respectively, for the duplication of one DNA molecule. Primer pairs were designed utilizing the genome browser Ensembl and the primer designing software Primer-Blast. All primers used in this study are listed in table 4.

Primer specificity was ensured considering the following aspects in primer design: (1) primer sequence length: 15-25 bp, (2) G/C content: 40-60%, (3) no matching properties to other homologue sequences. To maximize amplification efficiency, the formation of secondary structures during primer annealing was most widely avoided by controlling the folding structure with the mfold Web Server. The primer melting temperature was always set to about 60°C. In addition, the binding sites of all primers were placed at exon:exon boundaries of the target gene. This prevents the co-amplification of possible genomic DNA contaminants which would, otherwise, strongly limit gene expression studies.

5.6.5 Polymerase chain reaction (PCR)

Expression levels of TLR1, TLR2, TLR6 as well as the TLR4, MD-2, CD14 and NOD1 and NOD2 were measured by PCR analysis in unstimulated monocytes. Complementary DNA was amplified using the PCR amplification kit Perfect Taq Plus DNA Polymerase (5PRIME, Germany). Each PCR reaction was set up to a final volume of 20 µl containing 1x Perfect Taq Plus buffer, 1x

PerfectLoad Dye concentrate, 0.2 mM of each dNTP, Perfect Taq Plus DNA polymerase (1.25 U), 0.2 µM of each primer and 5 µl cDNA (ca. 30 ng/ml). The PCR cycler conditions are depicted in table 9. The Taq polymerase used herein has a 5`-3` exonuclease activity. The kit is based on the hot-start/cold-stop technology, in which a thermostable inhibitor competitively blocks the DNA polymerase at temperatures below 40°C in order to prevent nonspecific product amplification.

Table 9: PCR cycler conditions running on sqPCR

Step in amplification	[°C]	Time [min.]	
Initialization	94	2:00	
Denaturation	94	0:30	35 cycles
Primer annealing	60	0:30	
Elongation	72	0:20	
Final extension	72	2:00	
Final hold	10	∞	

5.6.6 PCR product analysis using agarose gel electrophoresis

The separation of nucleic acid sequences according to their molecular mass can be achieved with agarose gel electrophoresis. A 3% agarose gel was loaded with the PCR products already containing 1x loading dye. Agarose was diluted in Tris-acetate-EDTA (TAE) buffer by heating and ethidium bromide, that visualizes DNA through intercalation, was added during cooling (Table 10). The gel was run for 1.5 h at a voltage of 130 V. Images were taken using the Multi-imaging system Fusion FX7™ device. The amplicon size was estimated with a Low Range DNA Ladder (50 bp - 1 kb) (Jena Bioscience GmbH).

Table 10: Contents of agarose gel

TAE buffer:	0,04 M Tris-HCl, pH 8,5
	0,1% acetic acid
	2 mM EDTA
Agarose gel:	3% agarose in TAE buffer
	0,4 mg/ml ethidium bromide (Sigma-Aldrich)
	1 x loading dye

5.6.7 Gene expression analysis with real-time PCR (qPCR)

Real-time PCR was used for quantitative analysis of gene transcription. This method is based on visualizing the amplification of a targeted gene during PCR reaction cycles by an intercalating fluorescent dye (e.g., SYBR green). The PCR cycle at which the fluorescence signal raises above a defined threshold (Ct), and which is commonly placed slightly above the background fluorescence, enables the estimation of relative fold changes of potential genes. qPCR samples

were pipetted using the CAS-1200 pipetting robot (Qiagen). The PCR reaction volume was set to 20 µl containing 1x SensiMix SYBR No-Rox (Bioline), 0.2 µM of each primer and 4 µl of cDNA. Each sample was analyzed in duplicate on the Corbett-Rotor Gene 6000 (Qiagen). PCR cycling conditions were adjusted with an initial denaturation step at 95°C for 10 min followed by 40 cycles at 95°C for 15 sec, 60°C for 20 sec and 72°C for 20 sec. For each experiment, a RT-negative sample was included, adding water instead of SensiMix. The specificity of the PCR reaction was verified by melting curve analysis. The relative gene expression was calculated according to the efficiency correction method developed by Pfaffl (2001). The Ct-values of the target genes were normalized to housekeeping genes, whereby either PPIB (peptidylpropyl isomerase B) and/or HPRT1 (hypoxanthine phosphoribosyl-transferase 1) was used. Primer efficiency of all genes was tested beforehand by using a cDNA standard curve for each primer pair. The efficiency was calculated according to the equation m = -(1/log E), whereas m represents the slope of the calibration curve and E, the efficiency. An optimal efficiency in the exponential phase is achieved, when E = 2 (= one duplication/cycle). The stable expression of the housekeeping genes during different treatment conditions was clarified using the BestKeeper algorithm (Pfaffl et al. 2004).

5.6.8 Cultivation of Escherichia coli

E. coli were grown in LB medium with or without ampicillin (50 µg/ml). Bacterial cultures were incubated at 37°C either on agar plates (1.5% agar in LB medium) or in liquid LB-medium in shaking flasks at 220 rpm. Single colonies picked from petri dishes were used for the sterile inoculation of cultures. Ingredients of LB medium are listed in table 11.

Table 11: LB medium

10 g/l peptone
5 g/l yeast extract
10 g/l NaCl
LB-plates: adjustment of the ph value to 7 and adding 15 g/l agar.

5.6.9 Establishing of competent bacteria

Bacteria were made competent to incorporate plasmids and foreign DNA when treated with CaCl2. Therefore, 100 ml LB medium were inoculated with 1 ml of an overnight culture and grown to a density of 0.2 OD600. After 10 minutes of incubation on ice, cells were pelleted via centrifugation (6.000 rpm, 10 min, 4°C). While the supernatant was discarded, the bacterial pellet was resuspended in 20 ml of 100 mM ice-cold CaCl2 solution and incubated for another 30 min on ice. Cells were centrifuged again and resuspended in 500 µl ice-cold CaCl2 solution. E. coli cells were frozen at -80°C or immediately used for transformation.

5.6.10 Plasmid preparation and isolation

Plasmid preparation and isolation was performed according to the manufacturers' protocols using two different standard kits. In both cases, a single colony of transformed E. coli was grown overnight in 50 ml LB medium containing 50 µg/ml ampicillin at 37°C.

5.6.10.1 Plasmid preparation with PureYield™ Plasmid Midiprep Systems (Promega, USA)

Bacterial cells were harvested by centrifugation (5.000x g, 10 min) and the pellet resuspended in Cell Resuspension Solution. After adding and incubating bacterial cells with the provided Cell Lysis Solution, the reaction was stopped using Neutralization Solution and the cell lysate was centrifuged (15.000x g, 15 min). The supernatant was poured onto a Pure Yield™ Clearing Column, placed above a Pure Yield™ Binding Column to remove remaining debris. Bound plasmid DNA was washed by an endotoxin Removal Wash step. After further washing, plasmid-DNA was eluted by elution buffer and centrifugation (2000x g for 5 min). In a last step, quantity and purity of the purified plasmid DNA were measured using the NanoDrop 1000 Spectrophotometer (ThermoScientific, USA). Purified plasmid DNA was stored at -20°C. Vectors are listed in table 12.

Table 12: Purified plasmids

pGL4.32 [*luc*2P/NF-κB-RE/Hygro] Vector
pGL4.74 [*hRluc*/TK] Vector

5.6.11 Ethanol precipitation of DNA

Ethanol precipitation is a method used for the purification and concentration of DNA and RNA. Due to the highly negative charged phosphate backbone, DNA precipitates when mixed with less polar substances, e.g. pure ethanol. To 1 volume of DNA, 1/10 volume of 3 M sodium acetate (pH 5.2, final concentration of 0.3 M) was added in order to adjust the correct concentration of positive ions and to ensure complete recovery of the DNA. After adding 2 volumes of 95% ethanol, all contents were thoroughly mixed and incubated at -20°C for at least 30 minutes (or overnight). Precipitated DNA was centrifuged (13.000 rpm, 15 min, 0°C) and the supernatant carefully discarded. The DNA pellet was washed with 70% ethanol to remove residual salts. Finally, the DNA pellet was air-dried and afterwards redissolved in the appropriate amount of water or Tris-EDTA (TE) buffer (table 13). Purity and concentration of the DNA was measured with NanoDrop 1000 Spectrophotometer (Thermo Scientific, USA).

Table 13: TE buffer
95% Ethanol
3 M Sodium acetate ($C_2H_3NaO_2$)
10 mM Tris, pH 8.0
1 mM EDTA

5.6.12 Transfection of cells

5.6.12.1 Transfection with GeneCellin™ Transfection Reagent

The GeneCellin™ Transfection Reagent is polymer-based and, together with plasmid DNA, it builds nanoparticles that can be endocytosed by eukaryotic cells. 1.5 µg of the previously isolated plasmid DNA was diluted in 100 µl cell culture medium (pure RPMI medium), before adding 6 µl of the GeneCellin™ Transfection Reagent. This solution was shortly vortexed and then incubated for 15 min at RT. The GeneCellin™/DNA mixture was added dropwise onto $1*10^6$ cells that were seeded in 1.5 ml cell culture medium (RPMI medium supplemented with 10% FCS) in a 12-well tissue plate. After 24 h of incubation at 37°C in a CO_2- incubator, gene expression of target cells was analyzed by measuring luminescence with the help of Plate reader Tecan infinite® M200 (TECAN, Switzerland).

5.6.12.2 Transfection with Lipofectamine® 2000 Transfection Reagent

This chemical-based transfection method uses the stable formulation of liposomes, consisting of cationic lipids, which aggregate with the negatively charged DNA. The thereby formed vesicles with positively charged surface are able to fuse with the negatively charged cell membrane allowing the plasmids to enter the cell.

Cells were transfected according to the manufacturer's protocol. In short: Appropriate dilutions of the plasmid DNA (1.5 µg) in Opti-MEM® Medium (50 µl) and of Lipofectamine® 2000 Transfection Reagent (7.5 µl) in Opti-MEM® Medium (42.5 µl) were made. After 5 min of incubation at RT, the diluted DNA was combined with the diluted Lipofectamine® 2000 Reagent and incubated for another 20 min at RT. Then, 100 µl of the formed complexes was added dropwise to $1*10^6$ cells in 1.5 ml RPMI medium supplemented with 10% FCS. Medium was replaced after 4 h and gene expression was analyzed after 24 h of incubation at 37°C with the luminometer.

5.6.12.3 Transfection via electroporation

THP-1 cells and human monocytes were washed once in serum-free cell culture medium and counted (required number of cells: $1*10^6$ THP-1 cells, $5*10^6$ monocytes per sample). Mean-while, pmaxGFP vector as a provided positive control vector, as well as other plasmids were diluted in

100 µl Nucleofector™ Solution. After centrifugation and complete removal of the supernatant, cells were carefully resuspended in the DNA/Nucleofector solution and transferred to the bottom of the Nucleovette™ Vessels. Electroporation was carried out using the 4D-Nucleofector X-Unit (Lonza Group AG, Switzerland) (Table 14). For recovery of the stressed cells, 1 ml cell culture medium (RPMI 1640) containing 20% FCS or human serum was directly added to the cells in the cuvette and cells incubated for 2 h at 37°C. Then, cells were transferred into a 12-well cell culture plate and incubated for 24 h at 37°C before gene expression was analyzed via luminometer. Cells that were transfected with the NF-κB-containing plasmid pGL4.32 [luc2P/NF-κB-RE/Hygro] Vector were incubated again for 24 h with or without one of the following stimuli: LPS *E. coli* O111:B4 (100 ng/ml), Pam3CSK (200 ng/ml), MALP2 (10 ng/ml) or S100A12 (0,5 µg/ml). Transfection efficiency was calculated as percentage of transfected cells from all cells. Images were taken on a Zeiss Axio Vert.A1 fluorescent microsope using the filter set 38 for fluorescein isothiocyanate (FITC) (excitation: BP 470/40, beamsplitter: FT 495, emission: BP 525/50) at 20x magnification.

Table 14: Transfection conditions and kits

Monocytes:

Kit	P3 primary cell 4d-nucleofector X kit, Lonza Group AG, Switzerland	
Cell number	$5*10^6$	
Plasmids	Vector	Used amount
Positive control	pmax GFP™	2 µg
	pGL4.74 [*hRluc*/TK]	2,5 µg
	pGL4.32 [*luc*2P/NF-κB-RE/Hygro]	2,5 µg

THP-1 cells:

Kit	SG Cell Line 4D-Nucleofector® X Kit L, Lonza Group AG, Switzerland	
Cell number	$1*10^6$	
Plasmids	Vector	Used amount
Positive control	pmax GFP™	0,5 µg
	pGL4.74 [*hRluc*/TK]	0,5 µg
	pGL4.32 [*luc*2P/NF-κB-RE/Hygro]	0,5 µg

5.6.13 Luminescence measurement

Luminescence measurement was used to control the transfection efficiency of plasmid pGL4.74 [hRluc/TK], constitutively expressing a luciferase, and to adjust the concentrations of PAMPs in correlation to their pro-inflammatory response, using cells transfected with plasmid pGL4.32 [*luc*2P/NF-κB-RE/Hygro], expressing luciferase after a NF-κB promoter construct.

5.6. 13.1 Luminescence measurement with the Renilla Luciferase Assay System

The Renilla Luciferase Assay System (Promega, USA) was used to examine the transfection efficiency by measuring the expression of the constitutively expressed Renilla luciferase-gene encoded on plasmid pGL4.74 [hRluc/TK].

Transfected THP-1 cells ($1*10^6$ cells per sample) and human monocytes ($5*10^6$ cells per sample) were transferred from a 12-well cell culture plate into 1.5 ml tubes after 24 h of incubation (37°C, 5% CO_2) and were washed once with DPBS. After centrifugation and complete decantation of the supernatant, 30 µl of 1/5 diluted Renilla Luciferase Assay Lysis Buffer (in distilled water) were added to the cells, which then were incubated for 15 min at RT. To remove cellular debris, the cell lysate was centrifuged (microcentrifuge, maximum speed: 21.130x g, 10 sec) and the supernatant was transferred into new 1.5 ml tubes. 20 µl of the supernatant were transferred into a Nunc™ FluoroNunc™/LumiNunc™ 96-well plate(Thermo Scientific, USA) and then 100 µl of the 1/100 in Renilla Luciferase Assay Buffer diluted Renilla Luciferase Assay Substrate was added. Light emission was measured immediately after adding the Luciferase Assay Substrate for a period of 800 ms with Tecan infinite® M200.

5.6.13.2 Luminescence measurement with the Luciferase Reporter Gene Assay, high sensitivity

THP-1 cells ($1*10^6$ cells per sample) and human monocytes ($5*10^6$ cells per sample) were transfected with an NF-κB promoter construct-containing plasmid, were stimulated and incubated for 24 h at 37°C with or without one of the following stimuli: LPS *E. coli* O111:B4 (50 ng/ml or 100 ng/ml), Pam3CSK4 (200 ng/ml) or MALP2 (20 ng/ml). Cells were washed once with DPBS, before they were centrifuged again and the supernatant was completely discarded. Then, 30 µl of previously 1/5 in redist. water diluted lysis buffer were added to the cell pellet and incubated for 15 min at RT. To remove cellular debris, the cell lysate was centrifuged (microcentrifuge, maximum speed: 21.130x g, 10 sec) and the supernatant was transferred into new 1.5 ml tubes.

Expression of the inducible luciferase was carried out using the Luciferase Reporter Gene Assay, high sensitivity (Roche, Switzerland). The luciferase assay reagent was prepared by adding 10 ml of the reaction buffer to the lyophilized luciferase substrate. Not required material was stored in 1 ml aliquots at -20°C. Light emission was measured immediately after adding 100 µl of the luciferase assay reagent to 20 µl of the supernatant placed into a Nunc™ FluoroNunc™/LumiNunc™ 96-well plate (Thermo Scientific, USA) for a period of 800 ms with Tecan infinite® M200.

5.7 Methods of protein biochemistry

5.7.1 Enzym linked immunosorbent assay (ELISA)

Commercially available ELISA kits as listed in table 2 were used to measure and compare the amounts of produced cytokines (IL-6 and TNF-α) in supernatants of stimulated monocytes according to the manufacturers' recommendations.

Briefly, ELISA plates (Immuno Platte Maxi Sorp 96 well, VWR International, USA) were coated with the specific capture antibody, which binds specifically to the test antigen, diluted in coating buffer and incubated at 4°C overnight. After several washing steps, plates were blocked using a solution of non-reacting protein (DPBS with 10% FCS), in order to cover any plastic surface in the well which remains uncoated by the antibody in further steps. Reconstituted standard and appropriate dilutions of the samples were transferred to the wells and incubated for at least two hours at room temperature. Unbound material was removed by washing. Then, plates were incubated with the appropriate enzyme-linked detection antibody for one hour at RT. After washing, added tetramethylbenzidine (TMB)-solution was converted by the horseradish peroxidase (HRP). The reaction was stopped by adding 100 µl 2N H_2SO_4 and the read-out was done in a Tecan infinite® M200 Plate reader (Switzerland) measuring the absorbance at 450 nm.

5.7.2 Cell lysis and isolation of the total cellular protein content

Typically, cell counts of 1-3*10^6 cells/ml were used for protein extraction from human monocytes and THP-1 cells. Cells were harvested by scraping or centrifugation, washed once with DPBS to remove redundant serum proteins and then lysed (about 1*10^6 cells/ 200 µl lysis buffer; ingredients of lysis buffer are depicted in table 15). After one hour on ice, cell lysate was centrifuged for 10 min at 16,000x g. The supernatant contained all soluble cellular components, including cytoplasmic and numerous solubilized membrane proteins, and was either directly used for subsequent analysis or stored at -20°C. The use of Triton X-100 as detergent allows the solubilization of membrane proteins effecting only slightly the native conformation of most proteins.

Table 15: Lysis buffer HBSM buffer (Hepes-buffered saline magnesium):
20 mM Hepes, pH 7.2
150 mM NaCl
5 mM MgCl2
1% Triton X-100
Protease inhibitors: Protease inhibitor cocktail (1:200, Sigma-Aldrich, USA)
1 mM PMSF (Phenylmethylsulfonylfluorid)

5.7.3 SDS-polyacrylamide gel electrophoresis (SDS-page)

Separation of proteins according to their apparent molecular weight was performed using SDS-page in a TRIS-glycine buffer system (Table 16) using the Mini-PROTEAN®Trans cell electrophoresis system of Bio-Rad. Mini-PROTEAN TGX precast gradient (4-15%) gels (Bio-Rad) allowed an optimal protein separation between 20 and 200 kDa. Protein samples were diluted in 4x SDS sample buffer in a ratio of 4:1 and boiled for 5 min at 95°C. Sample preparation occurred either under non-reducing conditions or under reducing conditions by adding dithiothreitol (DTT) to a final concentration of 10 mM. DTT reduces protein disulfide bounds. The gel was run at a constant voltage of 180 V for 20-30 min. The molecular weights of isolated proteins were compared to marker proteins using a prestained marker (1 µl of PageRuler Prestained, 1-250 kDa, Thermo Scientific).

Table 16: 10x Running buffer

0.25 M Tris
1.92 M Glycine
1% SDS (w/v)

5.7.4 Staining of protein gels

5.7.4.1 Coomassie Brilliant Blue (CBB G250)-staining

Proteins in gels can be stained using Coomassie Brilliant Blue (CBB G250). The minimum detection size is limited to 200 – 400 ng protein per band.

After performing electrophoresis, gels were incubated for at least 20 min with CBB at RT on a tilting table. To destain the gel, it was swiveled in destaining solution for 2 h or overnight. CBB staining solutions are listed in detail in table 17.

Table 17: CBB-gel-staining solutions

CBB-staining solution:	CBB-destaining solution:
40% Ethanol (v/v)	40% Ethanol (v/v)
10% Acetic acid (v/v)	7,5% Acetic acid (v/v)
1‰ Serva Brilliant Blue G-250 (w/v)	

5.7.4.2 Silver staining

Silver staining of proteins is based on the formation of complexes between Ag^{+}-ions and Glu-, Asp- and Cys-groups of the proteins. These complexes will be reduced to Ag by adding alkaline formaldehyde. Silver staining is a very sensitive method for the detection of even lowest protein

concentrations (detection limit: ~5 ng protein per band). Protein amounts cannot be quantified due to the fact that the signaling intensities of different proteins show large variations. Another disadvantage is that besides proteins also nucleic acids, lipopolysaccharides, lipids and glycolipids can be stained.

The gel was incubated in fixing solution for at least 20 min (or was previously stained with CBB) to get rid of interfering compounds and was then washed three times with 50% ethanol/H_2O bidest. for 5 min to shrunk the gel. Then, the gel was incubated for 1 min in thiosulfate solution in order to prevent a silver mirror on the outside of the gel decreasing the sensitivity and contrast of the staining. Before and after incubation of the gel with silver-nitrate solution for 12 – 30 min the gel was washed three times with H_2O bidest. for 20 sec. Then, the gel was incubated in developing solution until reaching the desired color intensity. The reaction was stopped with fixing solution (Table 18).

Table 18: Silver-gel staining solutions

Fixing solution:	Thiosulfate solution:
50% Methanol	0,02% Sodium thiosulfate
12% Acetic acid	
Silver nitrate solution:	Developing solution:
0,08 g $AgNO^3$	3% Sodium carbonate
0,02% Formaldehyde	0,05% Formaldehyde
ad 50 ml	0,0005% Sodium thiosulfate

5.7.5 Western blot

Protein immunoblotting describes the transfer of proteins from a polyacrylamide gel matrix to a nitrocellulose (or PVDF) membrane, enabling the detection of proteins via antibody-based methods or diverse staining dyes. The transfer was achieved using the electroblotting tank system from Bio-Rad (Mini Trans-Blot®Cell) and carried out at a constant current of 280 mA at 4°C for 1.5-2 h. To verify successful transfer, proteins on the nitrocellulose membrane were visualized with Ponceau S (Table 19). After 1 minute Ponceau S staining, the membrane was washed with 1% acetic acid solution until protein bands were visible. Destaining was done with TBS.

Table 19: Buffer and staining solution for Western Blot analysis

10x Transfer buffer:	Ponceau S staining:
150 mM Glycine	2% Ponceau red (w/v)
20 mM Tris-HCl	30% TCA (v/v)
	30% Sulfosicylic acid (w/v)

The transfer buffer was applied in a 1x concentration containing 10% ethanol (v/v). The Ponceau S staining was diluted 1:4 in double distilled water before usage.

5.7.6 Immunochemical tests for the detection of proteins on blot membranes

For the detection of specific proteins, the blot membrane was blocked with 10% skimmed milk powder in Tris-buffered saline (TBS) for at least 2 h at 4°C or overnight. All following washing steps were carried out using either TBS or TBS supplemented with 0.1% Tween 20 (TBS-T) buffer (Table 20).

The blot membrane was washed and then incubated with an appropriate dilution of the primary antibody in TBS-T for 2 h at 4°C (or overnight). Afterwards, the blot was washed three times with TBS-T, before the secondary antibody (1:5000 in TBS-T) was added for another 2 h at 4°C. All secondary antibodies were conjugated with horseradish peroxidase (HRP) which catalyzes the oxidation of the chemiluminescent substrate luminol to 3-aminonaphthalate. To remove excessive secondary antibody, the blot was washed three times with TBS-T and then three times with TBS. The wet blot membrane was transferred into a transparent plastic foil, before the chemiluminescent solution, a 1:2 dilution of solution A (luminol, enhancer) and B (peroxidase buffer; SuperSignal West Pico Chemiluminescent Substrate, Thermo Scientific Pierce™), was added to the blot. The image was directly developed using the multi-imaging system Fusion FX7™. Exposure times varied and depended on the protein amount in the sample and the primary/secondary antibody combinations.

Table 20: TBS and TBS-T buffer

TBS buffer:	TBS-T buffer:
150 mM NaCl	TBS buffer + 0,1% Tween 20
10 mM Tris-HCl, pH 7,6	

5.7.7 Flow cytometry analysis of human monocytes

This laser-based, biophysical technology allows the simultaneously counting and sorting of cells as well as the detection of previously antibody-labeled target structures on or in the cells. Therefore, suspended single cells in a stream of fluid are passing a laser beam while the measured light scattering provide information of cell size (FSC = Forward Scatter) and intracellular granularity (SSC = Side Scatter). Antibodies, coupled to fluorescent dyes, may be used for additional data about cell type, state of the cells and their protein expression (antibody list see table 5).

Monocytes ($1*10^6$) were washed at least once with serum-free RPMI and once with FACS buffer (1% FCS, heat-inactivated (v/v) in DPBS). Meanwhile, appropriate dilutions of primary labeled antibodies in FACS buffer were prepared. Cells were resuspended in 100 µl of the prepared antibody dilutions per sample and incubated for 30 min on ice in the dark. To reduce the amount of unbound antibodies and prevent clotting, cells were washed with 5 mM EDTA in 10 ml PBS. Samples were washed once more with FACS buffer to eliminate remaining unbound antibodies and then analyzed in the Flow cytometer Aria II™ (BD Biosciences, Heidelberg). Unstained and isotype-labeled cells were included as negative controls and treated in the same manner. Cells were always kept on ice to limit endocytosis of surface receptors.

5.7.8 Sample Preparation for Mass Spectrometry

Mass Spectrometry can be used for qualitative and quantitative identification of cells or cell fractions (Fig. 3).

Cell preparation: MACS-separated and, thereafter, stimulated monocytes were purified once again by Fluorescence-Activated Cell Sorting (FACS). After several washing steps with DPBS, cells were lysed in 100 µl 4% SDS/DPBS and boiled for 5 min at 95°C. Cell lysates could be stored at -20°C and were thawed for further sample preparation.

Glycoprotein enrichment: DNA was digested by adding 1 µl Benzonase for 30 minutes at 37°C. To remove further contaminants, samples were centrifuged at high speed (21.000x g for 20 min). Supernatants were buffer exchanged by Size Exclusion Chromatography (SEC). In order to oxidize cis-diol-groups in sugars of polysaccharide moieties, 20 µl of 60 mM sodium meta-periodate ($NaIO_4$) were added to the flow-through containing proteins. After a 30 minute incubation period in darkness, samples were again buffer exchanged against PBS by SEC. Aldehydes of the oxidized glycoproteomic samples can react spontaneously with hydrazide groups on UltraLink Hydrazide-Beads forming stable hydrazone bonds. This coupling process is supported by aniline (9 µl/ml) as catalyst.

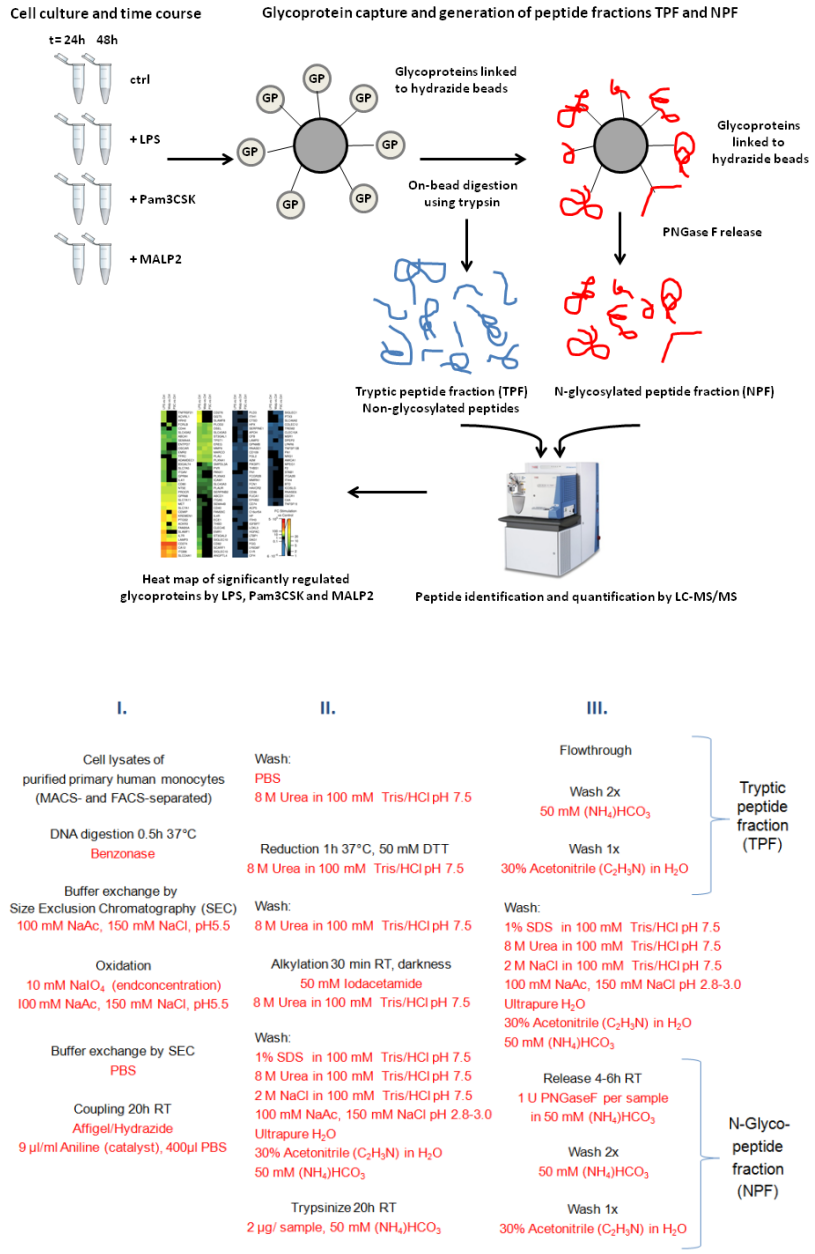

Fig.3: Workflow of sample preparation for LC-MS/MS.
(A) Cell lysates of monocytes, that were stimulated with either LPS, Pam3CSK, MALP2 or left untreated for 24 h or 48 h, are incubated with hydrazide beads. Aldehydes of the previously oxidized glycoproteins bind stably to hydrazide groups on the beads. In a first on-bead digestion step the tryptic peptide fraction (TPF) is gained. The N-glycosylated peptide fraction (NPF) is gained in a second incubation with PNGase F. Both peptide fractions are submitted to LC-MS/MS for peptide identification and further analysis. **(B)** Steps of glycoprotein enrichment at day I., II. and III. during sample preparation for LC-MS/MS. Black letters indicate the experimental procedure, used solutions and concentrations are given in red letters.

After overnight incubation at RT, beads were first washed with DPBS to remove aniline and in a second step with 8 M urea in 100 mM Tris/HCl (pH 7.5). This step is followed by disulfide reduction using dithiothreitol (50 mMDTT in 8 M urea in 100 mM Tris/HCl). The free sulfhydryl groups on the cysteine residues are then alkylated with iodoacetamide to irreversibly prevent the free sulfhydryl groups from reforming disulfide bonds. Extensive washing (five times with (1.) 1% SDS/Tris/HCl, (2.) 8 M urea in 100 mM Tris/HCl, (3.) 2 M NaCl/Tris/HCl, (4.) 100 mM NaAcetat and 150 mM NaCl, pH 2.8-3.0, (5.) H_2O, (6.) 30% acetonitrile/ H_2O and for two times with (7.) 50 mM ammonium carbonate, pH 8.0 in protein low-binding tubes (Protein LoBind Tubes, 1.5 ml, Eppendorf)) reduces non-specific binding of non-glycosylated proteins. The denatured, reduced and alkylated glycoproteins are digested by the endoproteinase trypsin in an overnight incubation at 37°C. Beads were washed twice with ammonium hydrogen carbonate

buffer, once with 30% acetonitrile buffer and supernatants, containing the tryptic peptides, were collected in new tubes. Then, supernatants were either kept at -20°C or dried using the Speed Vac (Thermo Scientific™ Savant™ SPD1010). In order to remove unbound tryptic peptides from glycopeptides, that are still bound to the UltraLink Hydrazide-Beads, beads were washed a second time as described above. After the last two washing steps with ammonium carbonate in new protein low-bind-tubes, glycopeptides are digested by adding Peptide-N-Glycosidase F (PNGase F, 1 U per sample), that cleaves between the innermost N-Acetyl-glucosamine (GlcNAc) and asparagine residues of high mannose hybride and complex oligosaccharides from N-linked glycoproteins in an overnight incubation (or 4-6 hours-incubation period) at 37°C. Again, beads were washed twice with ammonium hydrogen carbonate buffer, then once with 30% acetonitrile buffer and all supernatants, containing the glycopeptide fraction, were collected in new tubes and dried in a Speed Vac.

Each dried fraction was reconstituted in 0.3% formic acid and peptide concentrations were measured using a NanoDrop spectrometer. 2 µg of tryptic peptides and 0.5 µg of deglycosylated peptides were analyzed in each LC-MS/MS run in duplicates on an Orbitrap Fusion (Thermo Scientific) coupled to a Dionex Ultimate 3000 (Thermo Scientific) nanoelectrospray ion source. Samples were loaded on a 2 cm C18 trap column (Acclaim PepMap100, Thermo Scientific) and separated using a 2.5 h non-linear gradient (2-80% acetonitrile/ 0.1% formic acid, flow rate 300 nl/min) on a 50 cm C18 analytical column (75 µm i.d., PepMap RSLC, Thermo Scientific). Full MS scans were acquired with resolution 120.000 at m/z 400 in the Orbitrap analyzer (m/z range 400-1600, quadrupole isolation). MS1 parent ions were fragmented by higher energy collisional dissociation (HCD, 30% collision energy) and fragment ion spectra were acquired (in the order highest charge to least charge and least intense to highest intensity during a max. 4 sec cycle time) in the ion trap in rapid mode (m/z start 110). The following conditions were used: spray voltage of 2.0 kV, heated capillary temperature of 275°C, S-lens RF level of 60%, ion selection threshold of 50,000 counts for HCD, maximum ion accumulation times of 50 ms (AGC 5 x 10^5) for full scans and 35 ms (AGC 1 x 10^4) for HCD.

5.7.9 Limulus Amebocyte Lysate (LAL) test

The Limulus Amebocyte Lysate assay is a well-established method for the quantitative detection of even smallest amounts of endotoxin in samples. In the presence of endotoxin a protease cascade is activated. It catalyzes the cleavage of p-nitroaniline (pNA), resulting in yellow color, which can be quantified by measuring the absorbance at 405 nm (A405). In order to test whether the used

S100A12 is LPS-contaminated or not, the Kinetic Turbidimetric LAL Assay (PYROGENT™, Lonza) was performed according to the manufacturer's recommendation.

Briefly, Control Standard Endotoxin (CSE) was reconstituted and diluted in LAL Reagent Water (LRW) to prepare a standard series. Samples containing different dilutions of S100A12 of the different manufacturers, CSE standards and LRW as a negative control were dispensed as duplicates into the appropriate wells of a microplate. After incubating the microplate at 37°C for 10 min, the previously reconstituted LAL Reagent was added to all wells. Immediately after adding the LAL Reagent, color development was measured at 405 nm with the plate reader (Tecan infinite® M200, Switzerland).

5.7.10 Quantitative analysis of NF-κB activation in HEK-Blue-hTLR4 cells

Recruitment of transcription factors to DNA-binding sites can be analyzed using a promoter-reporter-gene construct. In general, reporter genes, e.g., those that encode for secreted embryonic alkaline phosphatase (SEAP), luciferases or fluorescence proteins, are coupled to the promoter sequences of the pathway of interest. SEAP is a widely used reporter gene that is secreted into cell culture supernatant and is therefore detectable by luminescent, fluorescent or colorimetric assays. The nuclear translocation and promoter-binding of NF-κB was herein quantified using the reporter SEAP expressed by HEK-Blue-hTLR4 cells.

HEK-Blue-hTLR4 cells were stimulated with constant concentrations of LPS *E.coli* O111:B4 (1 ng/ml or 10 ng/ml) and commercially available S100A12 (0.5 µg/ml) in the presence of different concentrations of LBP (none, 10 ng/ml, 100 ng/ml) or FCS (5%) in serum-free medium for 20 h. The second assay investigated the influence of polymyxin B (PMB) coincubation on LPS- and S100A12-stimulated cells. PMB is a well described inhibitor of LPS by binding to lipid A, the toxic component of LPS and, thus, inhibiting the LPS induced TLR4 activation. Cells were treated with either 10 ng/ml LPS *E.coli* O111:B4 or 0.5 µg/ml S100A12 with or without 100 µg/ml PMB for 20 h.

For all experiments, $3*10^4$ cells/200 µl were seeded in a 48-well plate and SEAP expression was quantified after 20 h of incubation at 37°. Since alkaline phosphatase is secreted into the cell culture supernatant, 10 and 20 µl of cell medium, each in triplicates, were removed and incubated with 200 µl of QUANTI-Blue™ detection solution (Invivogen) at 37°C. The colorimetric shift of the detection medium was measured at 635 nm at different time points after 15, 30 and 60 min. Untreated cells were included into all experiments as negative controls and their absorbance was substracted from all positive samples.

5.8 Statistical analysis

This chapter lists all statistical tests used for data interpretation of: 1) qPCR-, ELISA-, 2) Western blot- , 3) FACS- and 4) Mass spectrometry-based analysis. All differences with a p value <0.05 were considered as statistically significant. Statistical tests that were used to evaluate revealed data are also stated within each experiment.

5.8.1 Analysis of qPCR data and cytokine expression via ELISA

In a first step, variance heterogeneity between sample replicates was minimized by transforming real-time PCR data into log NRQ values (NRQ-normalized relative quantities) (Rieu and Powers 2009). Statistical comparisons between untreated and treated samples or between different treatments were assessed with the mean values of at least three sample replicates using the repeated measures one-way analysis of variance (ANOVA) and including the Bonferroni's post-hoc test.

5.8.2 Densitometric analysis of Western blot data

Protein expression measured by western blotting was quantitatively analyzed using ImageJ. Subsequently, densitometric data of the differently treated samples were compared applying the one-way ANOVA and the Bonferroni's post-hoc test.

5.8.3 Analysis of FACS data

MFIs of the different treatments were calculated in relation to the MFI of the untreated control for each donor in order to determine the relative fold change (FC). Afterwards, the mean value of all determined FCs per donor was calculated.

5.8.4 Analysis of mass spectrometry-based proteomic data

Protein identification and quantification were performed by matching all RAW files with the human UniProt database (Version 05.2016, reviewed sequences) using the MaxQuant version 1.5.5.1 (Max Planck Institute of Biochemistry (Cox and Mann 2008). The parameters were set as follows: main search peptide tolerance: 4.5 ppm; enzyme: trypsin, max. 2 missed cleavages; static modification: cysteine carbamidomethylation; variable modification in the tryptic peptide fraction: methionine oxidation; variable modification in PNGase F fractions: methionine oxidation and asparagine deamidation. PSM (peptide specific matches) and protein FDR was set to 0.01. For advanced identification the Second Peptide Search in MS2 spectra and the Match Between Runs feature were enabled. Label-free quantification of proteins with normalization was done in MaxQuant (Cox et al. 2014). LFQ min. ratio count was set to one. Peptides from both fractions

were integrated in the LFQ intensity calculations. Only unique and razor peptides, unmodified or modified, were used for quantification. LFQ protein intensities were then loaded into the Perseus framework (Max Planck Institute of Biochemistry (Tyanova et al. 2016)). Known contaminants (keratins and human plasma proteins) and reverse identified peptides/ proteins were discarded. Intensities were log(2) transformed and missing values were imputed from the normal distribution of the data set (width: 0.3, downshift 1.8). Two-sample t-test was used to calculate statistical differences of protein abundances in the control and LPS-treated groups. P-values were adjusted according to Benjamini and Hochberg (Benjamini and Hochberg) and proteins demonstrating at least a two-fold expression difference and an adjusted p-value < 0.05 were considered to be significantly changed in expression by LPS-, Pam3CSK- or MALP2- treatment.

Protein groups identified by MaxQuant were filtered for proteins annotated as “glycoproteins” in the UniProt data base and those annotated as transient O-GlcNAc-modified without any other N- or O-glycosylation annotated were discarded. Data analysis was performed in R using packages provided by Bioconductor. Putative TMDs were predicted using the transmembrane hidden Markov model (TMHMM) algorithm (TMHMM 2.0 server) (Krogh et al. 2001). For gene ontology classification the R-package “org.Hs.eg.db” version 3.1.2 was used and results were manually compiled. Functional annotation clustering was performed with DAVID (Huang da et al. 2009), Version 6.8.

5.9 Software

- Adobe Photoshop 6.0
- BestKeeper algorithm
- DAVID Bioinformatics Resources 6.8, NIAID/NIH
- Ensembl Genome Browser
- Graph Pad Prism 5.0
- ImageJ2
- Image Studio Lite 3.0
- MaxQuant, Max Planck Institute of Biochemistry
- mfold Web Server
- Microsoft Office Excel 2007
- Multiple Condition qPCR Manager
- PANTHER Classification System
- Perseus framework, Max Planck Institute of Biochemistry
- Primer-Blast software
- Rotor-Gene Q Series software 2.0.2
- TMHMM v2.0 server
- UniProt database

6. Results

6.1 Characterization of human monocytes

To investigate the phenomenon of endotoxin tolerance (ET), all experiments were carried out using either the acute monocytic leukemia cell line THP-1 or primary human peripheral blood monocytes isolated from healthy volunteers.

6.1.1 Human monocytes express TLR1, TLR2, TLR6, TLR4, CD14, MD-2, RAGE and NLRs

In order to assess the capability of monocytes to detect all stimuli used in this study (LPS *E. coli* O111:B4, Pam3CSK, MALP2, S100A12, iE-DAP and MDP) RT-PCR was performed to measure the basal gene expression of the required extra- and intracellular PRRs. All components of the TLR4 receptor complex (including TLR4, CD14 and MD-2) and of the TLR2 heterodimers (TLR1/TLR2 and TLR2/TLR6) as well as the receptor for advanced glycation endproducts (RAGE) and the nucleotide-binding oligomerization domain (NOD-) like receptors (NLRs: NOD1 and NOD2) showed a distinct basal gene expression in unstimulated, MACS-separated human monocytes (Fig. 4). Notably, NOD1 expression in human monocytes of all three donors analyzed was only faintly detectable in RT-PCR.

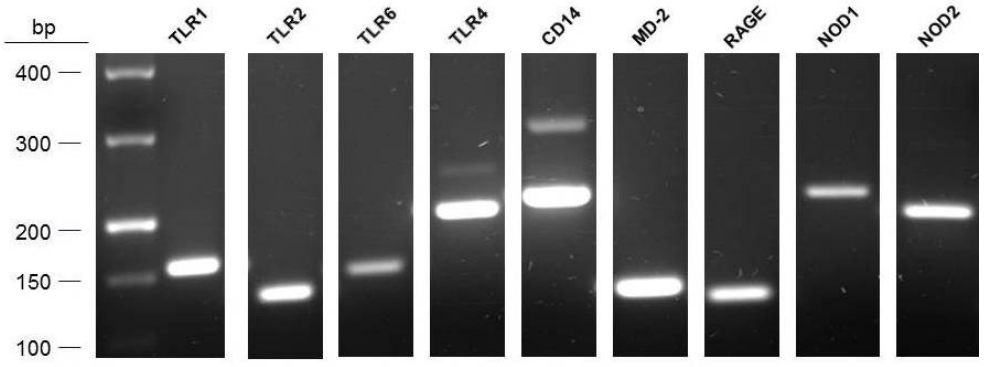

Fig. 4: Basal expression of TLR1, TLR2, TLR6, TLR4, CD14, MD2, RAGE and NLRs in primary human peripheral monocytes. Detection of TLR1 (157 bp), TLR2 (131 bp), TLR6 (144 bp), TLR4 (196 bp), CD14 (206 bp), MD-2 (120 bp), RAGE (110 bp), NOD1 (204 bp) and NOD2 (181 bp) in MACS-separated, unstimulated monocytes by RT-PCR and gel electrophoresis. Cells were lysed immediately after MACS separation. Data are representative for three independent experiments and donors.

6.2 Pro-inflammatory response and tolerance induction in monocytes by TLR- and NLR-agonists

Specific receptor agonists were proven to activate monocytes and to induce an adequate and similar pro-inflammatory response.

6.2.1 TNF-α mRNA expression of LPS-, Pam3CSK-, MALP2-, iE-DAP- or MDP-stimulated monocytes

To test for monocyte activation by the used PRR ligands, TNF-α expression in LPS-, Pam3CSK-, MALP2-, iE-DAP- or MDP-stimulated monocytes was examined on the transcriptional level using RT-qPCR in pilot experiments (Fig. 5).

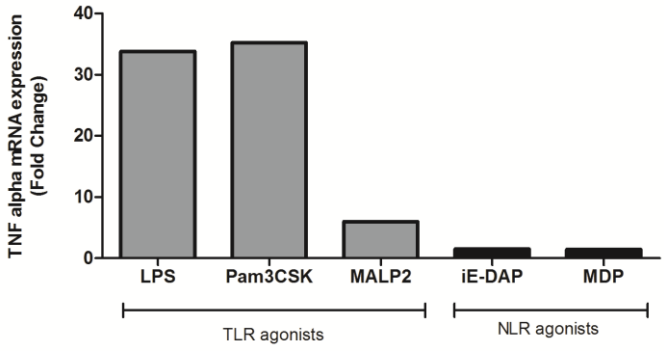

Fig. 5: TNF-α mRNA expression in LPS-, Pam3CSK-, MALP2-, iE-DAP- and MDP-stimulated human monocytes. Human monocytes ($8*10^6$ cells/2 ml medium) were incubated for 2 h with either 50 ng/ml LPS, 100 ng/ml Pam3CSK, 5 ng/ml MALP2 or for 4 h with iE-DAP 1 µg/ml or MDP 10 µg/ml or were left untreated. Total mRNA was isolated, reverse transcribed into cDNA and subjected to qPCR analysis. The results represent one experiment. The gene expression was normalized to the housekeeping gene HPRT. The fold ratio of mRNA levels relative to unstimulated cells was cal-culated according to Pfaffl et al. (2004).

A two-hour incubation period of monocytes with LPS, Pam3CSK and MALP2 led to increased expression of TNF-α compared to the non-treated control cells. Monocytes treated with either 50 ng/ml LPS or 100 ng/ml Pam3CSK showed a comparable ~33.- to 35.-fold upregulated TNF-α expression, whereas 5 ng/ml of MALP2 induced only a ~6.-fold upregulation. NOD-like receptor ligands, iE-DAP and MDP, did not affect TNF-α expression after 4 h in a significant manner (1.5- to 1.6-fold upregulation).

6.2.2 Kinetic analysis of the pro-inflammatory immune response of LPS-treated human monocytes

In order to determine the best suited time-period for pro-inflammatory and for tolerance induction on transcriptional level, human monocytes were stimulated with LPS for different times and the transcriptional regulation of TNF-α expression was analyzed by qPCR. TNF-α expression reached maximum levels with a 37.8-fold upregulation after stimulating cells for one hour with 50 ng/ml LPS (Fig. 6). Afterwards, expression levels of TNF-α declined and were already at 50% after two

hours. Therefore, LPS-restimulation over a period of one hour displays to be the most sensitive time point for the detection of TNF-α transcriptional changes.

Fig. 6: Transcriptional regulation of TNF-α gene expression in LPS-stimulated monocytes.

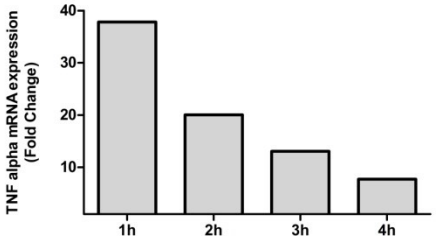

Human monocytes (8*10^6 cells) were stimulated for either 1, 2, 3, or 4 hours with 50 ng/ml LPS. Untreated controls were included for each time point. TNF-α gene expression was analyzed by qPCR and normalized to the housekeeping gene HPRT. The fold ratio of mRNA levels relative to untreated cells was calculated according to the Pfaffl method (2004). Data represent values from one experiment performed as pilot study.

6.2.3 TNF-α mRNA expression is suppressed in LPS-, Pam3CSK- or MALP2-prestimulated monocytes but not when pre-stimulated with a NLR-ligand

To test if TLR agonists induce the tolerant state in monocytes, tolerance induction in human monocytes by different PRR agonists was examined in a new experimental setting: Cells were exposed to either LPS (50 ng/ml), Pam3CSK (100 ng/ml), MALP2 (10 ng/ml), iE-DAP (1 µg/ml), MDP (10 µg/ml) or left untreated for 20 h and then restimulated with 50 ng/ml LPS for one hour. TNF-α mRNA expression was analyzed to reveal tolerance induction. TNF-α mRNA was significantly down-regulated in monocytes that were either prestimulated with LPS (1.9-fold, $p<0.001$) or with the TLR receptor agonists Pam3CSK (12.3-fold, $p<0.001$) or MALP2 (6.4-fold, $p<0.001$) compared to naïve monocytes that were stimulated with LPS for only one hour during the restimulation period (Fig. 7, white column, 69.15-fold).

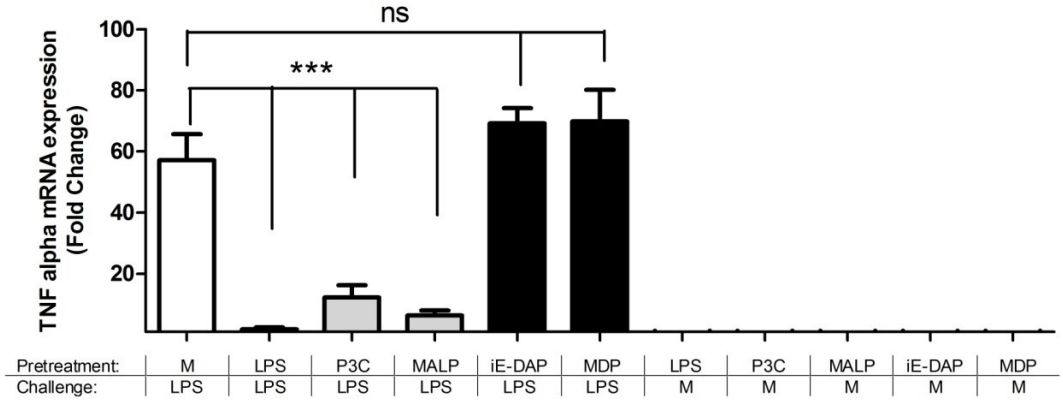

Fig. 7: Reduction of TNF-α gene expression in LPS-, Pam3CSK- and MALP2-prestimulated monocytes in qPCR analysis. Monocytes (8*10^{6}cells/ml) were prestimulated with one of the following stimuli: LPS *E. coli* O111:B4 (50 ng/ml), Pam3CSK (100 ng/ml), MALP2 (10 ng/ml), iE-DAP (1 µg/ml) or MDP (10 µg/ml) for 20 h, always including untreated cells as negative control, shown on the right part of the graph (M = medium). Pretreated monocytes were washed and incubated again with or without LPS *E. coli* O111:B4 (50 ng/ml) for 1 h. Data represent mean values (± SD) from three independent experiments. *** $p<0.001$, ns-not significant.

However, no reduction of the TNF-α transcript level was observed in monocytes that were pre-stimulated with one of the nucleotide-binding oligomerization domain (NOD)-like receptor

ligands. Neither the NOD-1 agonist iE-DAP nor the NOD-2 activator MDP were successful in inducing tolerance in monocytes due to unaltered high TNF-α mRNA expression levels (69.15- and 69.9-fold). Contrary, MDP indicated a slight pro-inflammatory trend when used as pre-stimulus, although significance was not reached. Monocytes that were only pretreated with one of the PRR agonists for 20 h but not restimulated showed no increased TNF-α mRNA levels. In summary, LPS-, Pam3CSK-, and MALP2-pretreatment of human monocytes led to tolerization of TNF-α response.

6.3 S100A12: an endogenous ligand and possible inducer of tolerance in monocytes

When NLR ligands iE-DAP and MDP failed in inducing tolerance in primary human monocytes, the question arose whether the endogenous RAGE and putative TLR4 agonist S100A12 would be able to induce tolerance in monocytes. In a first step, pro-inflammatory activation of monocytic THP-1 cells by S100A12 was tested, before further experiments were carried out using primary human monocytes.

6.3.1 Comparison of the pro-inflammatory effects of commercially obtained S100A12 and LPS in THP-1 cells

Initially, S100A12-stimulation experiments were carried out using commercially available S100A12 from R&D Systems (UK). In pilot studies, a two hours-incubation period with a high amount of S100A12 (5 µg/ml) or LPS (50 ng/ml) induced a 5.9-fold and 11.9-fold increase of TNF-α mRNA expression in THP-1 cells, respectively (Fig. 8).

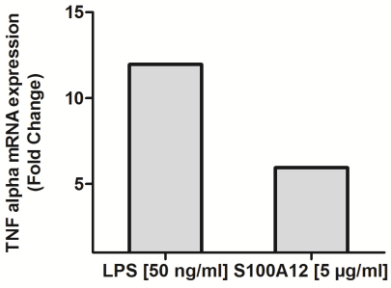

Fig. 8: Pro-inflammatory effect of commercially available S100A12 in THP-1 cells.
THP-1 cells ($1*10^6$ cells in 1 ml medium) were incubated with either 50 ng/ml LPS, 5 µg/ml S100A12 or left untreated for 2 h. Total mRNA was isolated, reverse transcribed into cDNA and subjected to qPCR analysis. The results represent one experiment. Gene expression was normalized to the housekeeping gene HPRT. The fold ratio of mRNA levels relative to unstimulated cells was calculated according to Pfaffl et al. (2004).

The result indicates that S100A12 has pro-inflammatory effects in THP-1 cells.

6.3.2 Confirmation of the purity of S100A12

Reconstituted proteins expressed in E. coli strains are often contaminated with LPS. To test the purity of S100A12 from R&D Systems and Sino Biological, two assays were developed to test for residual LPS concentrations. LPS-binding protein (LBP) is well-known to mediate and accelerate the binding of LPS to the TLR4:MD-2:CD14 receptor complex (Hailman et al. 1994). Thus, LBP- and FCS-dependency of LPS- and S100A12-signaling via TLR4 was tested in a first experimental approach using NF-κB reportergene expressing HEK-Blue-hTLR4 cells under serum free conditions.

As shown in Fig. 9, NF-κB activation in HEK-Blue-hTLR4 cells, grown in serum-free medium and stimulated with constant concentrations of LPS *E.coli* O111:B4 (1 ng/ml or 10 ng/ml), was considerably enhanced with increasing amounts of LBP (10 ng/ml, 100 ng/ml)**.** Comparable effects were observed for exogenously-added FCS, which contains LBP as an essential serum component. Unexpectedly, S100A12-induced NF-κB activation was also enhanced in a similar concentration-dependent manner in the presence of increasing amounts of LBP or in the presence of 5% serum. This was observed for both commercially available S100A12 proteins derived from R&D Systems and Sino Biological.

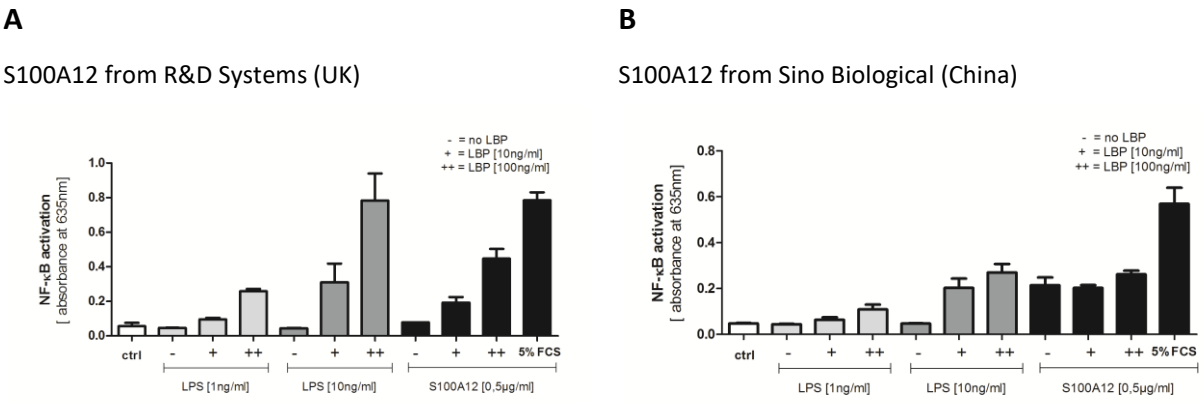

Fig. 9: Effects of LBP on S100A12 mediated NF-κB activation. A+B: HEK-Blue-hTLR4 cells (3*10^4/200 µl medium) were incubated in serum-free medium with different concentrations of LPS *E.coli* O111:B4 or with S100A12 purchased from either (A) R&D Systems (UK) or from (B) Sino Biological (China). NF-κB activation was studied in the presence of FCS or with increasing amounts of LBP. SEAP expression was quantified after 20 h of incubation. Medium treated cells as negative controls were always included. Data represent one experiment, measured in triplicates, respectively.

The second assay investigated the influence of polymyxin B (PMB) co-incubation on LPS- and S100A12-stimulated cells. PMB is well described to be a specific inhibitor of LPS through binding to lipid A, the toxic, negatively charged component of LPS. PMB inhibits the interaction with TLR4 receptor complex and, hence, LPS-mediated NF-κB signaling.

As expected, LPS-stimulated HEK-Blue-hTLR4 cells that were co-incubated with PMB, showed a strong, although not significant decrease of NF-κB activation. A similar effect of PMB on S100A12 stimulation was observed when cells were stimulated with 0.5 µg/ml S100A12 purchased from R&D Systems in the presence of PMB, leading to a significant reduction of 80.5% of the NF-κB activation (Fig. 10).

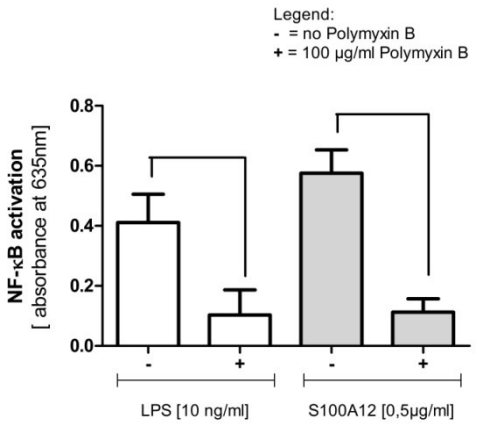

Fig. 10: Polymyxin B coincubation decreases the signaling of S100A12 on HEK-Blue-hTLR4 cells. Cells ($3*10^4$/200 µl medium) were stimulated with either LPS *E.coli* O111:B4 or S100A12 from R&D Systems (UK) in the presence or absence of 100 µg/ml polymyxin B. SEAP expression was quantified after 20 h of incubation at 37°C. Medium-treated cells as negative controls were always included and their absorbance substracted from all positive samples. Data represent two experiments measured in triplicates.

6.3.3 Confirmation of LPS contamination in commercially obtained S100A12 by LAL assay

According to the previously shown data, doubts about the purity of the commercially obtained S100A12 arose. Thus, purity of commercially obtained S100A12 from R&D Systems (UK) and from Sino Biological (China), as well as of S100A12 provided by Dirk Foell's (DF) working group was analyzed by Limulus Amebocyte Lysate (LAL-) assay, a specific and well-established method for the quantitative detection of even smallest amounts of endotoxin in biological material. The results show that both purchased S100A12 preparations, but not the one of the Foell's group were LPS-contaminated (about 0.39 ng LPS per 1 µg S100A12 of R&D Systems, and 0.3 ng LPS per 1 µg S100A12 of Sino Biological, Fig. 11).

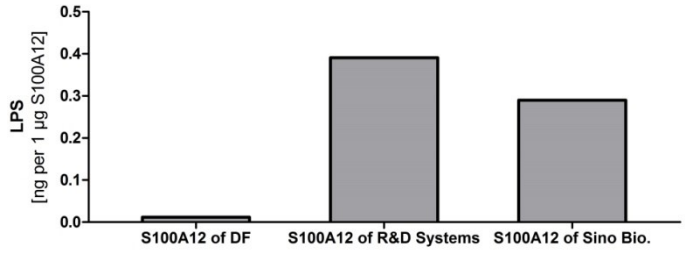

Fig. 11: Determination of possible endotoxin contamination of commercially obtained S100A12 in the Limulus Amebocyte Lysate (LAL)-test. LAL-assay of S100A12 allocated from Dirk Foell's group and obtained of R&D Systems (UK) or Sino Biological (China) was carried out according to the manufacturer's protocol. Data represent one experiment.

In summary, LPS contamination of S100A12 reconstituted proteins could be verified by: (1) enhanced signaling of S100A12 in HEK-Blue-hTLR4 cells when cells were co-incubated with

LBP, (2) reduction of S100A12-mediated NF-κB-activation in the presence of PMB and (3) the quantifiable proof performing the LAL-test.

Therefore, all further experiments were conducted using the LPS-free S100A12 of Dirk Foell's working group to ensure that all effects seen were caused by S100A12 itself and not by its LPS contamination.

6.3.4 Endotoxin-free S100A12 does not induce TNF-α expression on transcriptional level in THP-1 cells

In a first preliminary study, THP-1 cells were stimulated with three different concentrations of LPS-free S100A12 (0,5 µg/ml, 2 µg/ml or 5 µg/ml) or with LPS (50 ng/ml), included as positive control. Whereas the TNF-α mRNA expression of LPS-treated THP-1 cells was increased after 1 h, S100A12 did not induce an enhanced TNF-α expression at any test concentration (Fig. 12). Since THP-1 cells may differ from human monocytes in their responsiveness towards S100A12, further experiments were carried out using freshly isolated human monocytes. In a new experimental approach to rule out different kinetics in the responses of LPS and S100A12, secretion of TNF-α was measured after stimulating monocytes with a high dose of S100A12 (10 µg/ml) in three independent experiments performing cytokine-specific ELISA after 24 h of incubation.

Similar to the results obtained in the THP-1 cell model, S100A12 was not inducing TNF-α production, while LPS treatment increased TNF-α production.

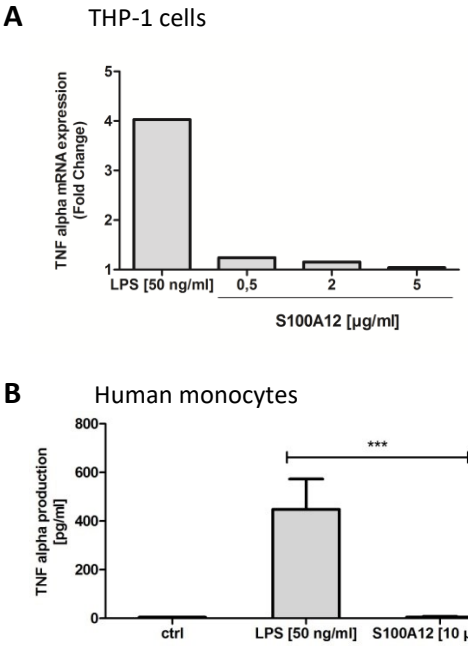

Fig. 12: LPS- and S100A12-induced TNF-α expression in THP-1 cells and human monocytes.

A: THP-1 cells ($2*10^6$ cells/1.5 ml medium) were incubated with increasing concentration of S100A12 and 50 ng/ml LPS for 1 h at 37°C. Total mRNA was isolated, reverse transcribed into cDNA and subjected to qPCR analysis. Data represent one experiment.

B: Human monocytes ($2*10^6$ cells/500 µl medium) were incubated with either LPS *E.coli*O111:B4 (50 ng/ml) or S100A12 (10 µg/ml) for 24 h at 37°C. TNF-α secretion was measured on protein level by specific ELISA measuring concentrations in supernatants of the stimulated human monocytes. The results are shown as the mean (±SD) of three independent experiments. *** $p<0.001$, Paired t-test.

Previously published data indicated that, besides TNF-α, gene expression of IL-1β and IL-6 is induced when monocytes are exposed to S100A12 (Foell et al. 2013). To test this, monocytes were stimulated with different concentrations of S100A12 and mRNA production of IL-1β and IL-6 was analyzed by qPCR. As shown in Fig. 13, cytokine gene expression remained nearly unaltered until high concentrations of 10 µg/ml S100A12 were used. Especially, the TNF-α gene expression was almost unchanged, whereas transcript levels of IL-1β (11.4-fold) and IL-6 (12.7-fold) were up-regulated when monocytes were stimulated with 10 µg/ml S100A12 (Fig. 13).

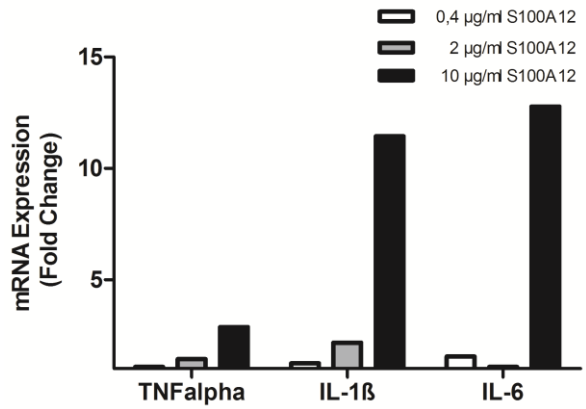

Fig. 13: qPCR analysis of S100A12-induced TNF-α, IL-1β and IL-6 gene expression in human monocytes.
Human monocytes (8*10^6 cells/2 ml medium) were incubated for 4 h with 0.4 µg/ml, 2 µg/ml, 10 µg/ml S100A12 or left untreated. The results represent one experiment. The gene expression was normalized to the housekeeping gene HPRT. The fold ratio of mRNA levels relative to unstimulated cells was calculated according to Pfaffl et al. (2004).

To prove if S100A12 can induce monocyte tolerance similar to LPS, IL-6 expression was chosen as new read out for subsequent experimental settings. LPS- or S100A12-pretreated monocytes were restimulated after 24 h with LPS or left untreated. IL-6 secretion was measured by ELISA in the supernatants after the pre- and restimulation period, respectively. Naïve monocytes that were stimulated only one-time with LPS showed increased IL-6 expression, whereas IL-6 production and release remained nearly unchanged when cells were exposed to S100A12. Moreover, the up-regulation of IL-6 expression on protein level remained completely unaffected when S100A12-pretreated monocytes were restimulated with LPS, particularly in comparison to the significantly down-regulated answer of LPS pretreated cells (Fig. 14).

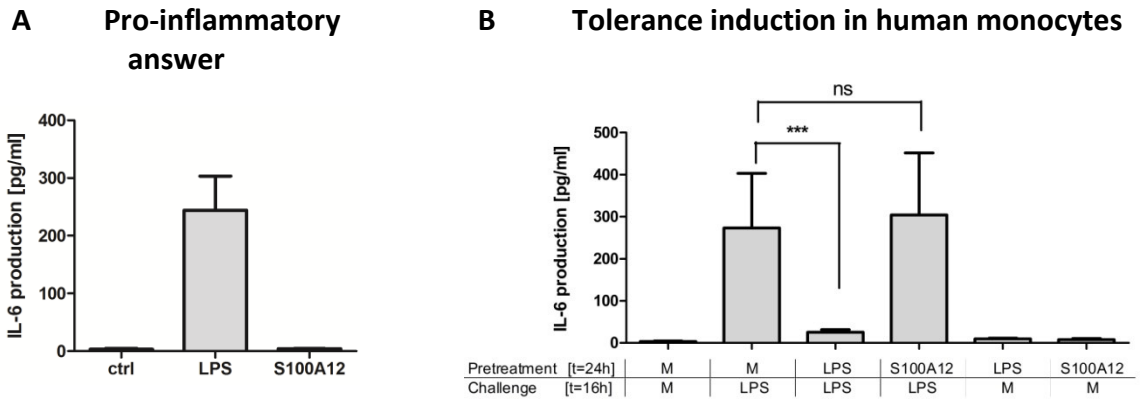

Fig. 14: Pro-inflammatory response and tolerance induction by S100A12 in human monocytes.
Human monocytes (2*10^6 cells in 500 µl medium) were pretreated with either LPS *E.coli* O111:B4 (50 ng/ml) or

S100A12 (10 µg/ml) or left untreated for 24 h at 37°C. Cells were carefully washed and allowed to rest for 30 min before they were restimulated with 50 ng/ml LPS for another 16 h. Unstimulated cells were included as control for each experiment. IL-6 production was measured on protein level by specific ELISA systems in supernatants of (A) the prestimulated human monocytes after 24 h and in (B) of the also restimulated or untreated monocytes after 40 h (24 h prestimulation+ 16 h restimulation), (M= medium). The results are shown as the mean (±SD) of three independent experiments. ***p<0.05, (Repeated measurements one-way ANOVA, Bonferroni post-hoc test (B)).

In summary, the results revealed that S100A12-(pre-)stimulation of human monocytes neither led to a detectable strong pro-inflammatory activation, nor was S100A12 stimulation able to induce the tolerant phenotype in monocytes as revealed by unaltered high protein expression levels of IL-6 in S100A12-pre- and LPS-restimulated cells. Thus, further experiments with the putative endogenous TLR4 agonist S100A12 were discontinued.

6.4 Adjustment of stimulation concentrations of TLR agonists

After confirming successful tolerance induction for the TLR4 agonist LPS *E.coli* O111:B4 and the TLR2 agonists Pam3CSK and MALP2 on transcriptional level, further tests were necessary to adjust the above-mentioned stimuli for equally strong pro-inflammatory responses for subsequent glycoproteomic experiments.

6.4.1 Standardization by an NF-κB-promoter reporter gene assay is not possible due to malfunctioning transient transfection

Several attempts were made to transfect THP-1 cells and monocytes in order to adjust concentrations of the used stimuli performing an NF-κB promoter reporter gene assay in dose-response experiments. Due to the fact, that gene transfer into primary cell lines and THP-1 cells has proven difficult (Gresch et al. 2004), different protocols, aiming at the transient insertion of plasmids into the cells, were tested.

Both, GeneCellin™ Transfection Reagent and Lipofectamine® 2000 Transfection Reagent, as chemical-based transfection methods failed in transfecting the purified NF-κB reporter gene containing plasmid (pGL4.32 [*luc*2P/NF-κB-RE/Hygro] Vector) and the Renilla-luciferase gene containing plasmid (pGL4.74 [*hRluc*/TK] Vector as positive control) into THP-1 cells and human monocytes. Many of the GeneCellin- and Lipofectamin-treated cells were considerably damaged and underwent apoptosis, while surviving cells showed no detectable luminescence in subsequent control experiments (data not shown).

Therefore, electroporation was used in a new experimental approach. Pmax GFP (green fluorescent protein) vector served as an additional positive control to determine transfection efficiency. Once inserted, the pmax GFP vector is constitutively expressed and, thus, GFP-labeled,

green fluorescent cells can be easily identified via fluorescence microscopy. Transfection efficiency by electroporation of monocytes was due to the pmax GFP vector only about 12-30%, dependent on the experiment and donor (Fig. 15).

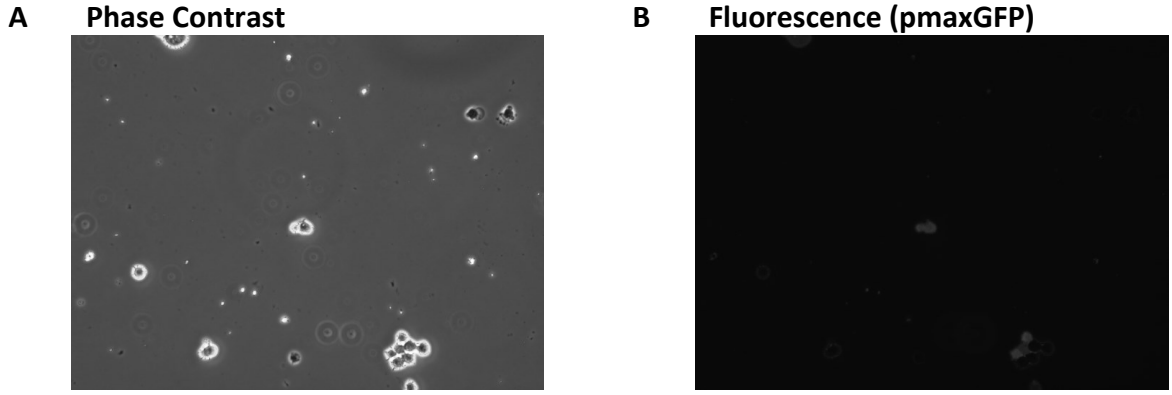

Fig. 15: Fluorescence and phase contrast micrographs of monocytes transfected with plasmid pmax GFP. Cells ($5*10^6$) were suspended in 100 µl Nucleofector solution containing 2 µg of the constitutively expressed pmax GFP vector. Transfection by electroporation was carried out according to the manufacturer's instructions. GFP expression was analyzed by fluorescence microscopy after incubating cells for 24 h at 37°C. Transfection efficiencies were of about 12-30%.

Similar attempts to insert the Renilla-luciferase gene containing plasmid or the NF-κB reporter gene containing plasmid in THP-1 cells and monocytes by using electroporation led to no successful transfection. Subsequent luminescence measurements, based on the activity of the constitutively expressed Renilla-luciferase gene containing plasmid (pGL4.74 [hRluc/TK]), showed no increased light emission of the actually transfected cells. Thus, further approaches of adjusting the stimuli by transfecting THP-1 cells and monocytes with an NF-κB reporter gene containing plasmid were discontinued.

6.4.2 TNF-α- and IL-6-production by naïve and prestimulated monocytes

Next, the adjustment of the utilized pro-inflammatory stimuli was tried by examining the cytokine production and release of TNF-α and of IL-6 by ELISA.

6.4.2.1 Monocytes show an upregulated IL-6- and TNF-α-secretion

The pro-inflammatory responsiveness of monocytes was tested by stimulating the cells with either LPS (50 ng/ml), Pam3CSK (100 ng/ml) or MALP2 (10 ng/ml) for 24 hours. IL-6 and TNF-α expression and secretion were analyzed in the supernatants of the stimulated monocytes by cytokine specific ELISA. The basal expression of both cytokines varied strongly among the donors and led to different intensity levels in the stimulus-induced upregulation of both cytokines. Nevertheless, IL-6 as well as TNF-α concentrations were highly increased after stimulation with LPS, Pam3CSK or MALP2 compared to non-stimulated monocytes (Fig. 16).

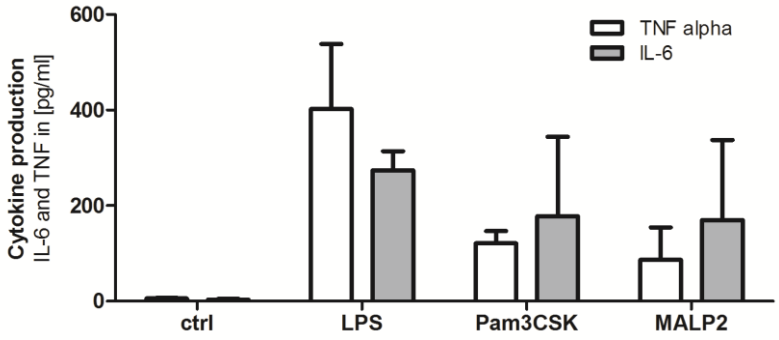

Fig. 16: Analysis of TNF-α and IL-6 release by LPS-, Pam3CSK- and MALP2-stimulated human monocytes. Monocytes ($2*10^6$ cells in 500 µl medium) were incubated with either LPS *E. coli* O111:B4 (50 ng/ml), Pam3CSK (100 ng/ml) or MALP2 (10 ng/ml) for 24 h at 37°C. TNF-α and IL-6 expression were analyzed in the collected supernatants by cytokine specific ELISA. Data represent mean values from two independent experiments (± SD).

6.4.2.2 TNF-α- and IL-6-production by monocytes after tolerance induction

It was further examined if the already described phenomenon of tolerance induction seen on transcriptional level was reproducible on protein level. Therefore, the pro-inflammatory cytokines, IL-6 and TNF-α, were measured in the supernatants of LPS (50 ng/ml)-, Pam3CSK (100 ng/ml)- and MALP2 (10 ng/ml)-prestimulated and LPS-restimulated monocytes. The data demonstrate a significant down-regulation of IL-6 as well as TNF-α for all three different pretreatments (LPS, Pam3CSK and MALP2) on protein level in three independent experiments (Fig. 17). In the case of IL-6, the expression levels were comparably reduced to about 15-18%, no matter which stimulus was used for prestimulation. Whereas the decrease of TNF-α seems to be stronger when prestimulation was carried out with LPS as Gram-negative stimulus or MALP2 as Gram-positive stimulus compared to a prestimulation with the second Gram-positive stimulus Pam3CSK.

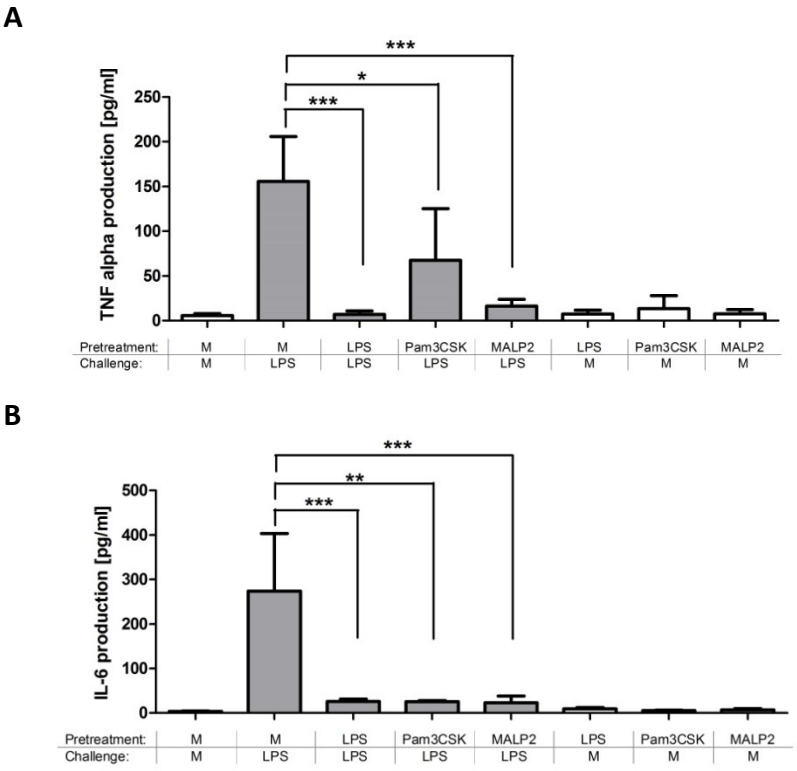

Fig. 17: Significant down regulation of cytokine production in tolerant human mono-cytes. Monocytes ($2*10^6$ cells in 500 µl medium) were incubated with either LPS *E. coli* O111:B4 (50 ng/ml), Pam3CSK (100 ng/ml) or MALP2 (10 ng/ml) for 24 h at 37°C and restimulated with LPS *E. coli* O111:B4 (50 ng/ml) again for 16 h (M = medium).
(A) TNF-α and (B) IL-6 expression were analyzed in the collected supernatants by cytokine specific ELISA. Data represent mean values from three independent experiments (± SD). *** p<0.001, **p<0.01, **p<0.05 (Repeated measurements one-way ANOVA, Bonferroni's post-hoc test).

In order to obtain comparable data, stimulus equalization was attempted by using different concentrations of each PRR agonist. In pilot studies, human monocytes ($2*10^6$ cells) were treated with different concentrations of one of the following stimuli: LPS *E. coli* O111:B4, Pam3CSK or MALP2 for 24 hours at 37°C. Untreated monocytes served as negative control. IL-6 and TNF-α expression and secretion were analyzed in the supernatants of the stimulated monocytes by cytokine specific ELISAs (Fig. 18). Again, the heterogeneous background among the donors led to great differences between the intensities in the stimulus-induced upregulation of cytokine expression. As depicted in Fig. 18, the expression of IL-6 and TNF-α proteins is shown for one individual donor. Similar results were observed for two more donors.

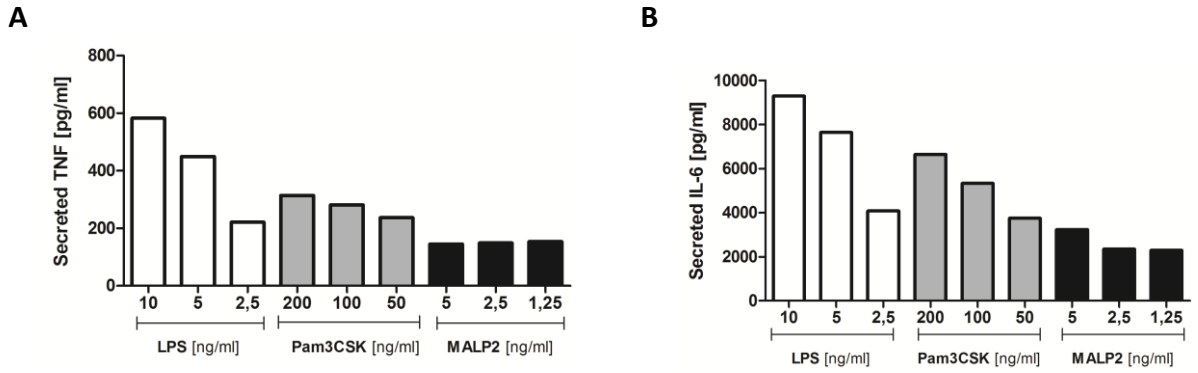

Fig. 18: Concentration series of LPS, Pam3CSK and MALP2 on human monocytes.
Monocytes ($2*10^6$ cells in 500 µl medium) were incubated with different concentrations of either LPS *E. coli* O111:B4 (2.5, 5 and 10 ng/ml), Pam3CSK (50, 100 and 200 ng/ml) or MALP2 (1.25, 2.5 and 5 ng/ml) for 24 h at 37°C. TNF-α (A) and IL-6 (B) expression were analyzed in the collected supernatants by cytokine specific ELISA. Data represent one experiment.

As shown in Fig. 18, already 2.5 ng/ml of LPS initiated higher IL-6- and TNF-α-secretion levels in monocytes compared to those stimulated with biological relevant high amounts of the TLR2 agonists MALP2. Moreover, simultaneously performed experiments showed that LPS concentrations (of 5 ng/ml and 10 ng/ml) that on the one hand were low enough to induce equivalent pro-inflammatory answers in monocytes as the TLR2 agonists did, on the other hand, were unable to reliably induce tolerance when monocytes were prestimulated with those amounts of endotoxin (data not shown). Although, measurement of cytokine expression turned out to be not sufficient in adjusting the concentrations of the TLR agonists, the usage of higher MALP2 concentrations than 5 ng/ml and as low concentrations of LPS as possible were indicated by the observed data.

6.4.3 Intercellular adhesion molecule-1 (ICAM-1) expression as a marker of the activation level of stimulated human monocytes

Next, the cell surface expression of ICAM-1 (CD54) was investigated by FACS analysis in order to determine the activation level of monocytes after PAMP stimulation and to ensure a comparable pro-inflammatory state of the differently treated cells that were used in further glycoproteomic analysis. ICAM-1 expression is a well-known parameter to identify the pro-inflammatory state of cells (Audran et al. 1996, Anbarasan et al. 2015). Concentrations of LPS, Pam3CSK and MALP2 were chosen due to the tendencies determined in previously performed experiments, e.g. cytokine concentration series and experiments of tolerance induction (see Chapter 6.4.2). Purified monocytes were additionally stained with FITC-labeled anti-CD14 antibody (eBioscience, USA) to discriminate the monocytes population from other blood cells. Stimulated cells were either left unstained or stained with an APC-labeled anti-CD54 antibody (ImmunoTools, Germany) and subjected to flow cytometry analysis. As shown in Fig. 19, a high basal expression of ICAM-1

was found in unstimulated monocytes (MFI=3.2*10^3). ICAM-1 expression was significantly upregulated (3.8-fold for donor 1 and 3.9-fold for donor 2 as can be seen in Fig. 19), when monocytes were stimulated with the 50 ng/ml LPS (MFI=12.6*10^3), 200 ng/ml Pam3CSK (MFI=12.6*10^3) or 10 ng/ml MALP2 (MFI=12.0*10^3), indicating equivalent activation levels. This was observed in two independent experiments.

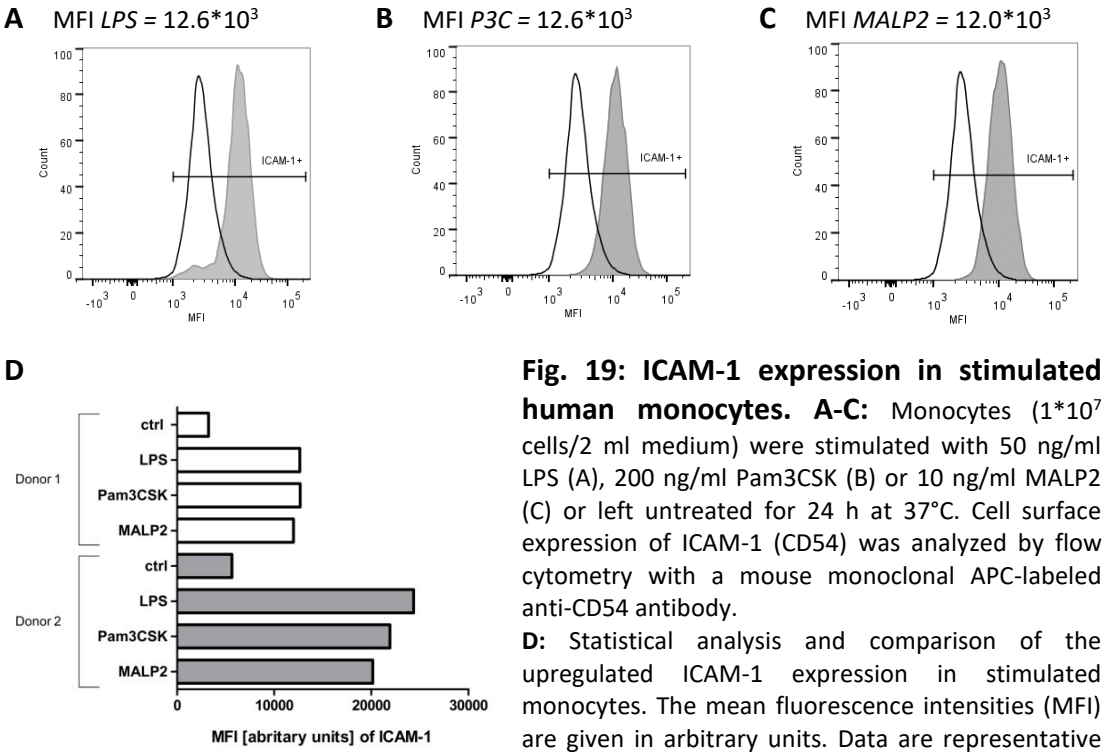

Fig. 19: ICAM-1 expression in stimulated human monocytes. A-C: Monocytes (1*10^7 cells/2 ml medium) were stimulated with 50 ng/ml LPS (A), 200 ng/ml Pam3CSK (B) or 10 ng/ml MALP2 (C) or left untreated for 24 h at 37°C. Cell surface expression of ICAM-1 (CD54) was analyzed by flow cytometry with a mouse monoclonal APC-labeled anti-CD54 antibody.
D: Statistical analysis and comparison of the upregulated ICAM-1 expression in stimulated monocytes. The mean fluorescence intensities (MFI) are given in arbitrary units. Data are representative for two independent experiments.

Therefore, further glycoproteomic studies were carried out using these concentrations of the stimuli named above.

6.5 Purity of monocytes for glycoproteomic analysis

Samples tested in the following glycoproteomic analysis have to be very pure and should contain exclusively monocytes. This is why the already MACS-sorted monocytes that were used for the stimulations with either LPS (50 ng/ml), Pam3CSK (200 ng/ml) or MALP2 (10 ng/ml) for 24 h or 48 h, were additionally labeled with an anti-CD14 antibody for a second purification step using fluorescence activated cell sorting (FACS analysis). To deplete contaminating platelets (anti-CD42b) and lymphocytes (anti-CD3 against T-lymphocytes and anti-CD19 against B-lymphocytes), these populations were labeled with the indicated antibodies and separated from CD14 positive cells in order to enrich the monocytic population (Fig. 20). Purity of CD14+ cells was increased to more than 97%. Unstimulated monocytes, that were always included as negative controls, showed poor survival after 48 hours of cultivation (data not shown).

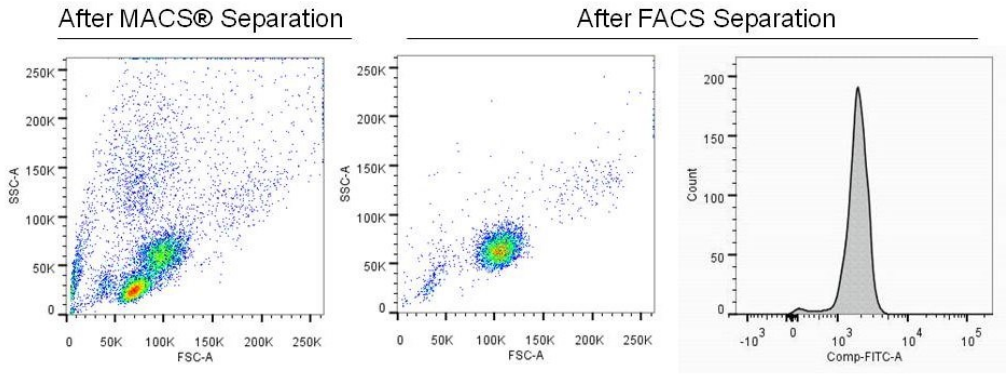

Fig. 20: Purification of monocytes via MACS® monocyte isolation kit and CD14+ fluorescence activated cell sorting (FACS). Purity of monocytes was assessed measuring the volume (FSC= forward scatter) and granularity (SSC=sideward scatter) of unstained cell fractions by flow cytometry analysis at different time points: 1. After MACS-separation and before incubation of the cells with the above-named stimuli. 2. After FACS-separation and prior to subsequent sample preparation for mass spectrometry analysis. High quality of monocyte isolation was ensured by additional staining against the monocyte surface marker CD14.

6.6 Mass spectrometry-based glycoprotein expression in monocytes

Analysis of whole membrane receptor profile of the differently treated monocytes was carried out in a glycoproteomic approach. Glycoproteomic data were assessed of monocytes stimulated with either LPS (50 ng/ml), Pam3CSK (200 ng/ml) or MALP2 (10 ng/ml) for 24 h and 48 h at 37°C in three independent experiments. Untreated cells were included for each experiment. Next, two different peptide fractions were gained by digesting the denatured, reduced and alkylated proteins bound to the UltraLink Hydrazide-Beads, first by the endoproteinase trypsin and in a second step by the added Peptide-N-Glycosidase F (PNGase F) (Details see chapter 5.8.8). Both fractions, the tryptic peptide fraction (TPF) from the first trypsin-digestion and the N-glycosylated peptide

fraction (NGF) from the second PNGase F-digestion, were subjected to subsequent analysis by liquid chromatography-tandem mass spectrometry (LC-MS/MS). Each biological replicate was measured in 3 technical replicates. Due to the poor survival rates of (especially not-stimulated) 48 hours-cultured monocytes, precise statistical data could be not obtained from the 48 hours-cultured monocytes. Only data of the 24 hours-cultured and stimulated monocytes were taken into consideration.

A similar number of glycoproteins (1003, 966 and 1033) were identified from each of the three biological replicates with a FDR of <0.01, respectively. These data were observed analyzing the whole data set and assuming 1 peptide being required for the identification of one protein. When using the threshold of a minimum of two unique peptides for the identification of one protein, we identified 802, 782 and 839 glycoproteins of donor 1, 2, and 3, respectively, but at the risk of missing possible glycoproteins, which contain only one glycosylation site (analysis based on the PNGase fraction). In total, 1210 annotated proteins were identified and quantified in the combined analysis of the NGP and TPG fractions of all stimulations, including 34 transient O-glycosylated (O-GlcNAc-modified) proteins which were excluded from further analysis. The hydrophobic transmembrane helix prediction algorithm (TMHMM v2.0 Server) revealed that 898 of the identified glycoproteins were predicted to contain at least one transmembrane domain (TMD) (Fig. 21).

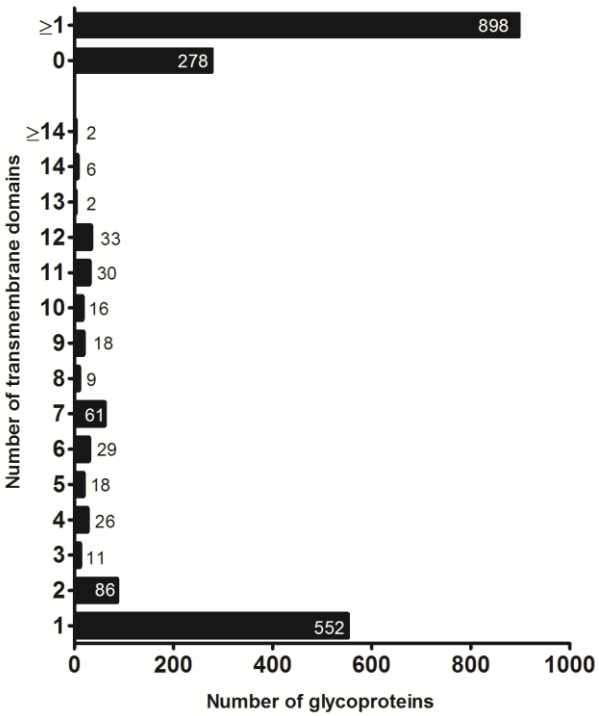

Fig. 21: Distribution of identified glycopro-teins according to the number of predicted transmembrane domains (TMDs).
Upper part: glycoproteins containing ≥1 or 0 TMD.
Lower part: TMD-comprising glycoproteins tabulated by number.

While the majority of 552 glycoproteins comprised one TMD, 346 (29.4%) glycoproteins were predicted to comprise two or more TMDs. Moreover, 61 of them were found to belong to the group

of seven transmembrane domain-containing proteins, which includes the group of drug-relevant G-protein coupled receptors being of major biomedical interest.

Next, we were interested in the subcellular localization of the identified glycoproteins. Based on subcellular compartment analysis, 617 glycoproteins (52%), and, therefore, the most abundant group, were annotated by gene ontology (GO) as “plasma membrane” associated (Fig. 22).

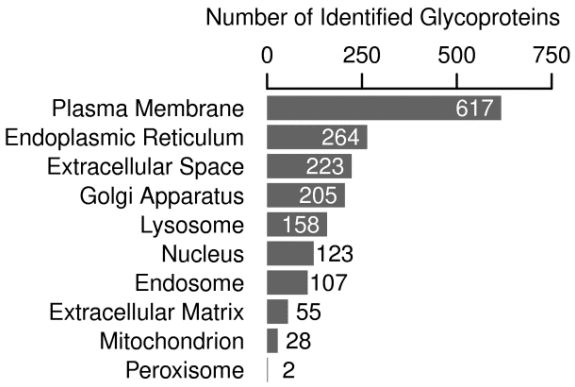

Fig. 22: Gene ontology-based cellular compo-nent analysis of all glycoproteins identified in monocytes.
Based on the identified glycoproteins in LC-MS/MS.

Proteins derived from the endoplasmic reticulum (264) and the golgi apparatus (205) formed together the second largest subset of about 40% when taking into account the non-exclusive assignment of the proteins to different subcellular compartments by gene ontology. Glycoproteins located in the lysosome (158), nucleus (123), endosome (107), mitochondrion (28) and peroxisome (2) were also identified. Besides these intracellular proteins, 223 glycoproteins were annotated as “extracellular space”, including secretory proteins, and 55 proteins were found to be part of the extracellular matrix.

6.6.1 LPS-, Pam3CSK- and MALP2-stimulated monocytes exhibit changes in their glycoprotein expression

For the purpose of identifying changes of the glycoprotein expression induced by LPS-, Pam3CSK- and MALP2-treatment, the glycoproteomes of untreated monocytes were compared to those stimulated for 24 hours. Fig. 23 shows differentially expressed glycoproteins in human monocytes depicted in a testing after stimulation with either LPS, Pam3CSK or MALP2. In total, 117 glycoproteins could be identified to be significantly regulated by at least one stimulus, of which the majority of 67 proteins was found upregulated. As the previously mentioned FACS analysis indicated, ICAM-1 that was previously chosen as marker-protein to adjust the concentrations of LPS, Pam3CSK and MALP2 stimuli showed very similar upregulated expression levels (3.56-fold, 3.23-fold and 3.10-fold, respectively) in the analyzed cells again.

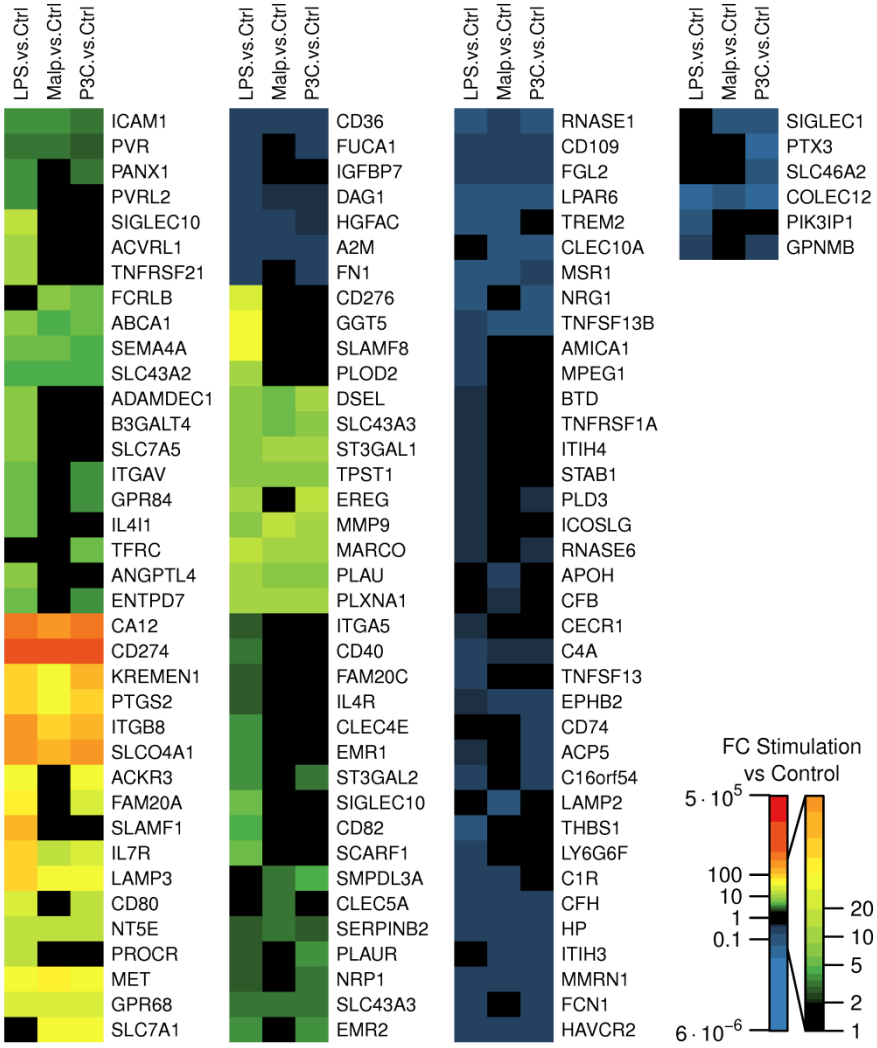

Fig. 23: Unpaired analysis: Significant up- or downregulated glycoproteins in LPS-, MALP2- and Pam3CSK-stimulated human monocytes. Heat map of glycoproteins significantly up- or downregulated in human monocytes post LPS, MALP2 or Pam3CSK treatment at 24 h according to unpaired analysis. As shown in the legend green, yellow and red boxes indicate upregulation, blue indicates

downregulation. Black boxes indicate either no fold change or fold changes reaching no significance. Gene names are given.

6.6.2 Comparison of the glycoprotein expression patterns of all three donors by Principal Component Analysis (PCA)

In order to visualize and compare the entire data set generated by combination of the glycoprotein expression patterns revealed for each donor and each stimulation, PCA was carried out reducing the dimensionality of the complex data (Fig. 24). The first two principal com-ponents (PC) accounted for >53% of the total data variance. Unstimulated control cells of all three donors showed considerably lower PC2 values compared to stimulated cells with either LPS, Pam3CSK or MALP2.

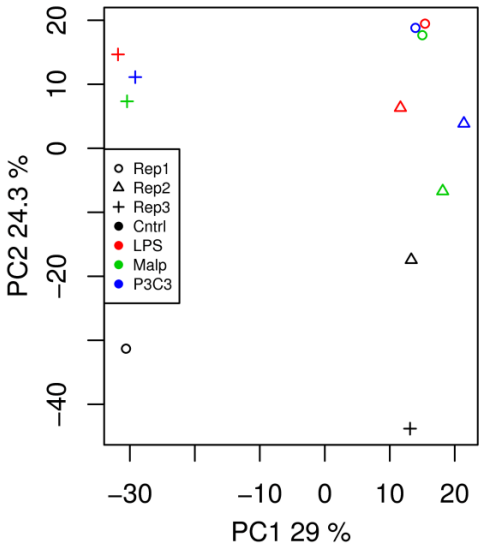

Fig. 24: Principal Component Analysis of the glycoprotein expression patterns all 3 replicates.
Each spot on the plot corresponds to one cell subpopulation of a donor, which was exposed to LPS (red), MALP2 (green) or Pam3CSK (blue) or left untreated (black) for 24 h. Replicate one is represented by circles, replicate two by triangles and replicate three by squares.

Although, PC2 values differed remarkably between the three controls, stimulated monocytes of all three donors, irrespective which stimulus was used, displayed similar shifts to higher PC2 values. Especially, the LPS-, Pam3CSK- and MALP2-treated cells of replicate 1 and 2 clustered in a very narrow range, indicating that these stimulated monocytes show similar glycoprotein expression profiles. The second observation one can make considering the whole spectra shown in Fig. 24 is that the values of the PC1 are widely scattered among the donors. In particular, PC1 values of donor 3 differ from those of replicate 1 and 2 and, therefore, causing the main variance of principal component 1. Besides contaminating non-glycosylated proteins, also differentially expressed HLA-proteins, were the glycoproteins found to have a major influence on PC1. This indicates that there is a higher variability among the different donors (interindividual differences + sample purity) than between the different stimuli. Therefore, a paired analysis was performed additionally.

6.6.3 Results of paired analysis

After paired analysis, all together, 135 glycoproteins showed significant alterations in their expression upon stimulation with either LPS, Pam3CSK or MALP2. LPS-treatment resulted in a significant up- or down-regulation of 119 glycoproteins, whereas both TLR2 agonists, Pam3CSK and MALP2, led to distinct changes in the expression of 83 and 75 glycoproteins, respectively (Fig. 25).

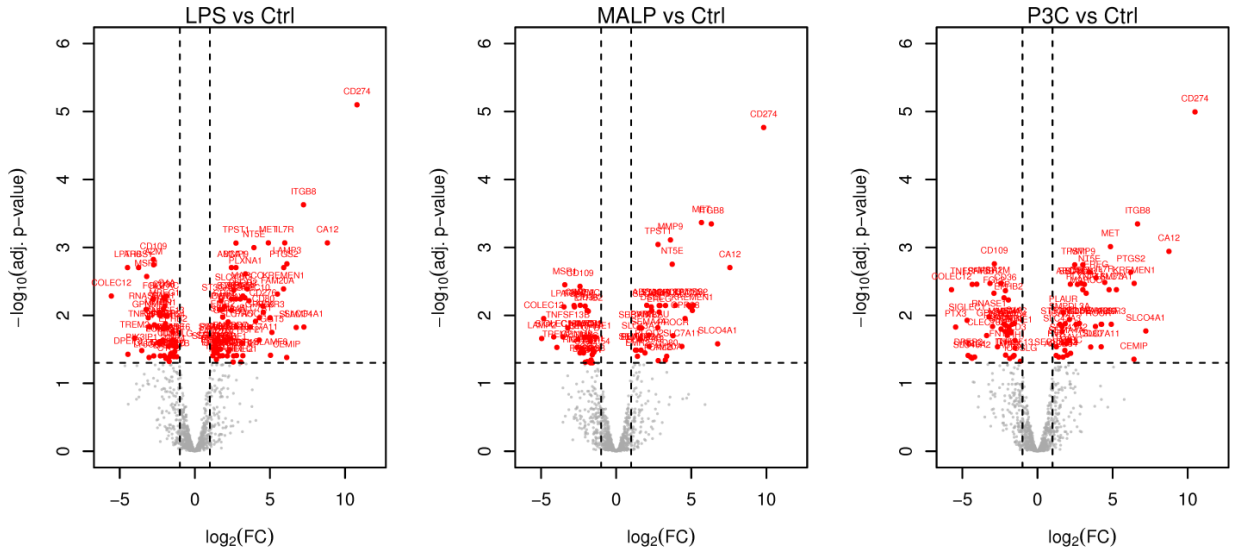

Fig. 25: Volcano plot of glycoproteins in LPS-, MALP2- and Pam3CSK-stimulated monocytes. The negative log of the t-test p-value was plotted against the protein fold change of differentially expressed glycoproteins after 24h of LPS (left), MALP2 (middle) and Pam3CSK (right) treatment. Red spots display significantly up- (upper right quadrant) or down- (upper left quadrant) regulated glycoproteins, while grey data points represent not significantly or unchanged proteins. Gene names are given.

Most of the glycoproteins displayed unaltered expression levels or alterations reached no significance (grey data points in the volcano plot; Fig. 25).

In total, 75 of 135, and, therefore, the majority of the significantly regulated glycoproteins, showed increased expression levels upon stimulation (Heat map, Fig. 26). 65 of them were integral members of the plasma membrane, while a large subset of 27 glycoproteins of the down regulated 60 glycoproteins was secreted or luminal localized. Expression of the LPS-sensing TLR4-receptor complex (consisting of TLR4, CD14 and MD-2) and the heterodimeric receptor complexes TLR2/1 and TLR2/6 for Pam3CSK and MALP2 were not affected in the course of the stimulation. Database for Annotation, Visualization and Integrated Discovery (DAVID) functional annotation clustering mapped 79 differentially expressed glycoproteins to 7 different Kyoto Encyclopedia of Genes and Genomes (KEGG) pathways, however, functional annotation clustering revealed no significant enrichment of these pathways. 18 glycoproteins were found to be involved in “cell adhesion” processes of which 11 demonstrated upregulated expression levels (CD274 molecule,

CD274; Integrin subunit beta 8, ITGB8; Atypical chemokine receptor 3, ACKR3; CD80 molecule, CD80; CD276 molecule, CD276; CD40 molecule, CD40; Integrin subunit alpha V, ITGAV; Scavenger receptor class F member 1, SCARF1; CD44 molecule, CD44; Intercellular adhesion molecule 1, ICAM1 and Poliovirus receptor, PVR (CD155 molecule)). Downregulated glycoproteins take mainly part in "complement and coagulation" signaling pathways (Alpha-2-macroglobulin, A2M; Complement C1r subcomponent, C1R; Complement factor H, CFH; Fibrinogen gamma chain, FGG; Complement C4-A, C4A; Prothrombin, F2; Plasminogen activator inhibitor 1, SERPINE1 and Complement factor B, CFB). Moreover, glycoproteins involved in the "acute phase" (F2; Fibronectin, FN1; Haptoglobin, HP and Inter-alpha-trypsin inhibitor heavy chain H4, ITIH4) and "inflammatory immune response" (C4A; Hepatitis A virus cellular receptor 2, HAVCR2 and Stabilin-1, STAB1) showed significantly decreased expression levels. HLA-DRA was not affected as previous data suggest (Wolk et al. 2000, del Fresno et al. 2009). The only MHC II-associated glycoprotein found to be significantly downregulated was CD74.

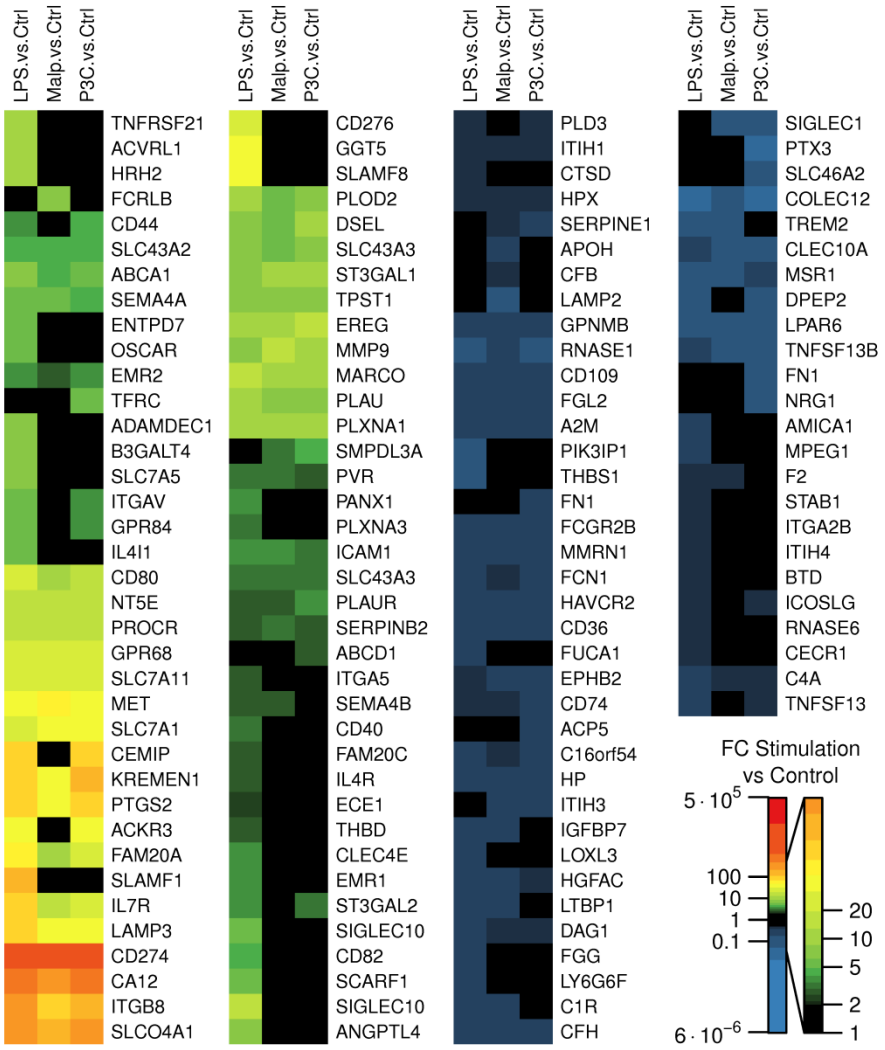

Fig. 26: Paired analysis: Significant up- or downregulated glycoproteins in LPS-, MALP2- or Pam3CSK-stimulated human monocytes. Heat map of glycoproteins significantly up- or downregulated in human monocytes post LPS, MALP2 or Pam3CSK treatment at 24 h according to paired analysis. As shown in the legend green, yellow and red boxes indicate upregulation, blue indicates downregulation. Black boxes indicate either no fold change or fold changes reaching no significance. Gene names are given.

Data of the heat map (Fig. 26) may, at first sight, give the impression of some glycoproteins (e.g. CD276; Signaling lymphocytic activation molecule family member 8, SLAMF8) to be specifically regulated by only one stimulus, because of 55 glycoproteins displaying altered expression levels that reach significance only in one of the three treatments (43 by LPS-, 8 by Pam3CSK- and 4 by MALP2-stimulation). However, these trends and tendencies might be artificial, taking into account that stimulation with one of the two other stimuli led to similar up- or downregulation of the glycoprotein expression, although these alterations did not reach significance (black boxes in the heat map). As can be seen in table 21, fold changes of these glycoproteins are comparable irrespectively of the stimulus.

Table 21: LPS-, Pam3CSK- and MALP2-regulated glycoproteins and their FCs at 24 h compared to unstimulated controls.

A: Significantly upregulated glycoproteins, at least one protein demonstrating more than >2 FC.

B: Significantly downregulated glycoproteins.

A	**Upregulated glycoproteins**		FC (Stimulus vs. ctrl)		
Gene name	Accession	Protein name	LPS	MALP	P3C
Membrane bound					
CD274	Q9NZQ7	Programmed cell death ligand 1	1781,20	905,32	1431,59
CA12	O43570	Carbonic anhydrase 12	453,95	190,17	430,94
SLCO4A1	Q96BD0	Solute carrier organic anion transporter family member 4A1	153,26	108,22	147,79
ITGB8	P26012	Integrin beta-8	150,34	80,42	101,49
SLAMF1	Q13291	Signaling lymphocytic activation molecule	107,23	11,46	33,46
LAMP3	Q9UQV4	Lysosome-associated membrane glycoprotein 3	70,00	28,06	27,26
IL7R	P16871	Interleukin-7 receptor subunit alpha	63,16	15,41	22,20
KREMEN1	Q96MU8	Kremen protein 1	59,75	33,51	86,90
FAM20A	Q96MK3	Protein FAM20A	45,23	9,68	19,19
GGT5	P36269	Gamma-glutamyltransferase 5	34,90	7,18	4,26
SLAMF8	Q9P0V8	SLAM family member 8	32,77	12,03	2,93
ACKR3	P25106	Atypical chemokine receptor 3	32,22	10,34	30,19
MET	P08581	Hepatocyte growth factor receptor	29,64	51,10	29,02
CD80	P33681	T-lymphocyte activation antigen CD80	23,57	10,31	11,70
CD276	Q5ZPR3	CD276 antigen	23,07	3,90	4,62
GPR68	Q15743	Ovarian cancer G-protein coupled receptor 1	19,78	24,09	18,84
SLC7A11	Q9UPY5	Cystine/glutamate transporter	19,59	20,84	18,93
SLC7A1	P30825	High affinity cationic amino acid transporter 1	16,43	30,15	37,96
NT5E	P21589	5-nucleotidase	15,30	13,29	10,97
PROCR	Q9UNN8	Endothelial protein C receptor	13,01	13,77	14,50
SIGLEC10	Q96LC7	Sialic acid-binding Ig-like lectin 10	12,14	1,90	3,97
MARCO	Q9UEW3	Macrophage receptor MARCO	11,32	9,71	9,48
PLXNA1	Q9UIW2	Plexin-A1	10,34	7,27	8,08
ACVRL1	P37023	Serine/threonine-protein kinase receptor R3	9,17	2,02	5,20
TNFRSF21	O75509	Tumor necrosis factor receptor superfamily member 21	8,75	2,22	5,88
HRH2	P25021	Histamine H2 receptor	8,40	1,94	5,67
EREG	O14944	Proepiregulin; Epiregulin	8,14	7,30	14,96
SLC7A5	Q01650	Large neutral amino acids transporter small subunit 1	6,73	3,10	4,19
ST3GAL1	Q11201	CMP-N-acetylneuraminate-beta-galactosamide-alpha-2,3-sialyltransferase 1	6,69	7,54	8,71
TPST1	O60507	Protein-tyrosine sulfotransferase 1	6,69	6,92	5,56
SLC43A3	Q8NBI5	Solute carrier family 43 member 3	6,00	5,05	6,32
B3GALT4	O96024	Beta-1,3-galactosyltransferase 4	5,98	3,26	2,29
DSEL	Q8IZU8	Dermatan-sulfate epimerase-like protein	5,42	5,13	7,56
ABCA1	O95477	ATP-binding cassette sub-family A member 1	5,41	4,08	4,58
ITGAV	P06756	Integrin alpha-V	5,39	2,91	3,53
ENTPD7	Q9NQZ7	Ectonucleoside triphosphate diphosphohydrolase 7	5,08	1,86	3,68

SCARF1	Q141623	Scavenger receptor class F member 1	4,96	2,40	1,72
SIGLEC10	Q96LC7	Sialic acid-binding Ig-like lectin 10	4,73	1,73	2,30
SEMA4A	Q9H3S1	Semaphorin-4A	4,63	4,50	3,77
GPR84	Q9NQS5	G-protein coupled receptor 84	4,51	2,51	3,27
OSCAR	Q8IYS5	Osteoclast-associated immunoglobulin-like receptor	4,46	1,94	3,85
SLC43A2	Q8N370	Large neutral amino acids transporter small subunit 4	4,03	3,79	4,20
CD82	P27701	CD82 antigen	3,92	2,25	2,08
TFRC	P02786	Transferrin receptor protein 1	3,64	2,40	4,60
EMR2	Q9UHX3	EGF-like module-containing mucin-like hormone receptor-like 2	3,60	2,67	3,60
CD44	P16070	CD44 antigen	3,60	3,58	3,95
ICAM1	P05362	Intercellular adhesion molecule 1	3,56	3,23	3,10
FCRLB	Q6BAA4	Fc receptor-like B	3,40	6,96	5,27
ST3GAL2	Q16842	CMP-N-acetylneuraminate-beta-galactosamide-alpha-2,3-sialyltransferase 2	3,35	1,92	2,81
PANX1	Q96RD7	Pannexin-1	3,28	2,69	2,87
CLEC4E	Q9ULY5	C-type lectin domain family 4 member E	3,21	1,97	2,30
EMR1	Q14246	EGF-like module-containing mucin-like hormone receptor-like 1	3,19	2,07	2,58
PVR	P15151	Poliovirus receptor	3,12	2,91	2,39
SLC43A3	Q8NBI5	Solute carrier family 43 member 3	2,81	3,05	3,10
PLXNA3	P51805	Plexin-A3	2,81	2,54	2,61
CD40	P25942	Tumor necrosis factor receptor superfamily member 5	2,78	1,57	1,90
THBD	P07204	Thrombomodulin	2,71	1,79	1,66
FAM20C	Q8IXL6	Extracellular serine/threonine protein kinase FAM20C	2,61	1,63	1,95
IL4R	P24394	Interleukin-4 receptor subunit alpha	2,57	1,55	1,90
PLAUR	Q03405	Urokinase plasminogen activator surface receptor	2,45	2,43	3,28
SEMA4B	Q9NPR2	Semaphorin-4B	2,43	2,55	1,93
ITGA5	P08648	Integrin alpha-5	2,40	2,05	1,87
ECE1	P42892	Endothelin-converting enzyme 1	2,29	1,67	1,63
ABCD1	P33897	ATP-binding cassette sub-family D member 1	1,84	1,66	2,67
Secreted or luminal localized					
CEMIP	Q8WUJ3	Cell migration-inducing and hyaluronan-binding protein	69,35	21,56	85,53
PTGS2	P35354	Prostaglandin G/H synthase 2	60,76	35,28	74,21
PLAU	P00749	Urokinase-type plasminogen activator	10,03	6,85	6,96
PLOD2	O00469	Procollagen-lysine,2-oxoglutarate 5-dioxygenase 2	9,18	4,59	5,92
ANGPTL4	Q9BY76	Angiopoietin-related protein 4	6,86	2,01	4,55
MMP9	P14780	Matrix metalloproteinase-9	6,67	12,23	8,07
ADAMDEC1	O15204	ADAM DEC1	5,85	2,85	2,65
IL4I1	Q96RQ9	L-amino-acid oxidase	4,74	2,99	3,08
SERPINB2	P05120	Plasminogen activator inhibitor 2	2,37	3,04	2,36
SMPDL3A	Q92484	Acid sphingomyelinase-like phosphodiesterase 3a	1,54	3,15	4,37

B	**Downregulated glycoproteins**		FC (Stimulus vs. ctrl)		
Gene name	Accession	Protein name	LPS	MALP	P3C
Membrane bound					
COLEC12	Q5KU26	Collectin-12	0,02	0,04	0,02
LPAR6	P43657	Lysophosphatidic acid receptor 6	0,05	0,09	0,06
TREM2	Q9NZC2	Triggering receptor expressed on myeloid cells 2	0,06	0,07	0,13
PIK3IP1	Q96FE7	Phosphoinositide-3-kinase-interacting protein 1	0,09	0,30	0,17
NRG1	Q02297	Neuregulin-1	0,10	0,19	0,06
RNASE1	P07998	Ribonuclease pancreatic	0,11	0,19	0,11
MSR1	P21757	Macrophage scavenger receptor types I and II	0,11	0,09	0,11
GPNMB	Q14956	Transmembrane glycoprotein NMB	0,12	0,16	0,13
LY6G6F	Q5SQ64	Lymphocyte antigen 6 complex locus protein G6f	0,12	0,16	0,41
TNFSF13B	Q9Y275	Tumor necrosis factor ligand superfamily member 13B	0,13	0,11	0,05
CD109	Q6YHK3	CD109 antigen	0,15	0,19	0,14
CLEC10A	Q8IUN9	C-type lectin domain family 10 member A	0,15	0,09	0,10
FGG	P02679	Fibrinogen gamma chain	0,20	0,28	0,33
AMICA1	Q86YT9	Junctional adhesion molecule-like	0,23	0,78	0,43
FCGR2B	P31994	Low affinity immunoglobulin gamma Fc region receptor II-b	0,23	0,26	0,18
DAG1	Q14118	Dystroglycan; Alpha-dystroglycan;Beta-dystroglycan	0,24	0,33	0,30
HAVCR2	Q8TDQ0	Hepatitis A virus cellular receptor 2	0,24	0,24	0,24
CD36	P16671	Platelet glycoprotein 4	0,24	0,26	0,23
SLC46A2	Q9BY10	Thymic stromal cotransporter homolog	0,24	0,20	0,05
HGFAC	Q04756	Hepatocyte growth factor activator	0,24	0,24	0,31
MPEG1	Q2M385	Macrophage-expressed gene 1 protein	0,25	0,58	0,51
TNFSF13	O43508	Tumor necrosis factor ligand superfamily member 13	0,26	0,38	0,34
C16orf54	Q6UWD8	Transmembrane protein C16orf54	0,28	0,33	0,26
CD74	P04233	HLA class II histocompatibility antigen gamma chain	0,30	0,32	0,23
CECR1	Q9NZK5	Adenosine deaminase CECR1	0,30	0,39	0,37
STAB1	Q9NY15	Stabilin-1	0,32	0,45	0,48
RNASE6	Q93091	Ribonuclease K6	0,36	0,53	0,42
ITIH1	P19827	Inter-alpha-trypsin inhibitor heavy chain H1	0,36	0,36	0,35
EPHB2	P29323	Ephrin type-B receptor 2	0,36	0,28	0,26
PLD3	Q8IV08	Phospholipase D3	0,37	0,44	0,36
ITGA2B	P08514	Integrin alpha-IIb	0,38	0,41	0,49
ICOSLG	O75144	ICOS ligand	0,43	0,57	0,46
SIGLEC1	Q9BZZ2	Sialoadhesin	0,65	0,06	0,04
LAMP2	P13473	Lysosome-associated membrane glycoprotein 2	0,66	0,03	0,66
Secreted or luminal localized					
DPEP2	Q9H4A9	Dipeptidase 2	0,05	0,09	0,04
FN1	P02751	Fibronectin	0,07	0,16	0,05
THBS1	P07996	Thrombospondin-1	0,08	0,53	0,53
FGL2	Q14314	Fibroleukin	0,15	0,15	0,13
A2M	P01023	Alpha-2-macroglobulin	0,15	0,24	0,19
C1R	P00736	Complement C1r subcomponent	0,15	0,17	0,25

IGFBP7	Q16270	Insulin-like growth factor-binding protein 7	0,18	0,22	0,32
CFH	P08603	Complement factor H	0,19	0,14	0,25
LOXL3	P58215	Lysyl oxidase homolog 3	0,19	0,24	0,42
MMRN1	Q13201	Multimerin-1	0,20	0,24	0,22
FCN1	O00602	Ficolin-1	0,23	0,31	0,23
FN1	P02751	Fibronectin	0,23	0,33	0,16
FUCA1	P04066	Tissue alpha-L-fucosidase	0,24	0,27	0,25
LTBP1	Q14766	Latent-transforming growth factor beta-binding protein 1	0,26	0,24	0,36
HP	P00738	Haptoglobin	0,27	0,19	0,21
C4A	P0C0L4	Complement C4-A	0,27	0,38	0,34
CTSD	P07339	Cathepsin D	0,31	0,36	0,33
ACP5	P13686	Tartrate-resistant acid phosphatase type 5	0,32	0,33	0,28
F2	P00734	Prothrombin	0,32	0,32	0,45
HPX	P02790	Hemopexin	0,33	0,33	0,32
PTX3	P26022	Pentraxin-related protein PTX3	0,34	0,13	0,02
ITIH3	Q06033	Inter-alpha-trypsin inhibitor heavy chain H3	0,38	0,21	0,23
ITIH4	Q14624	Inter-alpha-trypsin inhibitor heavy chain H4	0,40	0,43	0,50
APOH	P02749	Beta-2-glycoprotein 1	0,43	0,28	0,45
BTD	P43251	Biotinidase	0,43	0,50	0,64
SERPINE1	P05121	Plasminogen activator inhibitor 1	0,50	0,30	0,30
CFB	P00751	Complement factor B	0,54	0,31	0,48

The previous findings already indicated that changes of the monocytes glycoproteome tend to be very similar among the different stimuli (see FC table above). In a new statistical approach, fold changes (FCs) of significantly regulated glycoproteins induced by LPS treatment were calculated against FCs of significantly regulated glycoproteins from monocytes exposed to MALP2 or Pam3CSK (Fig. 27). The same was done with FCs of glycoproteins measured in MALP2- and Pam3CSK-stimulated cells, respectively. In this linear regression model we obtained a pearson ratio (ρ) of 0.949, 0.965 and 0.955 analyzing LPS vs. MALP2, MALP2 vs. Pam3CSK and Pam3CSK vs. LPS stimulation. The data indicate that most of the glycoproteins found to be regulated by LPS treatment of monocytes, were also regulated highly similar in cells that were stimulated with Pam3CSK or MALP2.

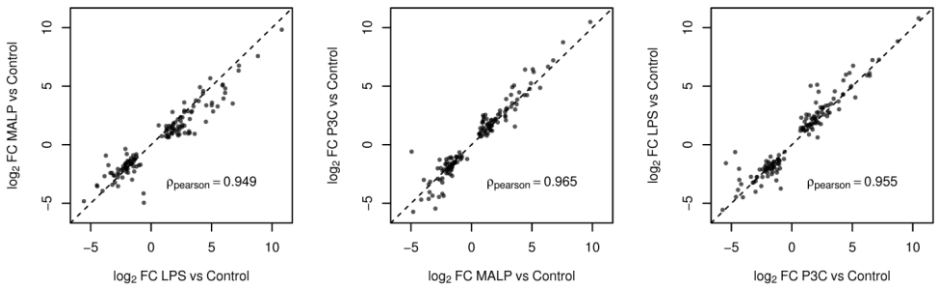

Fig. 27: Linear regression model of the glycoprotein expression of the differently treated monocytes. Pearson correlation was carried out calculating fold changes (FCs) of significantly up- or

downregulated glycoproteins of the different stimulations (Left: LPS vs. MALP2, Middle: MALP2 vs. Pam3CSK, Right: Pam3CSK vs. LPS) against each other. Pearson correlation coefficient (ρ) is given.

6.6.4 Subcellular localization of significantly regulated glycoproteins

In a next step, we analyzed if the distribution of significantly regulated glycoproteins among the different stimuli showed a distinct expression pattern regarding their subcellular location. Glycoproteins annotated as "plasma membrane" associated were not only the most abundant group of identified proteins, but included also the largest number of significantly regulated glycoproteins (Fig. 28). Upon exposure towards LPS, Pam3CSK and MALP2, the majority of regulated proteins derived from the plasma membrane, golgi apparatus and endoplasmic reticulum demonstrated increased expression levels. The second largest subset of proteins, showing distinctly altered expression levels, was annotated as "extracellular space". Together with glycoproteins denoted as belonging to the "extracellular matrix", they exhibited a slight tendency to be down regulated more often. Minor expression changes were detectable in proteins derived from the nucleus, lysosome and endosome. The different TLR agonists resulted in comparable expression changes of glycoproteins located in different cellular organells.

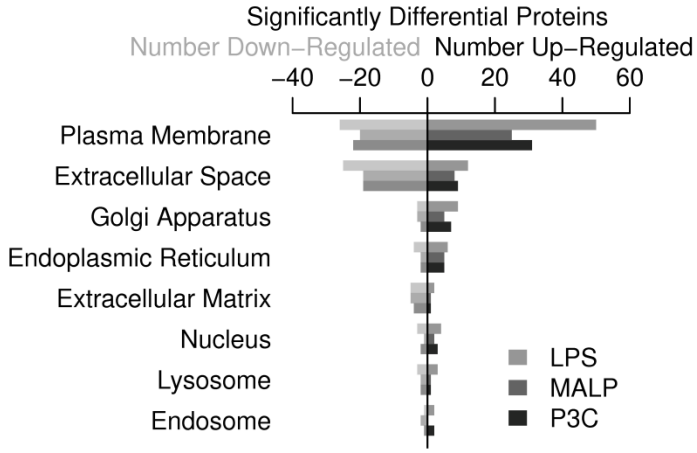

Fig. 28: Cellular component analysis of LPS-, MALP2- and Pam3CSK-regulated gly-coproteins.
Distribution of significantly different expressed glycoproteins after LPS (light grey bar), MALP2 (dark grey bar) or Pam3CSK (black bar) treatment in cellular organells assessed by LC-MS/MS.

6.6.5 Comprehensive analysis of CD antigen expression in the tolerant monocyte cell state

The majority of proteins affected by LPS, Pam3CSK and MALP2 treatment belonged to the subset of "plasma membrane" associated glycoproteins as shown in Fig. 29. Therefore, we further analyzed the CD antigen expression profile of unstimulated and treated monocytes in order to distinguish a specific CD antigen phenotype associated with the tolerant state.

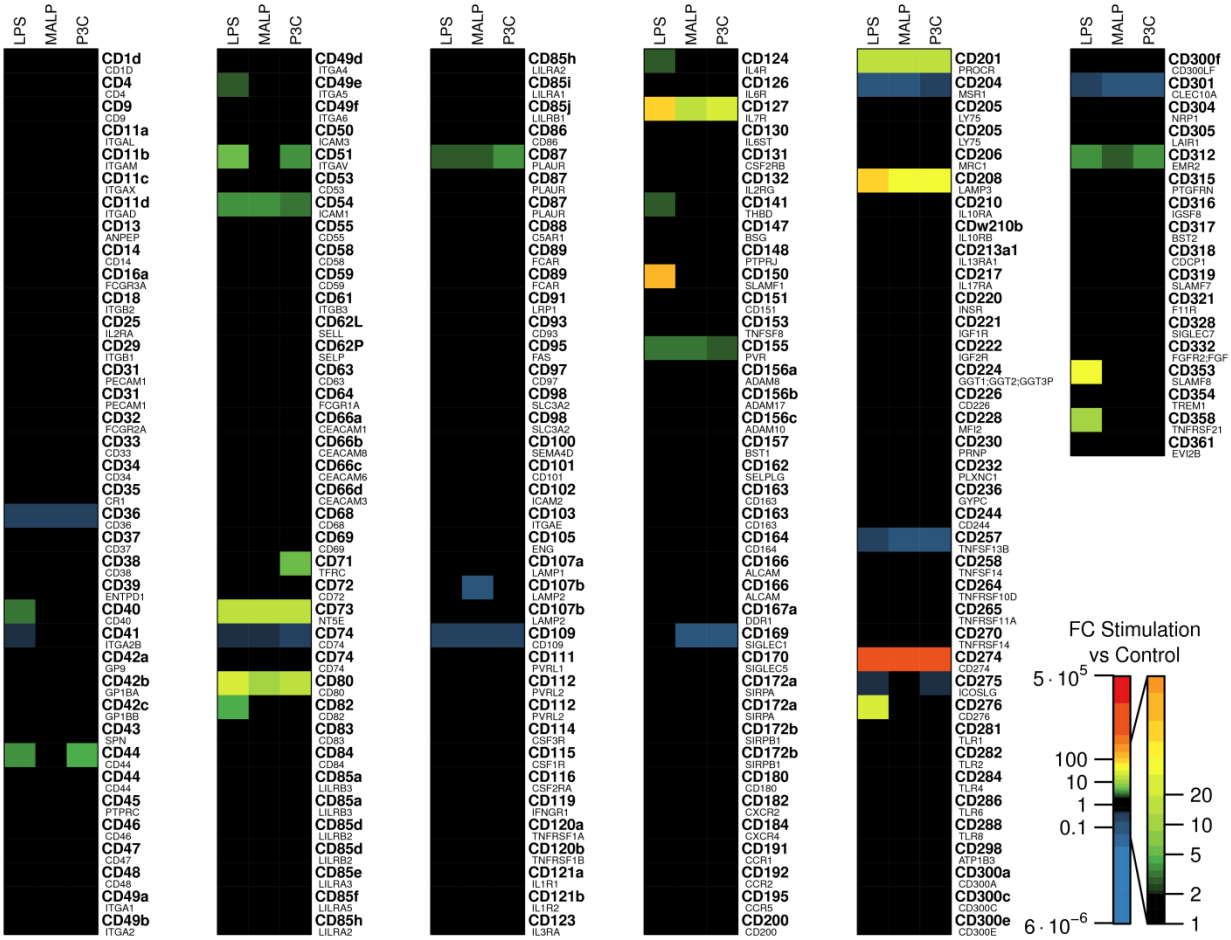

Fig. 29: CD antigen expression in stimulated monocytes. Heat map of CD antigens significantly up- or down-regulated in human monocytes by LPS, MALP2 or Pam3CSK treatment at 24 h. As shown in the legend green, yellow and red boxes indicate upregulation, blue indicates downregulation. Black boxes indicate either no fold change or fold changes reaching no significance. Gene names are given.

Altogether, 202 CD antigens expressed by human monocytes were identified, of which 32 showed distinct alterations in their expression when the cells were exposed to LPS, Pam3CSK or MALP2. Thus, CD antigens represent with 23.7% a large part of all 135 significantly up- or downregulated glycoproteins. The tolerant state after 24 h of prestimulation was predominantly associated with increased expression of CD molecules as 22 of the 32 detected and significantly regulated CD antigens showed a distinct upregulation of their expression, including Programmed cell death-ligand 1 (PD-L1, CD274), SLAM family member 1 (SLAMF1, CD150), Lysosome-associated

membrane glycoprotein 3 (LAMP3, CD208), Interleukin-7 receptor subunit (IL7R, CD127) as well as several others. Database for Annotation, Visualization and Integrated Discovery (DAVID) functional annotation clustering mapped 19 of the 22 upregulated CD molecules to 5 different KEGG pathways. As already described above, especially, CD antigens involved in cell adhesion processes like CD274, CD80, CD276, ITGAV (CD 51), CD44, ICAM-1 (CD54), PVR (CD155) and CD40 were observed to be significantly enriched and highly upregulated in the tolerant state, when significantly regulated CD antigens were searched against all 1176 identified glycoproteins (data not shown). However, adjusted p-values received by Benjamini-Hochberg multiple testing revealed no significant enrichments. Functional annotation clustering of the 10 down regulated CD antigens, e.g. Macrophage scavenger receptor types I and II (MSR1, CD204), TNF super family member 13B (CD257) and CD109 antigen, did not reveal any enrichment in functionality.

6.6.6 Modification of glycosylation enzyme expression in tolerant monocytes

The glycosylation pattern of glycoproteins is well-known to have a great impact on processes like enzyme activity, cell signaling, cell adhesion and numerous other processes (Dewald et al. 2016). Moreover, changes in the glycosylation might derogate the enrichment and quantification on protein level. Thus, we examined if expression levels of enzymes involved in the post-translational glycan maturation (GO-category: “protein glycosylation”; GO:0006486) showed distinct alterations in monocytes stimulated with LPS, Pam3CSK or MALP2 (Fig. 30). In total, 75 glycoproteins involved in glycosylation activities could be identified and quantified in the whole data set with only four showing altered expression levels. Three of them were upregulated (ST3 beta-galactoside alpha-2,3-sialyltransferase 1, ST3GAL1; Beta-1,3-galactosyl-transferase 4, B3GALT4 and ST3 beta-galactoside alpha-2,3-sialyltransferase 2, ST3GAL2) and just one (Thrombospondin 1, THBS1) displayed decreased expression levels upon stimulation with LPS, Pam3CSK and MALP2.

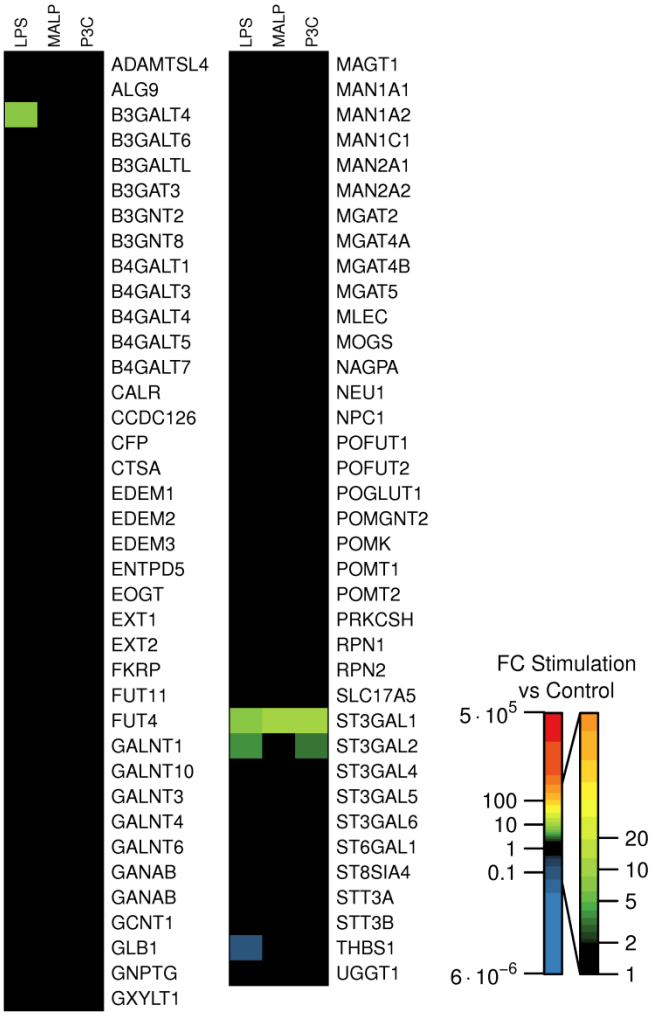

Fig. 30: Overview of 75 proteins annotated as being involved in various steps of "protein glycosylation" (GO:0006486).
Significance according to the color given in the legend.

Among the 3 elevated enzymes, two golgi apparatus-resident sialyltransferases, ST3GAL1 and ST3GAL2, could be identified, catalyzing the transfer of sialic acid in an α-2,3-linkage to terminal galactose residues on glycoproteins or glycolipids and, thereby, contributing to cell adhesion processes (Wu et al. 2016). The third upregulated glycosylation enzyme, B3GALT4, exhibits diverse enzyme functions, using different donor and acceptor sugars. The downregulated THBS1, annotated by GO to the category "proteins involved in protein glycosylation", is a subunit of a disulfide-linked homotrimeric, adhesive glycoprotein that, besides mediating cell-cell interaction, plays a major role in the activation of latent TGF-β (Schultz-Cherry et al. 1994). In summary, these results indicate no major changes in the glycosylation of the proteins which might have affected enrichment and quantification in course of LC-MS/MS analysis.

6.6.7 Changes of G protein-coupled receptor expression in tolerant monocytes

G protein-coupled receptors (GPCRs), a family of N-glycosylated seven-transmembrane domain receptors, act as the targets of over 40% of marketed drugs and, therefore, display to be of special biomedical interest (Lu and Wu 2016). Thus, expression and expression changes were examined in more detail revealing 54 proteins annotated as proteins with "G protein-coupled receptor activity" (GO:0004930) to be expressed in unstimulated monocytes (Fig. 31). Seven of them showed significantly up- or downregulated expression levels upon stimulation with LPS, Pam3CSK or MALP2. Lysophosphatidic acid receptor 6 (LPAR6) was found to be strongly down regulated whereas all other altered GPCRs, including Atypical chemokine receptor 3, ACKR3; G protein-coupled receptor 68, GPR68; G protein-coupled receptor 84, GPR84; Egf-like module containing, mucin-like, hormone receptor-like 1 and 2, EMR1, EMR2 and Histamine receptor H2, HRH2 demonstrated upregulated expression levels.

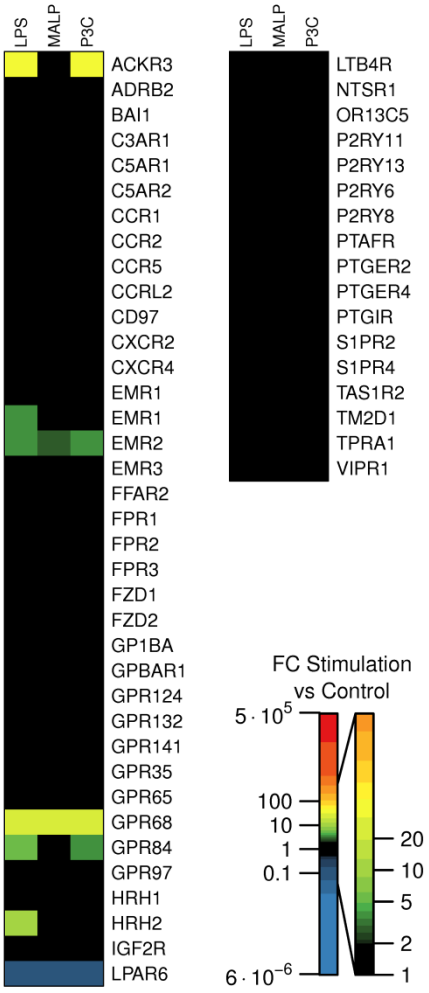

Fig. 31: Overview of 54 proteins annotated as proteins with "G protein-coupled receptor activity" (GO:0004930).
Significance according to the color given in the legend.

6.7 Confirmation of glycoproteomic data via qPCR, FACS and immunoblot analysis

In order to confirm the results obtained from mass spectrometry analysis, protein expression of several identified glycoproteins were checked by qPCR, FACS or western blot analysis.

Expression of ITGB8, LAMP3, MMP9, GPR84 and DPEP2 were measured by qPCR analysis in purified human monocytes stimulated with or without 50 ng/ml LPS for 2, 8, 24 or 48 h (Fig. 32). qPCR analysis revealed significantly upregulated expression levels of ITGB8 and LAMP3 in LPS-stimulated monocytes at all time points (ITGB8: 14, 36, 25 and 10 FCs and LAMP3: 10, 16, 29 and 22 FCs after 2, 8, 24 and 48 h of LPS-stimulation, respectively). MMP9 expression was not increased at the first two time points (FCs of about 1 after 2 h and 8 h), but significantly enhanced after 24 and 48 h of LPS-treatment (34 and 29 FCs, respectively). Although expression levels of GPR84 reached not significance, qPCR analysis demonstrated upregulated transcriptional levels of GPR84 at all time points. DPEP2, a glycoprotein found significantly downregulated in our glycoproteomic analysis, showed decreased expression levels of 0.06, 0.22 and 0. 66 FCs when monocytes were stimulated for 8, 24 or 48 h with LPS. However, only the 8 h-LPS-incubation period, which led to the greatest decrease of DPEP2 expression in monocytes, reached significance. Altogether, qPCR analysis revealed gene expression of differentially expressed glycoproteins of our glycoproteomic data set to be similarly regulated on transcriptional level.

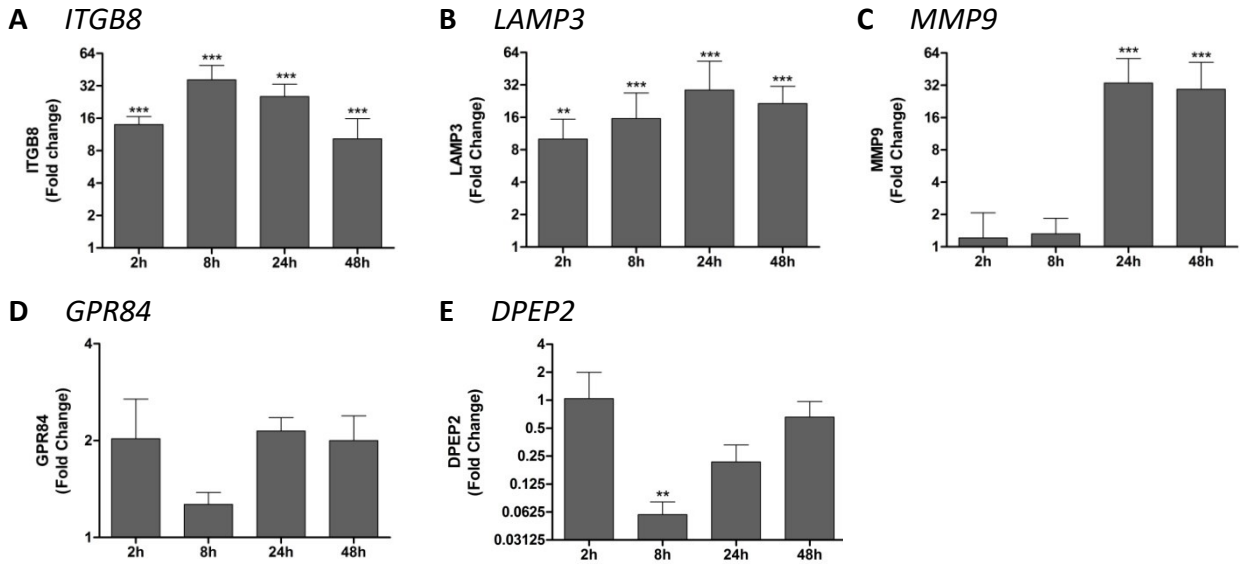

Fig. 32: qPCR analysis of LPS-induced ITGB8, LAMP3, MMP9, GPR84 and DPEP2 gene expression in purified human monocytes. A-E: Monocytes (4*10^{6}cells/2 ml) were stimulated with or without LPS *E. coli* O111:B4 (50 ng/ml) for 2, 8, 24 and 48 h, always including untreated cells as negative control. The gene expression was normalized to the housekeeping gene HPRT. Data represent mean values (± SD) from three independent experiments. ** p<0.01*** p<0.001.

Moreover, differential expression of 6 further identified glycoproteins was confirmed by FACS analysis. Therefore, MACS-separated monocytes gained from two different donors were stimulated with or without 50 ng/ml LPS for 24 or 48 h (Fig. 33). FACS analysis demonstrated upregulated cell surface expression of CD80, IL7R (CD127), PD-L1 (CD274) and SLAMF7 (CD319) at both time points, which have also shown increased expression levels in the previously obtained glycoproteomic data. LC-MS/MS-analysis has revealed reduced expression of CLEC12A (CD371) and FACS analysis confirmed decreased protein abundance of CLEC12A on the cell surface at both time points. CD86 that has been observed to be not regulated in monocytes stimulated for 24 h with LPS in our glycoproteomic data set, also showed unaltered cell surface expression after 24 h and decreased expression levels after 48 h of LPS-treatment.

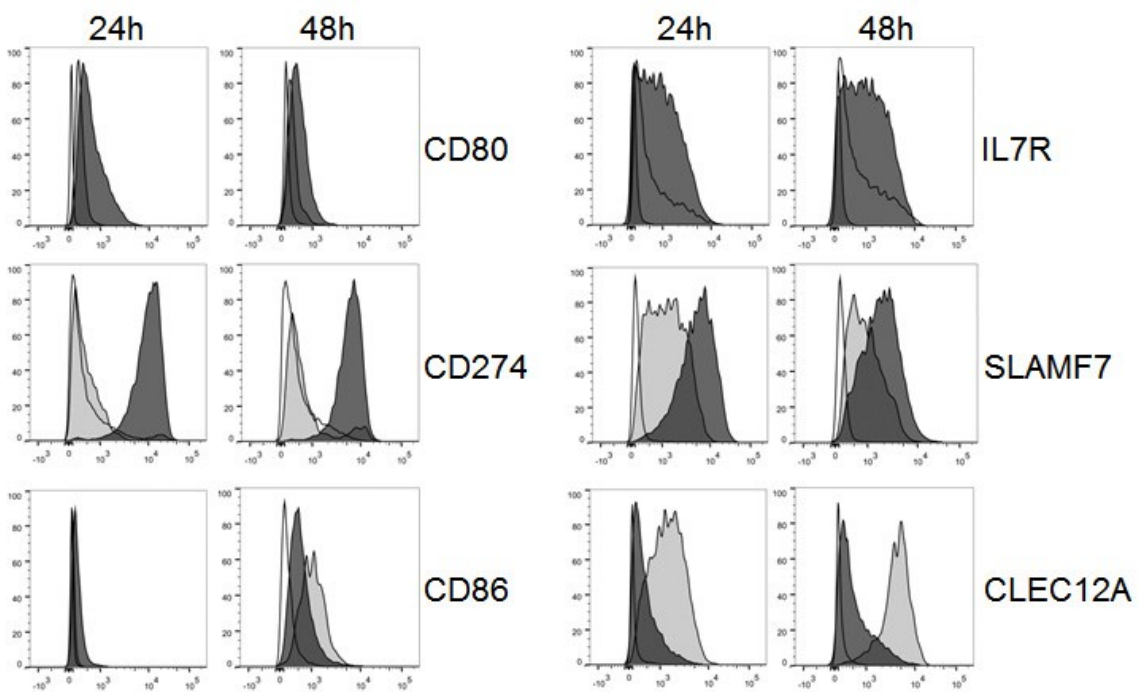

Fig. 33: Verification of proteomic results by FACS analysis: cell surface expression of CD80, IL7R, PD-L1, SLAMF7, CD86 and CLEC12A. Monocytes were stimulated for 24 h or 48 h with or without LPS *E. coli* O111:B4 (50 ng/ml) and labeled with specific fluorescent-dye conjugated antibodies (anti-CD14, anti-CD80, anti- CD127(IL7R) , anti-CD274 (PD-L1), anti- CD319 (SLAMF7), anti-CD86, anti-371 (CLEC12A)). White graphs: isotype controls, in light grey: expression at the indicated time point of unstimulated controls, in dark grey: expression at the indicated time points after LPS treatment. The data shown are representative of two different donors independently analyzed. Depicted are the intensity levels of the indicated proteins expressed on the CD14+ cell population.

In a third approach to confirm the obtained glycoproteomic data, expression of CEACAM-6 and TLR4 were quantitatively measured by western blot analysis (Fig. 34). MACS-separated monocytes were stimulated for 24 h with either LPS (50 ng/ml), Pam3CSK (200 ng/ml), MALP2 (10 ng/ml) or were left untreated. Mass spectrometry analysis has revealed unaltered expression levels for both selected target proteins. As shown in Fig. 34, LPS-, Pam3CSK- and MALP2-treatment of monocytes did not modulate the expression of CEACAM-6 and TLR4.

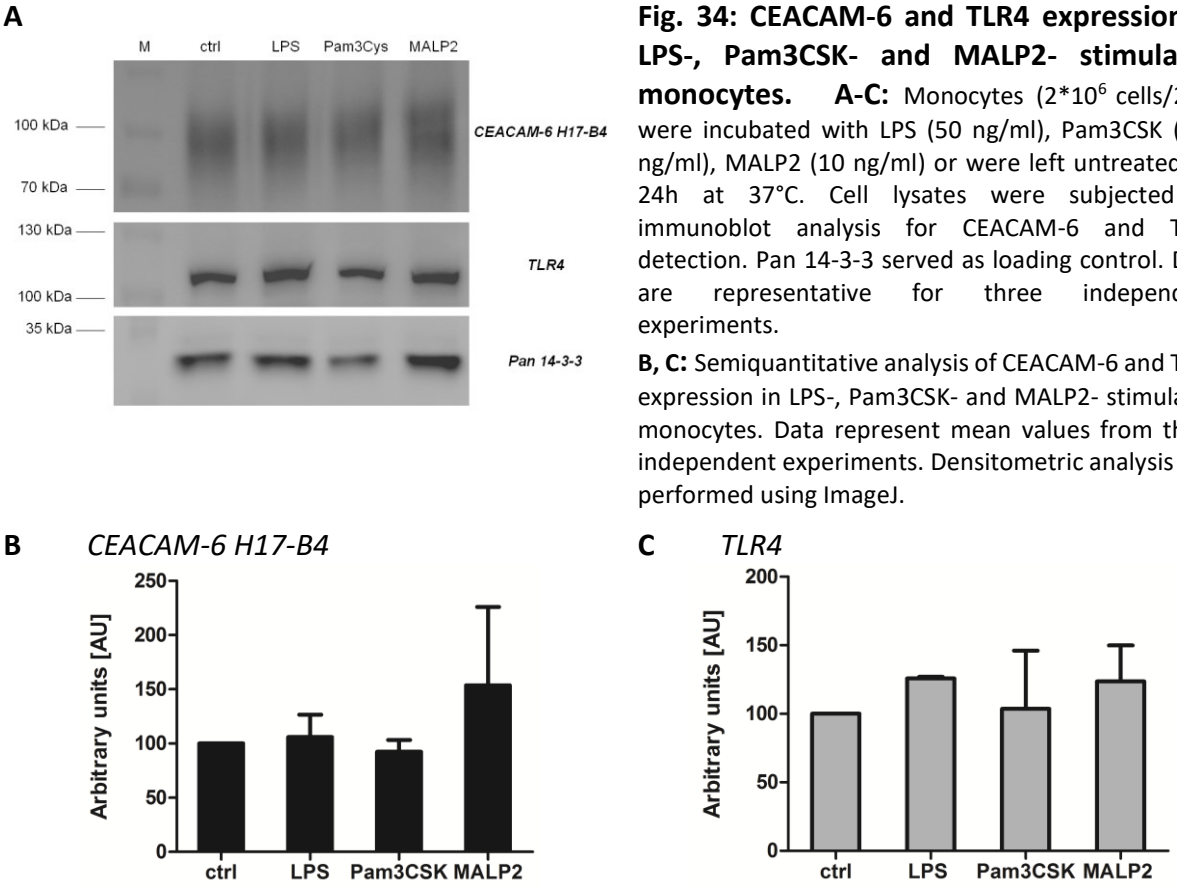

Fig. 34: CEACAM-6 and TLR4 expression in LPS-, Pam3CSK- and MALP2- stimulated monocytes. **A-C:** Monocytes ($2*10^6$ cells/2ml) were incubated with LPS (50 ng/ml), Pam3CSK (200 ng/ml), MALP2 (10 ng/ml) or were left untreated for 24h at 37°C. Cell lysates were subjected to immunoblot analysis for CEACAM-6 and TLR4 detection. Pan 14-3-3 served as loading control. Data are representative for three independent experiments.

B, C: Semiquantitative analysis of CEACAM-6 and TLR4 expression in LPS-, Pam3CSK- and MALP2- stimulated monocytes. Data represent mean values from three independent experiments. Densitometric analysis was performed using ImageJ.

7. Discussion

Immunodeficiency in septic patients surviving the initial hyperinflammatory phase is linked to an increased risk for secondary infections and mortality and one contributing mechanism of this phenomenon is monocyte tolerance. Monocytes exposed to low concentrations of PAMPs undergo a cellular reprogramming, which leads to decreased expression of pro-inflammatory cytokines, increased expression of anti-inflammatory cytokines and significantly altered expression of various (glyco-) proteins in subsequent encounters with PAMPs or pathogens. Due to glycosylation being one of the most common posttranslational modifications of cell surface-associated proteins, glycoproteins serve as an ideal source for the discovery of biomarkers and almost all of the frequently used biomarkers for disease detection, histological diagnosis and prognosis, as well as therapeutic intervention in diseases belong to the group of glycoproteins (Bausch-Fluck et al. 2015). Until now, no global characterization of the glycoprotein expression patterns of tolerant human monocytes has been carried out. An early identification of monocytes in the tolerant cell state based on differentially expressed cell surface markers might be a promising approach to detect patients suffering from sepsis-induced immunosuppression and could result in initiating a prompt treatment in order to improve the outcome of septic patients. We therefore induced tolerance in isolated and purified primary human monocytes and applied glycoprotein enrichment with subsequent mass-spectrometry analysis to investigate for changes of naïve and tolerized monocyte glycoproteomes.

7.1 Tolerance induction in human monocytes

The TLR4 agonist LPS is a well-described inducer of pro-inflammatory responses and also of tolerance in human monocytes and macrophages, resulting in the down regulation of pro-inflammatory cytokine expression and an upregulated anti-inflammatory cytokine expression in subsequent activations. Pro-inflammatory activation and tolerance induction in purified human monocytes were assessed by analyzing the regulation of TNF-α and IL-6 cytokine gene expression to investigate whether or not this capability is shared by TLR2 and its specific receptor ligands. Increased expression of TNF-α and IL-6 mRNA were observed in naïve monocytes exposed to the membrane-bound TLR agonists: LPS (TLR4), Pam3CSK (TLR2/1) and MALP2 (TLR2/6). LPS-restimulation of monocytes which were pretreated with either LPS, Pam3CSK or MALP2, led to a significant decrease of TNF-α and IL-6 production. While several studies consistently describe TLR4 agonist LPS to be capable in inducing tolerance in human monocytes, only few studies have been conducted using TLR2 agonists Pam3CSK and MALP2. Published reports examining TLR2 agonists to be potent tolerance inducers reveal conflicting data. Our findings support those of Kreutz et al. (1997), who were the first to describe TLR2/1 agonist Pam3CSK to induce tolerance in human monocytes to subsequent LPS- or Pam3CSK- challenges (cross- and homo-tolerance). This is also consistent with data of Siedlar et al. (2004), showing Pam3CSK to be an efficient cross-tolerance inducer in human monocytic Mono Mac 6 cells, while the group of Dobrovolskaia (2003) observed Pam3CSK to solely induce homo-tolerance in murine macrophages, but failed to induce cross-tolerance to a subsequent LPS-challenge.

Data on MALP2-mediated tolerance induction in human monocytes are even rarer: To our knowledge, there is no prior study examining TLR2/6 agonist MALP2 to be efficient in tolerance induction in human monocytes. Deiters et al. (2003) and two studies by Sato et al. (2000, 2002) found MALP2 to be a potent inducer of tolerance to a second LPS challenge in murine macrophages. Only one study using MALP2 as a PAMP was carried out in human monocytes by the group of Fernandes (2010) and showed that monocytes pretreated with LPS become refractory to further MALP2 challenges. The current study demonstrates TLR2/6 agonist MALP2 to induce cross-tolerance to further LPS-stimulation in human monocytes.

PAMP concentrations of LPS, Pam3CSK and MALP2 had to be adjusted to ensure, that they, on the one hand, were efficient in inducing (cross-) tolerance with comparable changes in monocytes and, on the other hand, were low enough to simulate biological relevant concentrations as close as possible to the ones observed in sepsis pathology. Previous studies by Kritselis et al. (2013) measured the concentrations of circulating LPS in blood samples from

septic patients on the first day of sepsis. They observed that LPS had to be present above a critical level of more than 1.60 Endotoxin Units (EU)/ml to induce significant endotoxin tolerance in monocytes of these patients. This is in accordance with our findings: low levels of 5-10 ng/ml LPS were not inducing tolerance in human monocytes reliably. Concentration adjustment of the different PRR ligands was first tried by transfecting primary human monocytes with an NF-κB-promoter gene containing plasmid and subsequent measurement of NF-κB activation by LPS, Pam3CSK and MALP2 in dose-response experiments. Although several attempts were made with different transfection protocols (GeneCellin^{TM} Transfection Reagent, Lipofectamine® 2000 Transfection Reagent and electroporation), the transfection efficiency of human monocytes remained very low giving inconsistent results in subsequent experiments. Thus, transfection rates of human monocytes were too low to produce meaningful data for stimulus adjustment. Analysis of cytokine expression by qPCR in LPS-, Pam3CSK- and MALP2-concentration series revealed that very high concentrations of TLR2/6 agonist MALP2 (more than 5 ng/ml) were needed in order to obtain similar activation levels seen by LPS- and Pam3CSK-stimulated monocytes. Concentrations of 50 ng/ml LPS, 200 ng/ml Pam3CSK and 10 ng/ml MALP2 demonstrated a similar upregulation of the cell surface associated cell adhesion molecule 1 (ICAM-1) in FACS analysis, which is a well-known parameter to identify pro-inflammatory activation of cells (Audran et al. 1996, Anbarasan et al. 2015). The determined concentrations of TLR2 and TLR4 ligands were therefore used in later performed glycoproteomic analysis.

Besides LPS, Pam3CSK and MALP2 which are ligands of membrane-bound PRRs, the synthetic NOD-like receptor ligands 1 and 2 (iE-DAP and MDP) were also tested to induce comparable pro-inflammatory responses in human monocytes. Both, NLR1 and NLR2, are located in the cytosol and, therefore, represent a mechanism for intracellular microbe sensing. Although monocytes were shown to express NLR1 and NLR2 on mRNA level (Fig. 4) and pro-inflammatory responses were described (Strober et al. 2006, Kufer et al. 2006), incubation of the cells with 1 µg/ml iE-DAP or 10 µg/ml MDP for 4 hours revealed marginal increased TNF-α mRNA expression levels (~1.5-fold, Fig. 5). The lack of pro-inflammatory TNF-α mRNA induction might be due to differences in the kinetics of PAMP sensing by intracellular and membrane-bound PRRs, and, thus, longer incubation periods with intracellular acting ligands would have been necessary to observe a strong pro-inflammatory activation of TNF-α at mRNA level in stimulated monocytes. However, if there would have been a pro-inflammatory activation of the cells by the used NLR ligands, not seen after 4 hours, but leading to a subsequent tolerant state towards a further LPS challenge, inhibition of pro-inflammatory TNF-α expression would have been detectable in the endotoxin tolerance model, which included a 20 hours-pretreatment with the NLR ligands. Unaltered induction of

TNF-α in monocytes, pretreated with either iE-DAP or MDP and restimulated with LPS, demonstrated no detectable tolerance induction by the NOD1 and NOD2 ligands (TNF-α FC levels: 69.15- and 69.9-fold, respectively; Fig. 7). In accordance with previously reported data, human monocytes of all three analyzed donors exhibited lesser expression levels of the cytosolic PRR NOD1 compared to NOD2 (Fig. 4), which might also contribute to the to the low pro-inflammatory activation by iE-DAP (Granland et al. 2014).

Moreover, we hypothesized that S100A12 can act as tolerance inducer. This host-derived endogenous alarmin and, as recently shown, putative TLR4 agonist, might be able to mediate a TLR4-dependent pro-inflammatory response, and, thereby, also a TLR4-dependent tolerance induction. Treatment of monocytic THP-1 cells with recombinant S100A12 proteins led to slightly augmented TNF-α levels. The recombinant proteins used in this study were produced in E. coli strains. As recombinant proteins derived from E. coli strains are often endotoxin contaminated, several experiments were performed to test the purity of the purchased S100A12 in order to ensure that the observed activation of the cells was truly caused by the protein S100A12 itself. Both, S100A12 preparations from R&D System (UK) and S100A12 preparations from Sino Biological (China), induced NF-κB activation in HEK-Blue-hTLR4 cells. Supplementation of LPS-binding protein (LBP), which mediates the binding of LPS to the TLR4 receptor complex, to S100A12-stimulated HEK-Blue-hTLR4 cells accelerated NF-κB activation, while co-incubation of S100A12 with polymyxin B, a well-known inhibitor of LPS, was found to decrease NF-κB activation. Together these findings hinted at a possible LPS-contamination in the commercially obtained S100A12 obtained from R&D Systems and Sino Biological, which was finally confirmed by Limulus Amebocyte Lysate (LAL) assay. The results indicated that 1 µg S100A12 protein from R&D Systems contained 0.39 ng LPS and 1 µg S100A12 protein from Sino Biological contained 0.3 ng LPS. As recently published, even these low levels of endotoxin contamination can lead to a notable activation and also to priming of human monocytes and dendritic cells (Schwarz et al. 2014).

S100A12 provided by Dirk Foell's group was also tested in the LAL assay and was found to be absolutely LPS-free. Unfortunately, this S100A12 preparation failed to induce a significant pro-inflammatory response (unchanged TNF-α expression on mRNA and protein level) in THP-1 cells, and only slightly enhanced the expression levels of IL-1β (~11-fold) and IL-6 mRNA (~13-fold) in monocytes using highest concentrations of S100A12 (10 µg/ml). Consistently, IL-6 protein secretion remained almost unaffected (~4 pg/ml IL-6) in further stimulations of monocytes with LPS-free S100A12 and no down-regulation of the upregulated IL-6 production (~304 pg/ml IL-6) in S100A12-pretreated and LPS-restimulated monocytes was observable (Fig. 14). Although the

correct folding of the used proteins could not be tested and denaturing during the transport and repeated freeze/thaw-cycles might have affected protein functionality, S100A12 was not further studied in the current study.

The results indicate that S100A12 treatment of THP-1 cells and human monocytes did not induce strong pro-inflammatory signaling with detectable increases of pro-inflammatory cytokines on mRNA level.

Moreover, the role of alarmins as putative pro-inflammatory signaling and tolerance inducers is lately conversely debated due to divergent findings. For example, several studies suggested HMGB1-preconditioning to be effective in inducing monocytes refractive to subsequent stimulations with LPS or LTA (Aneja et al. 2008, Robert et al. 2010). Other reports indicated that the pro-inflammatory effects of HMGB1-treatment were only due to LPS contaminations (Qin et al. 2009). Qin et al. found that HMGB1, which contained only low concentrations of LPS, failed in pro-inflammatory activation of mouse macrophages and TNF-α secretion of macrophages was positively correlated with the amount of contaminating LPS contained in several of the purchased HMGB1 preparations.

7.2 Glycoproteomic analysis of naïve and tolerant monocytes

7.2.1 Donor-dependent purity of isolated cells and impact on glycoproteomic analysis

Experiments performed with whole blood cell populations, PBMCs or monocyte subpopulations of heterogeneous purity are often difficult to interpret: Several cytokines can be produced both by mononuclear and polymorphonuclear cells present in whole blood cell populations and the responsiveness of each individual cell population may be differently affected by the performed treatment. Moreover, the presence of unknown factors within the plasma may mask or influence the individual behavior of leukocytes. In different donors also the ratio of leukocyte subpopulations can vary. Thus, an initial aim of our study was to establish an enrichment protocol to gain a highly purified CD14++CD16- monocyte population out of buffy coats from healthy donors. This way, it should be guaranteed that all measured effects are exclusively based on changes in the responsiveness of the major monocytes subset, CD14++ CD16- monocytes. The first step of monocyte enrichment and purification was performed by negative selection using the MACS isolation Kit II (Miltenyi Biotec, Germany). Although Zhou et al. (2012) reported positive selection to provide a higher purity of the enriched population of monocytes, we decided to use negative selection in order to prevent possible alterations of gene and protein expression caused by activation of the cells during the (CD14) antibody-mediated positive selection. FACS analysis of MACS-separated monocytes revealed a poor donor-dependent enrichment efficiency of about 66-70% purity. One possible reason for the low and different purities might be the significantly varying amounts of cell populations and also starting cell numbers between the different donors' buffy coats, leading to a possible subsequent overload of the cell separation columns during MACS purification. To gain higher purity, a second purification step was included. Remaining platelets (anti-CD42b) and lymphocytes (anti-CD3 against T-lymphocytes and anti-CD19 against B-lymphocytes) were stained with antibodies after MACS separation and separated from CD14 positive cells by an additional FACS sort. This increased the purity of the CD14++CD16- cell population to more than 97%.

Principal Component Analysis (PCA) of the glycoproteomic data from the 3 donors demonstrated that the three different stimuli LPS, Pam3CSK and MALP2 showed a higher resemblance of the global glycoproteomic expression patterns (in monocytes of one donor) than the different donors compared to each other. PC1 values were widely scattered among the three donors due to different amounts of contaminating proteins that arised from different numbers of contaminating leukocytes and platelets and also because of differential expression of glycosylated HLA molecules. Thus,

interindividual expression differences and purity of purified monocytes varied slightly and affected the statistical analysis causing a higher variance. Therefore, statistical analysis of the glycoproteomic monocyte data set was carried out with paired t-test analysis.

7.2.2 Changes in the glycoproteomes of LPS-, Pam3CSK- and MALP2-tolerized monocytes

In total, the mass spectrometry-based analysis of the CD14+ monocytic glycoproteome identified 1176 glycoproteins (~1000±33 annotated glycoproteins/donor) in the combined analysis of the NGP and TPG fractions using hydrazide enrichment and subsequent LC-MS/MS analysis. According to the hydrophobic transmembrane helix prediction algorithm (TMHMM v2.0 Server), 898 of the 1176 identified glycoproteins were predicted to contain at least one or more transmembrane domains (TDs), demonstrating that the glycoprotein enrichment protocol with SDS as a detergent was efficient in solubilizing a significant number of membrane-spanning or GPI-anchored glycoproteins from the cell surface and from various cellular organells. Identified glycoproteins derived from almost all cellular and subcellular compartments; the most abundant compartments were plasma membrane (671) and endoplasmic reticulum (264). Minor subsets of glycoproteins originated from the golgi apparatus, lysosome, nucleus, endosome, mitochondrion and peroxisome. Additionally to these intracellular glycoproteins, also 278 glycoproteins were detected, annotated as “extracellular matrix” and “extracellular space” including soluble and secreted glycoproteins. Besides the purified glycoproteins, a substantial number of non-glycosylated proteins, e.g. human keratins, histones and plasma proteins that were not completely removed by the numerous washing steps, were also detected by LC-MS/MS analysis. Non-glycosylated proteins and serum contaminants were excluded from further analysis since they represent contaminants and the performed experiments were not intended to find new glycoproteins that were to date not annotated as such.

Although several steps had been implemented in the sample preparation protocol in order to achieve a CD14+ monocyte population of highest purity, key cell surface markers for T cells (CD4), dendritic cells (CD123), hematopoietic stem cells (CD34), granulocytes (CD66b; CEACAM8 and CD66d; CEACAM3) and platelets (CD41, CD61 and CD62P) were identified in the glycoproteomic data set, though in low abundance. These findings could, on the one hand, hint at a possible contamination with the above named cell populations. On the other hand, several CD markers that were originally thought to be specific cell surface markers, were recently also reported to be expressed by (activated) human monocytes. For example, CD4, a putatively T-cell-specific surface marker, was also found to be expressed by human monocytes (Zhen et al. 2014). Other

classical T-cell surface marker like CD3 and CD8 were not detected in the analyzed glycoproteomic data set. Moreover, IL-4 stimulated monocytes were demonstrated to express the dendritic cell line-specific CD123 molecule (Borriello et al. 2015) and CD34, a hematopoietic stem cell marker, was also found to be expressed on the cell surface of a regulatory monocytes subpopulation (D'Aveni et al. 2015). Thus, CD123 and CD34 might be expressed by activated monocytes in the current study. Whether the detected expression of CD4, CD123 and CD34 indicates contamination with other leukocyte cell populations or is rather to interpret as activation markers being expressed by stimulated monocytes, can not be evaluated with absolute certainty. A low abundant contamination with granulocytes and platelets can not be ruled out due to the identification of the cell population specific CD markers (see above). Interestingly, except of downregulated expression levels of the platelet marker CD41 in LPS-stimulated monocytes, non of them demonstrated altered expression after LPS-, Pam3CSK- and MALP2-stimulation. Therefore, it could be assumed that the contaminating cell populations did not or did only slightly affect the statistic analysis of glycoproteins annotated in GO as CD antigens.

A well-described phenomenon in course of endotoxin tolerance is the impaired expression of HLA proteins associated with attenuated antigen presenting capacity and T-cell activation (Hynninen et al. 2003). Endotoxin tolerance was also shown to be accompanied by decreased cell surface expression of MHC II-related proteins CD74 (HLA class II histocompatibility antigen gamma chain) and HLA-DRA, as well as reduced expression of the Class II trans-activator (CIITA), a transactivator of HLA-DRA gene transcription. In patients, these human monocyte antigens were proven to be reliable markers for monocytic immunosuppression, the risk of secondary infections and for the prediction of mortality in septic patients (Cazalis et al. 2013, Cajander et al. 2016). Flow cytometry-based analysis of HLA-DR protein expression on monocytes was already used to identify critically ill patients in the Intensive Care Unit with immunosuppression in the clinical setting (Monneret and Venet 2014). In the data obtained in this study, LPS-, Pam3CSK- and MALP2-tolerized monocytes displayed significantly decreased expression levels of CD74. However, none of the other MHC II-related proteins demonstrated differential expression and CIITA, as non-glycosylated protein, was not detected in our glycoproteomic analysis. A possible explanation for the lack of differentially expressed HLA-DR antigens in monocytes analyzed in this study might be that according to findings of Monneret et al. (2014), HLA-DRA expression is only very slightly decreased in tolerant monocytes. Therefore, a possible reduction of HLA-DRA expression was not detected in the glycoproteomic data or, since we also detected intracellular glycoproteins, the overall amount of HLA-DR antigens is unchanged while cell surface expression might be reduced. Another contributing aspect might be that cell-cell interactions or

communication via soluble factors with other immune cells are required to induce this specific down-regulation of HLA-DRA expression. In our experimental setting, relative pure CD14+ monocyte populations were stimulated and other putative key players regulating the HLA-DR expression might be absent in this purified population. FACS analysis of HLA-DR did also not reveal down-regulated cell surface expression after 24 h (data not shown).
In accordance with data of Mendes et al. (2011), TLR4 and CD14 expression did not show altered expression in LPS-treated human monocytes. Moreover, prior studies observed that tolerance induced in macrophages by Gram-positive TLR2 agonists Pam3CSK or MALP2 did not affect TLR4 and TLR2 cell surface expression, which is consistent with unaltered expression levels of TLR4 and TLR2 in Pam3CSK- and MALP2-stimulated monocytes found in the current study (Dobrovolskaia et al. 2003, Sato et al. 2000). However, TLR4 and TLR2 expression on tolerant cells are controversially discussed in the literature: Sato et al. (2000) reported reduced TLR4 and CD14 expression on LPS-tolerized murine macrophages, while later studies indicated upregulated TLR4 cell surface expression on monocytes of septic patients (Calvano et al. 2003, Harter et al. 2004). Whereas our findings support those of Calvano et al. (2003), who found unaltered expression of TLR2 on monocytes of septic patients, the study of Harter et al.(2004) observed strongly enhanced cell surface expression of TLR2 on monocytes of septic patients. Again, these discrepant findings might be due to the properties of the experimental setting, stimulating purified monocytes in the absence of other immune cells, tissues and organs that all act in concert in the septic patient.

Taken together, the data of this study indicate that reduced TLR2, TLR4 and CD14 expression is not necessarily required for tolerance induction. Rather, modulation of signaling components in the intracellular down-streaming signaling cascades might be major regulatory mechanisms of endotoxin tolerance and, especially, cross-tolerance.

7.2.3 Effects of different TLR ligands

As mentioned above, detection of Gram-positive microbial compounds by TLR2 and Gram-negative bacterial cell wall components by TLR4 were both proven to efficiently induce tolerance. Although TLRs belong to a family of highly conserved receptors of the innate immunity and share common down-streaming signaling pathways, previous reports let suspect that TLR2- and TLR4-mediated tolerance differ due to differential engagement and affection of MyD88-dependent and MyD88-independent intracellular signaling pathways (Sato et al. 2002, Bagchi et al. 2007). Several studies indicated impaired expression of IRAK-1 to be a major mechanism of TLR2-mediated tolerance, but no such contribution to TLR4-induced tolerance was found (Siedlar et al.

2004, Li et al. 2006). Altogether, these findings suggest that TLR2- and TLR4-mediated tolerance in human monocytes might result in different global protein and also glycoprotein expression patterns. In the present study, data hint in another direction.

In LPS-, Pam3CSK- and MALP2-tolerized monocytes, 135 of the 1176 identified glycoproteins were significantly differentially expressed after a 24 hours-stimulation period. Further analysis revealed that LPS, Pam3CSK and MALP2 led to nearly identical changes in the monocytic glycoproteome, inducing almost similar levels of up- and down-regulation of the same glycoproteins. The high similarity of stimuli-induced glycoprotein expression changes in monocytes was indicated by equivalent fold changes of the regulated glycoproteins, although statistical significance (two sample t-test with FC >2 and adjusted $p<0.05$ according to Benjamini and Hochberg) was not reached for all differentially expressed proteins (see table 21). These findings could be confirmed in a linear regression model displaying highly similar pearson correlation coefficients (ρ) of 0.949, 0.965 and 0.955, when glycoprotein expression changes of LPS- vs. MALP2-, MALP2- vs. Pam3CSK- and Pam3CSK- vs. LPS-stimulated monocytes of all three donors were compared, respectively (Fig. 27).

As expected, cellular component analysis revealed a high resemblance in numbers and localization of significantly regulated glycoproteins between the different stimuli. Plasma membrane-resident glycoproteins and glycoproteins annotated as “extracellular space” comprised the largest numbers of significantly altered glycoproteins upon exposure of monocytes towards LPS, Pam3CSK and MALP2. The majority of plasma membrane proteins showed enhanced expression levels, while glycoproteins from the extracellular space displayed slightly higher numbers of downregulated proteins.

Altogether, the Gram-negative stimulus LPS and both Gram-positive stimuli Pam3CSK and MALP2 induced highly similar alterations in the monocyte glycoproteomes of all three donors analyzed. This is contrary to our first hypothesis that different TLR agonists might lead to dissimilar changes in the global glycoprotein expression patterns based on different usage of down-streaming signaling pathways. Despite the previously described differences in the intracellular signaling of tolerant cells, our findings indicate different TLRs to induce highly similar changes in the monocyte glycoproteome.

7.2.4 Cell surface signature of tolerant monocytes

Due to the majority of cell surface proteins being glycosylated, mass spectrometry-based analysis of the tolerant monocytes glycoproteome offers a unique opportunity to identify global alterations of the monocytes surfaceome as well as specific marker proteins of the tolerant state. Tolerance-specific biomarkers might facilitate the identification of critically ill patients suffering from sepsis-induced immunosuppression or even might be possible new drug targets to reverse immunosuppression in future. Therefore, glycoproteins annotated in GO to be plasma membrane-associated were analyzed in more detail.

202 CD antigens and 54 GPCRs were identified among the glycoproteins annotated as plasma membrane-associated. Plasma membrane-resident glycoproteins, as mentioned above, comprised the highest number of significantly regulated glycoproteins, including 32 CD molecules and 4 GPCRs with altered expression levels. An enrichment of CD antigens involved in cell adhesion processes was found when GO-annotation pathway analysis (DAVID) was carried out analyzing regulated CD glycoproteins against all 1176 identified glycoproteins. Other categories were not detected to be significantly enriched.

Interestingly, the majority of the regulated plasma membrane-associated glycoproteins in tolerant human monocytes displayed increased expression levels. PD-L1 (CD274), ITGB8 and IL-7R (CD127) were among the most highly upregulated cell surface-located glycoproteins. In accordance with our findings, previous studies showed that PD-L1 expression is upregulated in monocytes by several PAMPs and PD-L1 expression levels on monocytes in septic patients to be increased (Sharpe et al. 2007, Francisco et al. 2010, Zhang et al. 2011). Data of PD-L1 in the present study confirm efficient activation of monocytes by the chosen concentrations of LPS, Pam3CSK and MALP2 and, again, demonstrated an equivalent activation level of the differently treated monocytes due to highly similar fold change levels of PD-L1 expression. Additionally, PD-L1 expression on monocytes was recently identified to be an independent predictor for 28 day-mortality in septic patients (Shao et al. 2016). Inhibition of PD-L1 (by antibodies directed against PD-L1) resulted in reduced T-cell exhaustion and improved survival rates in a septic mouse model (via cecal ligation and puncture (CLP)) and was found to reverse monocytes dysfunction in an *ex vivo* performed blockade of PD-L1 on immune cells from septic patients (Zhang et al. 2010, Chang et al. 2014). Remarkably, blockade of ICAM-1, a cell adhesion molecule, which was found to be upregulated in our data set as well, was shown to be effective in decreasing PD-L1 expression levels in tissues and organs like spleen and thymus of septic mice (Zhao et al. 2014). Therefore, ligation of ICAM-1 with specific antibodies might also decrease enhanced expression levels of PD-L1 on tolerant human monocytes and, in this way, improve the outcome of septic patients.

Another candidate to distinguish tolerant from naïve monocytes and that, probably, might serve as prospective therapeutic target is integrin β8 (ITGB8). Our studies identified, for the first time, strongly enhanced expression levels of ITGB8 in PAMP-activated tolerant monocytes. The integrin β8 subunit non-covalently binds to an αV subunit to form a heterodimeric complex and was recently shown to play a major role in the activation of latent TGF-β 1 and 3 (Mu et al. 2002, Travis and Sheppard 2014). TGF-β family members have pleiotropic functions: Especially TGF β1 is described to be produced in significant amounts by hematopoietic cells and to control inflammation. Effects of this immunological mediator are highly context specific, but it mainly acts as an immunosuppressive cytokine by downregulating the differentiation of naïve T-cells to Th1- and Th2-cells on the one hand and promoting the development of suppressive regulatory T-cells on the other hand (Travis and Sheppard 2014). Mice lacking the integrin β8 subunit exhibited multiple phenotypes consistent with loss of TGF-β, e.g. severe multiorgan inflammation, decrease of Tregs cells and increase of spontaneously activated $CD4^+$ and $CD8^+$ T-cells (Aluwihare et al. 2009, Travis and Sheppard 2014). Upregulated numbers of Tregs were found to contribute to immunological anergy in the immunosuppressive phase of septic patients (Venet et al. 2009). Due to the predominantly inhibitory effects of TGF-β in immune signaling processes, inhibition of the TGF-β activator ITGB8 might be a possible new therapeutic target in reversing immunosuppression in (post-) septic patients. Other integrin beta subunits like ITGB7 are already subjects of extensive investigation within the pharmacological industry, e.g. Etrolizumab, a humanized monoclonal antibody that selectively binds the integrin β7 subunit of α4β7- and αEβ7-heterodimers, was shown to be beneficial in the treatment of inflammatory bowel disease (Mitroulis et al. 2015). Moreover, other enzymatic regulators of latent TGF-β activation demonstrated also significantly altered expression levels in our data set, e.g. matrix metalloprotease 9 (MMP9) and cathepsin D (CTSD) (Travis and Sheppard 2014). Several studies found a positive correlation of highly upregulated serum levels of MMP9 and tissue inhibitor of matrix metalloproteinases 1 (TIMP-1) and mortality in septic patients (reviewed by Lorente et al. 2014). Both, MMP9 and TIMP-1, showed enhanced expression levels in our data analysis, indicating that activated monocytes might be a source for upregulated serum levels in septic patients.

A cytokine affecting T-cell homeostasis is interleukin 7 (IL-7). IL-7 is produced by antigen-presenting cells and induces the differentiation of naïve and memory T-cells to effector T-cells, as well as it acts as survival signal protecting lymphocytes from cell death. Recent studies by Grealy et al. (2013) showed that IL-7 production in monocytes of septic patients was diminished on transcriptional level. Simultaneously, the group of Julie Demaret found elevated plasma levels of

soluble IL-7 receptor alpha chain (sCD127) positively correlating with an increased risk of death in septic shock patients (Demaret et al. 2014). Interestingly, the present study demonstrates highly augmented protein abundance of IL-7 receptor in tolerant human monocytes, a receptor for IL-7 and thymic stromal lymphopoietin (TSPL). IL-7 and IL-7 receptor are already targets of particular pharmacological investigations in cancer and sepsis pathology. First attempts of recombinant human (rh)IL-7 substitution led to a restoration of lymphocyte functions, when cells of septic patients were treated *ex vivo* with rhIL-7 (Venet et al. 2012). Similar to the rescue signal in lymphocytes, treatment of tolerant monocytes with rhIL-7 might be a novel and promising strategy to reverse monocytic tolerance and prevent cell death. Thus, effects of IL-7 receptor activation in activated tolerant monocytes should be tested in future. Shindo et al. (2015) suggest a combined immuno-therapy with rhIL-7 and anti-PD-L1 because they differ in their effects to reverse sepsis-induced immunosuppression. Outcome and survival of septic patients might be even more improved with ITGB8 as third therapeutic target to down-regulate TGF-β-signaling.

Although most of the significantly regulated glycoproteins displayed upregulated expression levels, there are also some interesting downregulated candidates, which might help to distinguish tolerant from naïve monocytes including collectin 12 (COLEC12) and lysophosphatidic acid receptor 6 (LPAR6). Collectin 12 (COLEC12), a C-type lectin and member of the scavenger receptor family, showed the greatest decrease in its expression in all three differently tolerized monocyte subsets. Whereas most collectins belong to the group of soluble pattern recognition receptors, COLEC12 also recognizes invading pathogens as a membrane-bound receptor and initiates opsonophagocytosis (Ma et al. 2015). This finding is inconsistent with the described enhanced phagocytotic capabilities of tolerant monocytes (del Fresno et al. 2009). Besides COLEC12, lysophosphatidic acid receptor 6 (LPAR6) showed the second largest expression decrease. LPAR6 is a member of the G protein-coupled receptor (GPCR) family and is stimulated upon binding of lysophosphatidic acid (LPA). Moreover, LPAR6-mediated signaling results in the upregulation of pentraxin 3 (PTX3), a secreted glycoprotein which is involved in the innate immunity through binding to the C1q component and activating the complement cascade (Gustin et al. 2008). In accordance with the down regulated expression level of LPAR6 found in tolerant monocytes, also PTX3 exhibited significantly reduced expression in our data set. Substantial reduction of both, LPAR6 and PTX3 protein levels, might contribute to the diminished immunological function of monocytes during the sepsis-induced immunosuppressive phase.
Of the other 53 identified GPCRs 6 further receptors demonstrated altered expression levels. All of them (ACKR3, GPR68, GPR84, EMR1, EMR2 and HRH2) were upregulated. The most interesting one might be GPR84, a GPCR that functions as a selectively medium-chain (C7-C12)

fatty-acid sensing pro-inflammatory receptor (Suzuki et al. 2013, Yonezawa et al. 2013). Bouchard et al. (2007) observed increased expression of GPR84 on monocytes in mice suffering from endotoxemia. Recent reports emphasize its role in enhancing pro-inflammatory responses, e.g. LPS-stimulated macrophages from GPR84 knock-out mice were found to show markedly reduced expression of several pro-inflammatory cytokines (Nicol et al. 2015). Thus, GPR84 might be an interesting drug target to downregulate pro-inflammatory responses in the early course of sepsis or to restore pro-inflammatory responses in immunosuppressed sepsis survivors with tolerant monocytes.

7.2.5 Induction of sialyltransferases and SIGLECs

Changes in the expression of enzymes involved in protein glycosylation might influence cell-cell adhesion and cell signaling, as well as it might have affected the enrichment and, thereby, also protein quantification within the LC-MS/MS analysis. Therefore, glycoproteins annotated in GO to be involved in protein glycosylation were analyzed in more detail, revealing 3 glycosylation enzymes of a total of 75 identified members of this category with significantly altered expression levels. Beta-1,3-galactosyltransferase 4 (B3GALT4) and two golgi apparatus-resident sialyltransferases, ST3GAL1 and ST3GAL2, showed increased protein abundance. These enzymes are described to be specific in the usage of donor and acceptor substrates and, therefore, major changes mediated by the altered expression of these 3 enzymes affecting the whole glycoproteome seem unlikely. Both, ST3GAL1 and ST3GAL2, catalyze the transfer of sialic acid in an α-2,3-linkage to terminal galactose residues on glycoproteins or glycolipids, changing the negative charge of proteins (Wu et al. 2016). Sialylated glycoproteins are detected by the family of sialic acid (Sia)-binding Ig-like lectins (SIGLECs), which mediate cell-cell interactions and cell signaling processes and were also found in our data set to be significantly regulated. SIGLEC 10, a CD33-related SIGLEC, bearing an immunoreceptor tyrosine-based inhibition motif (ITIM) motif and, thus, is strongly suggested to down-regulate pro-inflammatory signaling pathways (Crocker and Redelinghuys 2008), was upregulated after LPS, Pam3CSK and MALP2 treatment. In contrast, significantly reduced expression levels were found for SIGLEC1 (sialoadhesin), a sialic acid binding lectin specifically restricted to monocytes and macrophages (Munday et al. 2001, Hartnell et al. 2001). SIGLEC1 mediates mainly cell adhesion of monocytes and macrophages, but until now there is little evidence of SIGLEC1 mediating signaling functions via its cytoplasmic domain which lacks signaling motifs (Crocker and Redelinghuys 2008).

7.3 Perspectives

This study identified 135 glycoproteins to be putative tolerance markers in human monocytes, which might help to identify septic patients with monocytes in the immunosuppressed cell state. Up- or down-regulated expression of 60 of those candidates reached significance in all three (LPS-, Pam3CSK- and MALP2-) stimulations. Although, pro-inflammatory cytokine production of 24 h-LPS-, Pam3CSK- and MALP2-pretreated monocytes was significantly down-regulated, indicating monocytes to be tolerant, it is not clarified with absolute certainty whether these differentially expressed glycoproteins are specific markers of the tolerant state or only activations markers of the stimulated monocytes. In order to proof if these glycoproteins are specific markers of the tolerant state, NLR-stimulated monocytes should be analyzed for the expression of glycoprotein-biomarker candidates. NLR ligands iE-DAP and MDP were shown to induce a slight pro-inflammatory response in human monocytes, but failed in the induction of tolerance. Thus, significantly regulated glycoproteins after LPS-, Pam3SK- or MALP2-stimulation should show no alterations of their expression levels upon exposure towards NLR ligands 1 and 2. Otherwise, those glycoproteins are likely to be activation markers of stimulated monocytes unrelated to the used stimulus, but no tolerance markers.

In a next step, glycoprotein biomarkers should be evaluated *in vivo*: So far, all experiments were carried out with purified monocytes from buffy coats of healthy male donors and *ex vivo*-stimulations with the above named TLR agonists. Due to the manifoldness of influence factors *in vivo* and the special features of the herein used experimental settings, further studies in patients are necessary to validate putative candidates. Moreover, prior studies demonstrated monocyte tolerance to be present even 28 days after sepsis onset in the patients (Poehlmann et al. 2009), which, with regard to circulating monocytes having a life span of 2-3 days, suggests a cellular reprogramming at the level of monocytic progenitor cells or stem cells in the bone marrow. Thus, it would be interesting to investigate the glycoproteomes of tolerant human monocytes at later time points after sepsis diagnosis, due to the fact that isolated human monocytes undergoing apoptosis during such long *ex vivo* cultivation periods. Verified biomarkers of the tolerant state might then help to differentiate between patients suffering from sepsis-induced immunosuppression and patients who enter the recovery phase. Improved tools for staging patients according to their individual risk could be a step towards a more personalized medicine with timely initiated, individual pro- or anti-inflammatory therapies.

8. Conclusions

Aim of this study was to examine and compare changes in the glycoproteomes of purified peripheral human CD14+ monocytes that were stimulated with different PRR ligands and analyzed in the tolerant state. We hypothesized that the TLR agonists LPS, Pam3CSK, MALP2 and the endogenous alarmin S100A12, as well as the two NLR ligands iE-DAP and MDP were able to induce pro-inflammatory responses in human monocytes, and, thus, might also be able to induce monocyte tolerance to subsequent stimulations with LPS. The data obtained in this study revealed that stimulation of human monocytes with the Gram-negative TLR4 ligand LPS or with the Gram-positive TLR2 agonists, Pam3CSK or MALP2, led to a pro-inflammatory activation of monocytes with subsequent hyporesponsiveness towards a further LPS challenge.

RAGE and TLR4 ligand S100A12 was found to induce a pro-inflammatory activation of human monocytes only when it contained measurable amounts of LPS. Purified granulocyte-derived, LPS-free S100A12 was not capable of inducing pro-inflammatory effects or monocyte tolerance.

IE-DAP and MDP which bind to the intracellular located NLR1 and NLR 2 were found to induce quantifiable pro-inflammatory responses in human monocytes. However, unaltered induction of pro-inflammatory cytokines in iE-DAP- or MDP-pretreated and LPS-restimulated monocytes indicated that both NLR ligands failed to induce monocyte tolerance.

Taken together, LPS, Pam3CSK and MALP2 were proven to be effective in inducing tolerance and cross-tolerance in human monocytes, whereas S100A12, iE-DAP and MDP did not.

We further hypothesized that adjusted concentrations of LPS, Pam3CSK and MALP2 which induce similar pro-inflammatory responses in human monocytes, may lead to segregation of glycoproteomic signatures according to differential usage of downstream signaling pathways. Equivalent cell surface expression of ICAM-1 on stimulated monocytes revealed 50 ng/ml of LPS, 200 ng/ml Pam3CSK and 10 ng/ml MALP2 to induce similar pro-inflammatory activation levels in human monocytes.

Analysis of global alterations in the glycoproteomes of LPS-, Pam3CSK- or MALP2-activated monocytes and statistical evaluation of the recorded data for the discovery of segregating signatures to classify tolerant human monocytes and naïve monocytes, discovered highly similar changes in the glycoproteomes induced by all three TLR ligands. Altogether, 135 of 1176 identified glycoproteins, derived from almost all cellular and subcellular compartments, displayed significant alterations in their expression after 24 h of stimulation, the time point when tolerance induction was measured. The largest subset of identified and also of regulated glycoproteins was annotated in Gene Ontology (GO) as “plasma membrane”-associated. Of 202 identified CD

antigens, 35 comprised significant differentially expression levels and KEGG pathway analysis revealed an enrichment of CD antigens involved in cell adhesion processes. 54 glycoproteins were annotated in GO as glycoproteins with ““G-protein coupled receptor activity”, of which 7 displayed distinct alterations in their expression.
Glycoproteomics identified well-known cell surface markers to be upregulated after monocyte stimulation like PD-L1 and IL-7R, as well as several, so far, not described glycoprotein biomarkers, which were unknown to be differentially expressed by monocytes in the tolerant state like ITGB8.

In summary, the tolerant state of human monocytes is associated with significant alterations in the monocytic glycoproteome, especially of glycoproteins located on the cell surface. LPS-, Pam3CSK- and MALP2-induced changes of the glycoprotein expression pattern revealed highly similar glycoprotein expression changes, independent of the ligand used for the first activation, targeting TLR2 or TLR4. The identified expression changes of new biomarker candidates for monocyte tolerance should now be evaluated in *in vivo*-models to test their validity to characterize tolerant monocytes.

9. References

Achouiti A, Föll D, Vogl T, van Till JW, Laterre PF, Dugernier T, Wittebole X, Boermeester MA, Roth J, van der Poll T, van Zoelen MA. 2013. S100A12 and soluble receptor for advanced glycation end products levels during human severe sepsis. Shock, 40 (3):188-194.

Akira S, Uematsu S, Takeuchi O. 2006. Pathogen recognition and innate immunity. Cell, 124 (4):783-801.

Aluwihare P, Mu Z, Zhao Z, Yu D, Weinreb PH, Horan GS, Violette SM, Munger JS. 2009. Mice that lack activity of alphavbeta6- and alphavbeta8-integrins reproduce the abnormalities of Tgfb1- and Tgfb3-null mice. J Cell Sci, 122 (Pt 2):227-232.

Anbarasan C, Bavanilatha M, Latchumanadhas K, Ajit Mullasari S. 2015. ICAM-1 molecular mechanism and genome wide SNP's association studies. Indian Heart J, 67 (3):282-287.

Aneja RK, Tsung A, Sjodin H, Gefter JV, Delude RL, Billiar TR, Fink MP. 2008. Preconditioning with high mobility group box 1 (HMGB1) induces lipopolysaccharide (LPS) tolerance. J Leukoc Biol, 84 (5):1326-1334.

Audran R, Lesimple T, Delamaire M, Picot C, Van Damme J, Toujas L. 1996. Adhesion molecule expression and response to chemotactic agents of human monocyte-derived macrophages. Clin Exp Immunol, 103 (1):155-160.

Aziz M, Jacob A, Yang WL, Matsuda A, Wang P. 2013. Current trends in inflammatory and immunomodulatory mediators in sepsis. J Leukoc Biol, 93 (3):329-342.

Bagchi A, Herrup EA, Warren HS, Trigilio J, Shin HS, Valentine C, Hellman J. 2007. MyD88-dependent and MyD88-independent pathways in synergy, priming, and tolerance between TLR agonists. J Immunol, 178 (2):1164-1171.

Barbalat R, Lau L, Locksley RM, Barton GM. 2009. Toll-like receptor 2 on inflammatory monocytes induces type I interferon in response to viral but not bacterial ligands. Nat Immunol, 10 (11):1200-1207.

Barbe F, Douglas T, Saleh M. 2014. Advances in Nod-like receptors (NLR) biology. Cytokine Growth Factor Rev, 25 (6):681-697.

Bausch-Fluck D, Hofmann A, Bock T, Frei AP, Cerciello F, Jacobs A, Moest H, Omasits U, Gundry RL, Yoon C, Schiess R, Schmidt A, Mirkowska P, Hartlova A, Van Eyk JE, Bourquin JP, Aebersold R, Boheler KR, Zandstra P, Wollscheid B. 2015. A mass spectrometric-derived cell surface protein atlas. PLoS One, 10 (3):e0121314.

Benjamini Y, Hochberg Y. Controlling the False Discovery Rate: A Practical and Powerful Approach to Multiple Testing.

Bertin J, Nir WJ, Fischer CM, Tayber OV, Errada PR, Grant JR, Keilty JJ, Gosselin ML, Robison KE, Wong GH, Glucksmann MA, DiStefano PS. 1999. Human CARD4 protein is a novel CED-4/Apaf-1 cell death family member that activates NF-kappaB. J Biol Chem, 274 (19):12955-12958.

Biswas SK, Lopez-Collazo E. 2009. Endotoxin tolerance: new mechanisms, molecules and clinical significance. Trends Immunol, 30 (10):475-487.

Bohannon JK, Hernandez A, Enkhbaatar P, Adams WL, Sherwood ER. 2013. The immunobiology of toll-like receptor 4 agonists: from endotoxin tolerance to immunoadjuvants. Shock, 40 (6):451-462.

Boheler KR, Bhattacharya S, Kropp EM, Chuppa S, Riordon DR, Bausch-Fluck D, Burridge PW, Wu JC, Wersto RP, Chan GC, Rao S, Wollscheid B, Gundry RL. 2014. A human pluripotent stem cell surface N-glycoproteome resource reveals markers, extracellular epitopes, and drug targets. Stem Cell Reports, 3 (1):185-203.

Borriello F, Longo M, Spinelli R, Pecoraro A, Granata F, Staiano RI, Loffredo S, Spadaro G, Beguinot F, Schroeder J, Marone G. 2015. IL-3 synergises with basophil-derived IL-4 and IL-13 to promote the alternative activation of human monocytes. Eur J Immunol, 45 (7):2042-2051.

Bouchard C, Page J, Bedard A, Tremblay P, Vallieres L. 2007. G protein-coupled receptor 84, a microglia-associated protein expressed in neuroinflammatory conditions. Glia, 55 (8):790-800.

Brandenburg K, Andra J, Muller M, Koch MH, Garidel P. 2003. Physicochemical properties of bacterial glycopolymers in relation to bioactivity. Carbohydr Res, 338 (23):2477-2489.

Buckley JM, Wang JH, Redmond HP. 2006. Cellular reprogramming by gram-positive bacterial components: a review. J Leukoc Biol, 80 (4):731-741.

Cajander S, Tina E, Backman A, Magnuson A, Stralin K, Soderquist B, Kallman J. 2016. Quantitative Real-Time Polymerase Chain Reaction Measurement of HLA-DRA Gene Expression in Whole Blood Is Highly Reproducible and Shows Changes That Reflect Dynamic Shifts in Monocyte Surface HLA-DR Expression during the Course of Sepsis. PLoS One, 11 (5):e0154690.

Calvano JE, Agnese DM, Um JY, Goshima M, Singhal R, Coyle SM, Reddell MT, Kumar A, Calvano SE, Lowry SF. 2003. Modulation of the lipopolysaccharide receptor complex (CD14, TLR4, MD-2) and toll-like receptor 2 in systemic inflammatory response syndrome-positive patients with and without infection: relationship to tolerance. Shock, 20 (5):415-419.

Caroff M, Karibian D. 2003. Structure of bacterial lipopolysaccharides. Carbohydr Res, 338 (23):2431-2447.

Caruso R, Warner N, Inohara N, Nunez G. 2014. NOD1 and NOD2: signaling, host defense, and inflammatory disease. Immunity, 41 (6):898-908.

Cazalis MA, Friggeri A, Cave L, Demaret J, Barbalat V, Cerrato E, Lepape A, Pachot A, Monneret G, Venet F. 2013. Decreased HLA-DR antigen-associated invariant chain (CD74) mRNA expression predicts mortality after septic shock. Crit Care, 17 (6):R287.

Chang K, Svabek C, Vazquez-Guillamet C, Sato B, Rasche D, Wilson S, Robbins P, Ulbrandt N, Suzich J, Green J, Patera AC, Blair W, Krishnan S, Hotchkiss R. 2014. Targeting the programmed cell death 1: programmed cell death ligand 1 pathway reverses T cell exhaustion in patients with sepsis. Crit Care, 18 (1):R3.

Cox J, Mann M. 2008. MaxQuant enables high peptide identification rates, individualized p.p.b.-range mass accuracies and proteome-wide protein quantification. Nat Biotechnol, 26 (12):1367-1372.

Cox J, Hein MY, Luber CA, Paron I, Nagaraj N, Mann M. 2014. Accurate proteome-wide label-free quantification by delayed normalization and maximal peptide ratio extraction, termed MaxLFQ. Mol Cell Proteomics, 13 (9):2513-2526.

Crocker PR, Redelinghuys P. 2008. Siglecs as positive and negative regulators of the immune system. Biochem Soc Trans, 36 (Pt 6):1467-1471.

D'Aveni M, Rossignol J, Coman T, Sivakumaran S, Henderson S, Manzo T, Santos e Sousa P, Bruneau J, Fouquet G, Zavala F, Alegria-Prevot O, Garfa-Traore M, Suarez F, Trebeden-Negre H, Mohty M, Bennett CL, Chakraverty R, Hermine O, Rubio MT. 2015. G-CSF mobilizes CD34+ regulatory monocytes that inhibit graft-versus-host disease. Sci Transl Med, 7 (281):281ra242.

Das U. 2014. HLA-DR expression, cytokines and bioactive lipids in sepsis. Arch Med Sci, 10 (2):325-335.

Deiters U, Gumenscheimer M, Galanos C, Muhlradt PF. 2003. Toll-like receptor 2- and 6-mediated stimulation by macrophage-activating lipopeptide 2 induces lipopolysaccharide (LPS) cross tolerance in mice, which results in protection from tumor necrosis factor alpha but in only partial protection from lethal LPS doses. Infect Immun, 71 (8):4456-4462.

del Fresno C, Garcia-Rio F, Gomez-Pina V, Soares-Schanoski A, Fernandez-Ruiz I, Jurado T, Kajiji T, Shu C, Marin E, Gutierrez del Arroyo A, Prados C, Arnalich F, Fuentes-Prior P, Biswas SK, Lopez-Collazo E. 2009. Potent phagocytic activity with impaired antigen

presentation identifying lipopolysaccharide-tolerant human monocytes: demonstration in isolated monocytes from cystic fibrosis patients. J Immunol, 182 (10):6494-6507.

Demaret J, Villars-Mechin A, Lepape A, Plassais J, Vallin H, Malcus C, Poitevin-Later F, Monneret G, Venet F. 2014. Elevated plasmatic level of soluble IL-7 receptor is associated with increased mortality in septic shock patients. Intensive Care Med, 40 (8):1089-1096.

Dewald JH, Colomb F, Bobowski-Gerard M, Groux-Degroote S, Delannoy P. 2016. Role of Cytokine-Induced Glycosylation Changes in Regulating Cell Interactions and Cell Signaling in Inflammatory Diseases and Cancer. Cells, 5 (4).

van Dissel JT, van Langevelde P, Westendorp RG, Kwappenberg K, Frolich M. 1998. Anti-inflammatory cytokine profile and mortality in febrile patients. Lancet, 351 (9107):950-953.

Dobrovolskaia MA, Medvedev AE, Thomas KE, Cuesta N, Toshchakov V, Ren T, Cody MJ, Michalek SM, Rice NR, Vogel SN. 2003. Induction of in vitro reprogramming by Toll-like receptor (TLR)2 and TLR4 agonists in murine macrophages: effects of TLR "homotolerance" versus "heterotolerance" on NF-kappa B signaling pathway components. J Immunol, 170 (1):508-519.

Fernandes ML, Mendes ME, Brunialti MK, Salomao R. 2010. Human monocytes tolerant to LPS retain the ability to phagocytose bacteria and generate reactive oxygen species. Braz J Med Biol Res, 43 (9):860-868.

Foell D, Wittkowski H, Kessel C, Luken A, Weinhage T, Varga G, Vogl T, Wirth T, Viemann D, Bjork P, van Zoelen MA, Gohar F, Srikrishna G, Kraft M, Roth J. 2013. Proinflammatory S100A12 can activate human monocytes via Toll-like receptor 4. Am J Respir Crit Care Med, 187 (12):1324-1334.

Foster SL, Hargreaves DC, Medzhitov R. 2007. Gene-specific control of inflammation by TLR-induced chromatin modifications. Nature, 447 (7147):972-978.

Francisco LM, Sage PT, Sharpe AH. 2010. The PD-1 pathway in tolerance and autoimmunity. Immunol Rev, 236:219-242.

Gogos CA, Drosou E, Bassaris HP, Skoutelis A. 2000. Pro- versus anti-inflammatory cytokine profile in patients with severe sepsis: a marker for prognosis and future therapeutic options. J Infect Dis, 181 (1):176-180.

Gordon S. 2007. The macrophage: past, present and future. Eur J Immunol, 37 Suppl 1:S9-17.

Granland C, Strunk T, Hibbert J, Prosser A, Simmer K, Burgner D, Richmond P, Currie AJ. 2014. NOD1 and NOD2 expression and function in very preterm infant mononuclear cells. Acta Paediatr, 103 (5):e212-218.

Grealy R, White M, Stordeur P, Kelleher D, Doherty DG, McManus R, Ryan T. 2013. Characterising cytokine gene expression signatures in patients with severe sepsis. Mediators Inflamm, 2013:164246.

Gresch O, Engel FB, Nesic D, Tran TT, England HM, Hickman ES, Korner I, Gan L, Chen S, Castro-Obregon S, Hammermann R, Wolf J, Muller-Hartmann H, Nix M, Siebenkotten G, Kraus G, Lun K. 2004. New non-viral method for gene transfer into primary cells. Methods, 33 (2):151-163.

Gustin C, Delaive E, Dieu M, Calay D, Raes M. 2008. Upregulation of pentraxin-3 in human endothelial cells after lysophosphatidic acid exposure. Arterioscler Thromb Vasc Biol, 28 (3):491-497.

Hailman E, Lichenstein HS, Wurfel MM, Miller DS, Johnson DA, Kelley M, Busse LA, Zukowski MM, Wright SD. 1994. Lipopolysaccharide (LPS)-binding protein accelerates the binding of LPS to CD14. J Exp Med, 179 (1):269-277.

Harter L, Mica L, Stocker R, Trentz O, Keel M. 2004. Increased expression of toll-like receptor-2 and -4 on leukocytes from patients with sepsis. Shock, 22 (5):403-409.

Hartnell A, Steel J, Turley H, Jones M, Jackson DG, Crocker PR. 2001. Characterization of human sialoadhesin, a sialic acid binding receptor expressed by resident and inflammatory macrophage populations. Blood, 97 (1):288-296.

Hedl M, Li J, Cho JH, Abraham C. 2007. Chronic stimulation of Nod2 mediates tolerance to bacterial products. Proc Natl Acad Sci U S A, 104 (49):19440-19445.

Hotchkiss RS, Monneret G, Payen D. 2013. Sepsis-induced immunosuppression: from cellular dysfunctions to immunotherapy. Nat Rev Immunol, 13 (12):862-874.

Huang da W, Sherman BT, Lempicki RA. 2009. Systematic and integrative analysis of large gene lists using DAVID bioinformatics resources. Nat Protoc, 4 (1):44-57.

Hynninen M, Pettila V, Takkunen O, Orko R, Jansson SE, Kuusela P, Renkonen R, Valtonen M. 2003. Predictive value of monocyte histocompatibility leukocyte antigen-DR expression and plasma interleukin-4 and -10 levels in critically ill patients with sepsis. Shock, 20 (1):1-4.

Inohara N, Koseki T, del Peso L, Hu Y, Yee C, Chen S, Carrio R, Merino J, Liu D, Ni J, Nunez G. 1999. Nod1, an Apaf-1-like activator of caspase-9 and nuclear factor-kappaB. J Biol Chem, 274 (21):14560-14567.

Jawad I, Luksic I, Rafnsson SB. 2012. Assessing available information on the burden of sepsis: global estimates of incidence, prevalence and mortality. J Glob Health, 2 (1):010404.

Jiang Z, Georgel P, Du X, Shamel L, Sovath S, Mudd S, Huber M, Kalis C, Keck S, Galanos C, Freudenberg M, Beutler B. 2005. CD14 is required for MyD88-independent LPS signaling. Nat Immunol, 6 (6):565-570.

Kawai T, Akira S. 2011. Toll-like receptors and their crosstalk with other innate receptors in infection and immunity. Immunity, 34 (5):637-650.

Kessel C, Holzinger D, Foell D. 2013. Phagocyte-derived S100 proteins in autoinflammation: putative role in pathogenesis and usefulness as biomarkers. Clin Immunol, 147 (3):229-241.

Kono H, Rock KL. 2008. How dying cells alert the immune system to danger. Nat Rev Immunol, 8 (4):279-289.

Kreutz M, Ackermann U, Hauschildt S, Krause SW, Riedel D, Bessler W, Andreesen R. 1997. A comparative analysis of cytokine production and tolerance induction by bacterial lipopeptides, lipopolysaccharides and Staphyloccous aureus in human monocytes. Immunology, 92 (3):396-401.

Kritselis I, Tzanetakou V, Adamis G, Anthopoulos G, Antoniadou E, Bristianou M, Kotanidou A, Lignos M, Polyzos K, Retsas T, Sassopoulou P, Papaioannou AI, Sinapidis D, Sereti K, Vittoros V, Ghanas P, Gogos C, Giamarellos-Bourboulis EJ. 2013. The level of endotoxemia in sepsis varies in relation to the underlying infection: Impact on final outcome. Immunol Lett, 152 (2):167-172.

Krogh A, Larsson B, von Heijne G, Sonnhammer EL. 2001. Predicting transmembrane protein topology with a hidden Markov model: application to complete genomes. J Mol Biol, 305 (3):567-580.

Kufer TA, Banks DJ, Philpott DJ. 2006. Innate immune sensing of microbes by Nod proteins. Ann N Y Acad Sci, 1072:19-27.

Kumar S, Ingle H, Prasad DV, Kumar H. 2013. Recognition of bacterial infection by innate immune sensors. Crit Rev Microbiol, 39 (3):229-246.

Le Bourhis L, Benko S, Girardin SE. 2007. Nod1 and Nod2 in innate immunity and human inflammatory disorders. Biochem Soc Trans, 35 (Pt 6):1479-1484.

Li CH, Wang JH, Redmond HP. 2006. Bacterial lipoprotein-induced self-tolerance and cross-tolerance to LPS are associated with reduced IRAK-1 expression and MyD88-IRAK complex formation. J Leukoc Biol, 79 (4):867-875.

Li HB, Jin C, Chen Y, Flavell RA. 2014. Inflammasome activation and metabolic disease progression. Cytokine Growth Factor Rev, 25 (6):699-706.

Lorente L, Martin MM, Sole-Violan J, Blanquer J, Labarta L, Diaz C, Borreguero-Leon JM, Orbe J, Rodriguez JA, Jimenez A, Paramo JA. 2014. Association of sepsis-related mortality with early increase of TIMP-1/MMP-9 ratio. PLoS One, 9 (4):e94318.

Lu M, Wu B. 2016. Structural studies of G protein-coupled receptors. IUBMB Life, 68 (11):894-903.

Ma YJ, Hein E, Munthe-Fog L, Skjoedt MO, Bayarri-Olmos R, Romani L, Garred P. 2015. Soluble Collectin-12 (CL-12) Is a Pattern Recognition Molecule Initiating Complement Activation via the Alternative Pathway. J Immunol, 195 (7):3365-3373.

Martin GS, Mannino DM, Eaton S, Moss M. 2003. The epidemiology of sepsis in the United States from 1979 through 2000. N Engl J Med, 348 (16):1546-1554.

Matzinger P. 1994. Tolerance, danger, and the extended family. Annu Rev Immunol, 12:991-1045.

Matzinger P. 2002. The danger model: a renewed sense of self. Science, 296 (5566):301-305.

Mendes ME, Baggio-Zappia GL, Brunialti MK, Fernandes Mda L, Rapozo MM, Salomao R. 2011. Differential expression of toll-like receptor signaling cascades in LPS-tolerant human peripheral blood mononuclear cells. Immunobiology, 216 (3):285-295.

Mitroulis I, Alexaki VI, Kourtzelis I, Ziogas A, Hajishengallis G, Chavakis T. 2015. Leukocyte integrins: role in leukocyte recruitment and as therapeutic targets in inflammatory disease. Pharmacol Ther, 147:123-135.

Monneret G, Venet F. 2014. Monocyte HLA-DR in sepsis: shall we stop following the flow? Crit Care, 18 (1):102.

Monneret G, Finck ME, Venet F, Debard AL, Bohe J, Bienvenu J, Lepape A. 2004. The anti-inflammatory response dominates after septic shock: association of low monocyte HLA-DR expression and high interleukin-10 concentration. Immunol Lett, 95 (2):193-198.

Mu D, Cambier S, Fjellbirkeland L, Baron JL, Munger JS, Kawakatsu H, Sheppard D, Broaddus VC, Nishimura SL. 2002. The integrin alpha(v)beta8 mediates epithelial homeostasis through MT1-MMP-dependent activation of TGF-beta1. J Cell Biol, 157 (3):493-507.

Munday J, Kerr S, Ni J, Cornish AL, Zhang JQ, Nicoll G, Floyd H, Mattei MG, Moore P, Liu D, Crocker PR. 2001. Identification, characterization and leucocyte expression of Siglec-10, a novel human sialic acid-binding receptor. Biochem J, 355 (Pt 2):489-497.

Nicol LS, Dawes JM, La Russa F, Didangelos A, Clark AK, Gentry C, Grist J, Davies JB, Malcangio M, McMahon SB. 2015. The role of G-protein receptor 84 in experimental neuropathic pain. J Neurosci, 35 (23):8959-8969.

Ogura Y, Inohara N, Benito A, Chen FF, Yamaoka S, Nunez G. 2001. Nod2, a Nod1/Apaf-1 family member that is restricted to monocytes and activates NF-kappaB. J Biol Chem, 276 (7):4812-4818.

Park BS, Song DH, Kim HM, Choi BS, Lee H, Lee JO. 2009. The structural basis of lipopolysaccharide recognition by the TLR4-MD-2 complex. Nature, 458 (7242):1191-1195.

Pena OM, Hancock DG, Lyle NH, Linder A, Russell JA, Xia J, Fjell CD, Boyd JH, Hancock RE. 2014. An Endotoxin Tolerance Signature Predicts Sepsis and Organ Dysfunction at Initial Clinical Presentation. EBioMedicine, 1 (1):64-71.

Pfaffl MW. 2001. A new mathematical model for relative quantification in real-time RT-PCR. Nucleic Acids Res, 29 (9):e45.

Pfaffl MW, Tichopad A, Prgomet C, Neuvians TP. 2004. Determination of stable housekeeping genes, differentially regulated target genes and sample integrity: BestKeeper--Excel-based tool using pair-wise correlations. Biotechnol Lett, 26 (6):509-515.

Poehlmann H, Schefold JC, Zuckermann-Becker H, Volk HD, Meisel C. 2009. Phenotype changes and impaired function of dendritic cell subsets in patients with sepsis: a prospective observational analysis. Crit Care, 13 (4):R119.

Qin YH, Dai SM, Tang GS, Zhang J, Ren D, Wang ZW, Shen Q. 2009. HMGB1 enhances the proinflammatory activity of lipopolysaccharide by promoting the phosphorylation of MAPK p38 through receptor for advanced glycation end products. J Immunol, 183 (10):6244-6250.

Reinhart K, Bauer M, Riedemann NC, Hartog CS. 2012. New approaches to sepsis: molecular diagnostics and biomarkers. Clin Microbiol Rev, 25 (4):609-634.

Rietschel ET, Brade H, Holst O, Brade L, Muller-Loennies S, Mamat U, Zahringer U, Beckmann F, Seydel U, Brandenburg K, Ulmer AJ, Mattern T, Heine H, Schletter J, Loppnow H, Schonbeck U, Flad HD, Hauschildt S, Schade UF, Di Padova F, Kusumoto S, Schumann RR. 1996. Bacterial endotoxin: Chemical constitution, biological recognition, host response, and immunological detoxification. Curr Top Microbiol Immunol, 216:39-81.

Rieu I, Powers SJ. 2009. Real-time quantitative RT-PCR: design, calculations, and statistics. Plant Cell, 21 (4):1031-1033.

Robert SM, Sjodin H, Fink MP, Aneja RK. 2010. Preconditioning with high mobility group box 1 (HMGB1) induces lipoteichoic acid (LTA) tolerance. J Immunother, 33 (7):663-671.

Sato S, Takeuchi O, Fujita T, Tomizawa H, Takeda K, Akira S. 2002. A variety of microbial components induce tolerance to lipopolysaccharide by differentially affecting MyD88-dependent and -independent pathways. Int Immunol, 14 (7):783-791.

Sato S, Nomura F, Kawai T, Takeuchi O, Muhlradt PF, Takeda K, Akira S. 2000. Synergy and cross-tolerance between toll-like receptor (TLR) 2- and TLR4-mediated signaling pathways. J Immunol, 165 (12):7096-7101.

Schultz-Cherry S, Lawler J, Murphy-Ullrich JE. 1994. The type 1 repeats of thrombospondin 1 activate latent transforming growth factor-beta. J Biol Chem, 269 (43):26783-26788.

Schwarz H, Schmittner M, Duschl A, Horejs-Hoeck J. 2014. Residual endotoxin contaminations in recombinant proteins are sufficient to activate human CD1c+ dendritic cells. PLoS One, 9 (12):e113840.

Shao R, Fang Y, Yu H, Zhao L, Jiang Z, Li CS. 2016. Monocyte programmed death ligand-1 expression after 3-4 days of sepsis is associated with risk stratification and mortality in septic patients: a prospective cohort study. Crit Care, 20 (1):124.

Sharpe AH, Wherry EJ, Ahmed R, Freeman GJ. 2007. The function of programmed cell death 1 and its ligands in regulating autoimmunity and infection. Nat Immunol, 8 (3):239-245.

Shindo Y, Unsinger J, Burnham CA, Green JM, Hotchkiss RS. 2015. Interleukin-7 and anti-programmed cell death 1 antibody have differing effects to reverse sepsis-induced immunosuppression. Shock, 43 (4):334-343.

Siedlar M, Frankenberger M, Benkhart E, Espevik T, Quirling M, Brand K, Zembala M, Ziegler-Heitbrock L. 2004. Tolerance induced by the lipopeptide Pam3Cys is due to ablation of IL-1R-associated kinase-1. J Immunol, 173 (4):2736-2745.

Sosa-Bustamante GP, Amador-Licona N, Barbosa-Sabanero G, Guizar-Mendoza JM, Lopez-Briones S, Mulgado-Aguas CI, Torres-Pedroza A. 2011. Intercellular adhesion molecules and mortality for sepsis in infants younger than 1 year of life. Rev Invest Clin, 63 (6):601-606.

Strober W, Murray PJ, Kitani A, Watanabe T. 2006. Signalling pathways and molecular interactions of NOD1 and NOD2. Nat Rev Immunol, 6 (1):9-20.

Suzuki M, Takaishi S, Nagasaki M, Onozawa Y, Iino I, Maeda H, Komai T, Oda T. 2013. Medium-chain fatty acid-sensing receptor, GPR84, is a proinflammatory receptor. J Biol Chem, 288 (15):10684-10691.

Takeuchi O, Akira S. 2010. Pattern recognition receptors and inflammation. Cell, 140 (6):805-820.

Tekin D, Dalgic N, Kayaalti Z, Soylemezoglu T, Diler B, Kutlubay BI. 2012. Importance of NOD2/CARD15 gene variants for susceptibility to and outcome of sepsis in Turkish children. Pediatr Crit Care Med, 13 (2):e73-77.

Travis MA, Sheppard D. 2014. TGF-beta activation and function in immunity. Annu Rev Immunol, 32:51-82.

Tsuchiya S, Yamabe M, Yamaguchi Y, Kobayashi Y, Konno T, Tada K. 1980. Establishment and characterization of a human acute monocytic leukemia cell line (THP-1). Int J Cancer, 26 (2):171-176.

Tyanova S, Temu T, Sinitcyn P, Carlson A, Hein MY, Geiger T, Mann M, Cox J. 2016. The Perseus computational platform for comprehensive analysis of (prote)omics data. Nat Methods, 13 (9):731-740.

Vaure C, Liu Y. 2014. A comparative review of toll-like receptor 4 expression and functionality in different animal species. Front Immunol, 5:316.

Venet F, Foray AP, Villars-Mechin A, Malcus C, Poitevin-Later F, Lepape A, Monneret G. 2012. IL-7 restores lymphocyte functions in septic patients. J Immunol, 189 (10):5073-5081.

Venet F, Chung CS, Kherouf H, Geeraert A, Malcus C, Poitevin F, Bohe J, Lepape A, Ayala A, Monneret G. 2009. Increased circulating regulatory T cells (CD4(+)CD25 (+)CD127 (-)) contribute to lymphocyte anergy in septic shock patients. Intensive Care Med, 35 (4):678-686.

Wolk K, Docke WD, von Baehr V, Volk HD, Sabat R. 2000. Impaired antigen presentation by human monocytes during endotoxin tolerance. Blood, 96 (1):218-223.

Wu H, Shi XL, Zhang HJ, Song QJ, Yang XB, Hu WD, Mei GL, Chen X, Mao QS, Chen Z. 2016. Overexpression of ST3Gal-I promotes migration and invasion of HCCLM3 in vitro and poor prognosis in human hepatocellular carcinoma. Onco Targets Ther, 9:2227-2236.

Yonezawa T, Kurata R, Yoshida K, Murayama MA, Cui X, Hasegawa A. 2013. Free fatty acids-sensing G protein-coupled receptors in drug targeting and therapeutics. Curr Med Chem, 20 (31):3855-3871.

Yu B, Wright SD. 1996. Catalytic properties of lipopolysaccharide (LPS) binding protein. Transfer of LPS to soluble CD14. J Biol Chem, 271 (8):4100-4105.

Zhang H, Li XJ, Martin DB, Aebersold R. 2003. Identification and quantification of N-linked glycoproteins using hydrazide chemistry, stable isotope labeling and mass spectrometry. Nat Biotechnol, 21 (6):660-666.

Zhang Y, Zhou Y, Lou J, Li J, Bo L, Zhu K, Wan X, Deng X, Cai Z. 2010. PD-L1 blockade improves survival in experimental sepsis by inhibiting lymphocyte apoptosis and reversing monocyte dysfunction. Crit Care, 14 (6):R220.

Zhang Y, Li J, Lou J, Zhou Y, Bo L, Zhu J, Zhu K, Wan X, Cai Z, Deng X. 2011. Upregulation of programmed death-1 on T cells and programmed death ligand-1 on monocytes in septic shock patients. Crit Care, 15 (1):R70.

Zhao YJ, Yi WJ, Wan XJ, Wang J, Tao TZ, Li JB, Wang JF, Deng XM. 2014. Blockade of ICAM-1 improves the outcome of polymicrobial sepsis via modulating neutrophil migration and reversing immunosuppression. Mediators Inflamm, 2014:195290.

Zhen A, Krutzik SR, Levin BR, Kasparian S, Zack JA, Kitchen SG. 2014. CD4 ligation on human blood monocytes triggers macrophage differentiation and enhances HIV infection. J Virol, 88 (17):9934-9946.

Zhou L, Somasundaram R, Nederhof RF, Dijkstra G, Faber KN, Peppelenbosch MP, Fuhler GM. 2012. Impact of human granulocyte and monocyte isolation procedures on functional studies. Clin Vaccine Immunol, 19 (7):1065-1074.

10. Appendix

10.1 List of figures

ID	Title	Page
Fig. 1	Theory of host immune response in sepsis	6
Fig. 2	Simplified model of the TLR4 intracellular signaling cascade and its negative regulation in endotoxin tolerance	10
Fig. 3	Workflow of sample preparation for LC-MS/MS	41
Fig. 4	Basal expression of TLR1, TLR2, TLR6, TLR4, CD14, MD2, RAGE and NLRs in primary human peripheral monocytes	47
Fig. 5	TNF-α mRNA expression in LPS-, Pam3CSK-, MALP2-, iE-DAP- and MDP-stimulated human monocytes	48
Fig. 6	Transcriptional regulation of TNF-α gene expression in LPS-stimulated human monocytes	49
Fig. 7	Reduction of TNF-α gene expression in LPS-, Pam3CSK- and MALP2-prestimulated monocytes in qPCR analysis	49
Fig. 8	Proinflammatory effect of commercially available S100A12 in THP-1 cells	50
Fig. 9	Effects of LBP on S100A12 mediated NF-κB activation	51
Fig. 10	Polymyxin B coincubation decreases the signaling of S100A12 on HEK-Blue-hTLR4 cells	52
Fig. 11	Determination of possible endotoxin contamination of commercially obtained S100A12 in the Limulus Amebocyte Lysate (LAL)-test	52
Fig. 12	LPS- and S100A12-induced TNF-α expression in THP-1 cells and human monocytes.	53
Fig. 13	qPCR analysis of S100A12-induced TNF-α, IL-1β and IL-6 gene expression in human monocytes	54
Fig. 14	Pro-inflammatory response and tolerance induction by S100A12 in human monocytes	54
Fig. 15	Fluorescence and phase contrast micrographs of monocytes transfected with plasmid pmaxGFP	56
Fig. 16	Analysis of TNF-α and IL-6 release by LPS-, Pam3CSK- and MALP2-stimulated human monocytes	57
Fig. 17	Significant down regulation of cytokine production in tolerant human monocytes	58

Fig. 18	Concentration series of LPS, Pam3CSK4 and MALP2 on human monocytes	59
Fig. 19	ICAM-1 expression in stimulated human monocytes	60
Fig. 20	Purification of monocytes via MACS® monocyte isolation kit and CD14+ fluorescence activated cell sorting (FACS)	61
Fig. 21	Distribution of identified glycoproteins according to the number of predicted transmembrane domains (TMDs)	62
Fig. 22	Gene-ontology based cellular component analysis of all glycoproteins identified in monocytes	63
Fig. 23	Unpaired analysis: Significant up- or downregulated glycoproteins in LPS-, MALP2- and Pam3CSK-stimulated human monocytes	64
Fig. 24	Principal Component Analysis of the glycoprotein expression patterns all 3 replicates	65
Fig. 25	Volcano plot of glycoproteins in LPS-, MALP2- and Pam3CSK-stimulated monocytes	66
Fig. 26	Paired analysis: Significant up- or downregulated glycoproteins in LPS-, MALP2- or Pam3CSK-stimulated human monocytes	68
Fig. 27	Linear regression model of the glycoprotein expression of the differently treated monocytes	72
Fig. 28	Cellular component analysis of LPS, MALP2 and Pam3CSK-regulated glycoprotein	73
Fig. 29	CD antigen-expression in stimulated monocytes	74
Fig. 30	Overview of 75 proteins annotated as being involved in various steps of “protein glycosylation” (GO:0006486)	76
Fig. 31	Overview of 54 proteins annotated as proteins with “G-protein coupled receptor activity” (GO:0004930)	77
Fig. 32	qPCR analysis of LPS-induced ITGB8, LAMP3, MMP9, GPR84 and DPEP2 gene expression in monocytes	78
Fig. 33	Verification of proteomic results by FACS analysis: cell surface expression of CD80, IL7R, PD-L1, SLAMF7, CD86 and CLEC12A	79
Fig. 34	CEACAM-6 and TLR4 expression in LPS-, Pam3CSK- and MALP2-stimulated monocytes	80

10.2 List of tables

ID	Title	Page
Table 1	List of laboratory devices	18
Table 2	List of expendable materials	19
Table 3	List of used PRR agonists	20
Table 4	Primer list	21
Table 5	Primary antibodies for flow cytometry and western blot	22
Table 6	Secondary antibodies used in western blot (WB) analysis	22
Table 7	Mix composition using the High Capacity cDNA Reverse Transcription Kit (Thermo Scien., USA)	28
Table 8	Program of the thermo cycler used for cDNA synthesis	28
Table 9	PCR cycler conditions running on sqPCR	29
Table 10	Contents of agarose gel	29
Table 11	LB medium	30
Table 12	Purified plasmids	31
Table 13	TE buffer in DNA precipitation	32
Table 14	Transfection conditions and kits	33
Table 15	Lysis buffer for isolation of the total cellular protein content	35
Table 16	10x Running buffer for SDS-page	36
Table 17	CBB-gel-staining solutions	36
Table 18	Silver-gel staining solutions	37
Table 19	Buffer and staining solution for Western Blot analysis	37
Table 20	TBS and TBS-T buffer	39
Table 21	LPS-, Pam3CSK- and MALP2-regulated glycoproteins and their FC at 24 h compared to unstimulated control	69

Ehrenwörtliche Erklärung

Hiermit erkläre ich, dass mir die Promotionsordnung der Medizinischen Fakultät der Friedrich Schiller-Universität bekannt ist,

ich die Dissertation selbst angefertigt habe und alle von mir benutzten Hilfsmittel, persönlichen Mitteilungen und Quellen in meiner Arbeit angegeben sind,

mich folgende Personen bei der Auswahl und Auswertung des Materials sowie bei der Herstellung des Manuskripts unterstützt haben: Prof. Dr. Hortense Slevogt, Dr. rer. nat. Mario Müller, Dipl.-Ing. Dominik Driesch, Dr. med. Tony Bruns und Dr. rer. nat. Tilman Klassert.

die Hilfe eines Promotionsberaters nicht in Anspruch genommen wurde und dass Dritte weder unmittelbar noch mittelbar geldwerte Leistungen von mir für Arbeiten erhalten haben, die im Zusammenhang mit dem Inhalt der vorgelegten Dissertation stehen,

dass ich die Dissertation noch nicht als Prüfungsarbeit für eine staatliche oder andere wissenschaftliche Prüfung eingereicht habe und

dass ich die gleiche, eine in wesentlichen Teilen ähnliche oder eine andere Abhandlung nicht bei einer anderen Hochschule als Dissertation eingereicht habe.

Ort, Datum Unterschrift des Verfassers

Danksagung

In der Tat wäre diese Doktorarbeit wohl nie ohne die Unterstützung einer Reihe von Personen zustande gekommen, bei denen ich mich an dieser Stelle bedanken möchte:

Zuerst gilt mein aufrichtiger Dank Prof. Dr. Hortense Slevogt für die Betreuung und Möglichkeit an ihrem Institut promovieren zu dürfen.

Ein ganz besonders großer Dank gebührt Dr. Mario Müller der mir stets mit Expertise und Geduld bei kleinen und größeren Problemen mit Rat und Tat zur Seite stand.

Bedanken möchte ich mich auch bei dem gesamten *Host Septomics* Team in dem ich mich von Anfang an sehr wohlgefühlt habe und in Moira, Simone, Cora, Carolin, Cris und Tilman nicht nur „Labor-Gefährten“, sondern mehr noch wertvolle neue Freunde gefunden habe.

Ebenfalls bedanken möchte ich mich bei Dipl.-Ing. Dominik Driesch für seine Hilfe in allen statistischen Fragen und bei Dr. Tony Bruns für die Übernahme der Zweitbetreuung.

Dank des Stipendiums des *Center for Sepsis Control and Care* wurde es mir ermöglicht mich uneingeschränkt meiner Doktorarbeit zu widmen. Auch dafür herzlichen Dank!

Abschließend möchte ich mich auch bei meiner Familie und meinen Freunden bedanken, die mir immer den nötigen Rückhalt gaben und mit einem offenen Ohr zur Seite standen.